Assessing water stress of desert vegetation using remote sensing

The case of the Tamarugo forest in the Atacama Desert (Northern Chile)

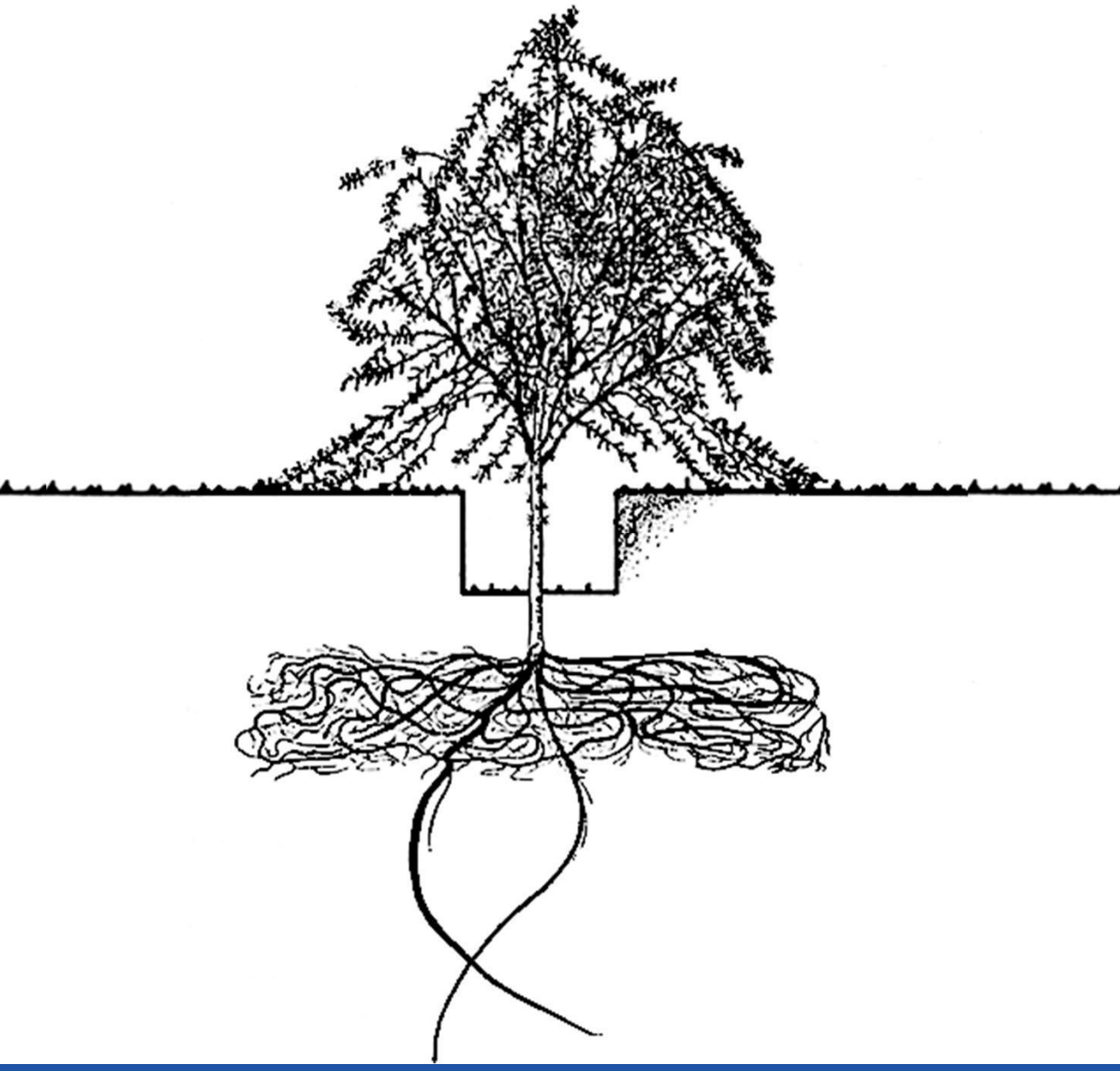

Roberto O. Chávez

Assessing water stress of desert vegetation using remote sensing

The case of the Tamarugo forest in the Atacama Desert (Northern Chile)

Roberto O. Chávez

Thesis committee

Promotor
Prof. Dr M. Herold
Professor of Geo-information Science and Remote Sensing
Wageningen University

Co-promotors
Dr J.G.P.W. Clevers
Associate professor, Laboratory of Geo-information Science and Remote Sensing
Wageningen University

Prof. Dr E. Acevedo
Professor at Departamento de Producción Agrícola, Facultad de Ciencias Agronómicas, Universidad de Chile, Chile

Other members
Prof. Dr G.M.J. Mohren, Wageningen University
Prof. Dr A.K. Skidmore, University of Twente, Enschede, The Netherlands
Prof. Dr A. Karnieli, Ben-Gurion University of the Negev, Beer-Sheva, Israel
Dr S. Lhermitte, KU Leuven, Belgium

This research was conducted under the auspices of the C.T. de Wit Graduate School of Production Ecology & Resource Conservation (PE&RC)

Assessing water stress of desert vegetation using remote sensing

The case of the Tamarugo forest in the Atacama Desert (Northern Chile)

Roberto O. Chávez

Thesis
submitted in fulfilment of the requirements for the degree of doctor
at Wageningen University
by the authority of the Rector Magnificus
Prof. Dr M.J. Kropff,
in the presence of the
Thesis Committee appointed by the Academic Board
to be defended in public
on Tuesday 16 September 2014
at 4 p.m. in the Aula.

Roberto O. Chávez
Assessing water stress of desert vegetation using remote sensing.
The case of the Tamarugo forest in the Atacama Desert (Northern Chile)
174 pages.

PhD thesis, Wageningen University, Wageningen, NL (2014)
With references, with summaries in Dutch, English and Spanish

ISBN 978-94-6257-079-5

Table of Contents

Chapter

1

General Introduction

1.1. Remote sensing of desert vegetation

Can we see desert vegetation in satellite images? At the present time, we can use remote sensing to 'see' sparse desert vegetation (Figure 1.1). Recent advances in remote sensing not only have enabled a high spatial resolution of satellite images (< 1 m pixel resolution), but also a high number of spectral bands at a high spatial detail. For example, the WorldView-3 satellite (expected to be launched in 2014) will provide 16 spectral bands: eight covering the visible (VIS) and near-infrared (NIR) regions at 1.24 m resolution and eight bands covering the shortwave-infrared (SWIR) region at 3.7 m resolution. Current operational very high spatial resolution satellites such as QuickBird-2 (launched in 2001), GeoEye-1 (launched in 2008) and WorldView-2 (launched in 2009) have enabled the retrieval of important bio-physical parameters of small desert vegetation features, such as single trees, shrubs or grass patches (Aksoy et al. 2012; Blaschke 2010; Gibbes et al. 2010; Karydas and Gitas 2011; Laliberte et al. 2007). Therefore, assessing the health condition of desert vegetation nowadays seems a feasible task.

Remote sensing has not been used for desert vegetation as intensively as for other vegetation types (e.g. tropical forests) and some dimensions of the light-canopy interaction of desert plants are not fully understood yet. Desert plant species have evolved remarkable adaptations to survive aridness (Alpert and Oliver 2002), and some of these adaptations can have an important effect on remote sensing observations that need to be quantified.

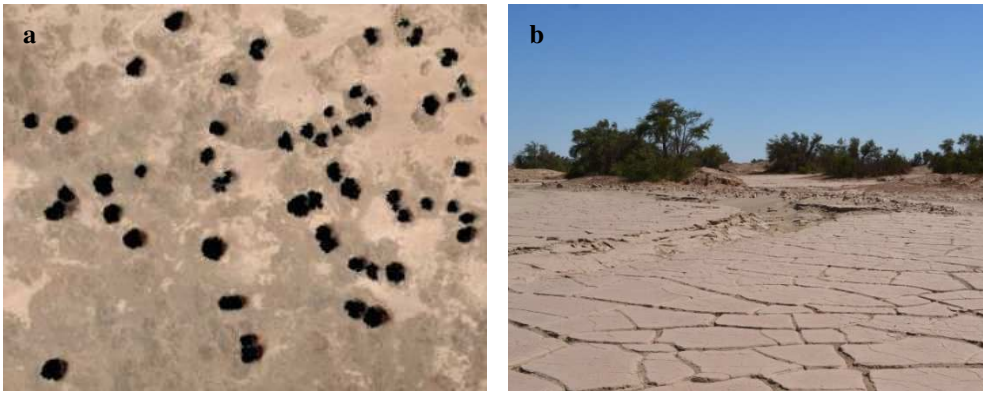

Figure 1.1. Natural Tamarugos in the Atacama Desert (Northern Chile) as seen from a WorldView2 satellite image **(a)** and from a digital picture in the field **(b)**.

For example, many desert plants can track the sun in such a way that they avoid direct sun rays on the leaves (paraheliotropism) (Ehleringer and Forseth 1980; Koller 2001). Consequently, these plants are able to photosynthesize longer than other plants under high solar irradiation and temperature (Pastenes et al. 2005; Pastenes et al. 2004). These light-driven leaf movements can cause changes in the canopy reflectance of desert vegetation during the day, as the sun moves across the sky, and during the season, as solar irradiation changes in intensity. Yet, no research has been done so far to quantify the effects of solar tracking on remote sensing based estimations of desert vegetation properties. Furthermore, very high spatial resolution satellite images have a limited temporal resolution and a relatively short historical timespan, making it difficult to study the temporal dynamic of spectral reflectance due to desert plant adaptations (e.g. phenology or paraheliotropism). Coarser satellite images providing a higher spatial resolution and timespan must be used, such as Landsat images (30 m resolution) or MODIS images (250 m resolution), for which the small fractional cover of desert vegetation remains the main limitation (Asner and Heidebrecht 2002).

Important economic activities take place in desert ecosystems (e.g. mining and fuel extraction), putting pressure on water demands and threatening natural ecosystems (Danielopol et al. 2003). Thus, water stress assessments of natural vegetation are needed for environmental impact assessments and water management of desert ecosystems. We cannot assess water stress of a desert species using remote sensing without knowing the light-canopy interaction governing canopy spectral

reflectance. In this thesis, we aim at providing insights on the use of remote sensing for assessing water stress of desert vegetation, exemplified in the case of the Tamarugo (*Prosopis tamarugo* Phil.) trees in the Atacama Desert, Northern Chile.

1.2. The water conflict in desert ecosystems

Water sources and vegetation spots are very important in deserts for both conservation of biodiversity and supporting human activities (Filella and Penuelas 1994). Unfortunately, there is an intrinsic trade-off between these two objectives, because vegetation and water sources are limited and strongly interdependent, and human activities such as mining, oil extraction and agriculture are highly demanding on water resources (Danielopol et al. 2003; Filella and Penuelas 1994; Portnov and Safriel 2004). These activities are interrelated since a growing industry attracts people to work in the factories and to live in the cities or towns nearby, and consequently, they together create an increasing demand for water resources (Portnov and Safriel 2004). Furthermore, the biological activity of deserts occurs at a slow rate, thus recovery from human perturbation can take a long time, even when active restoration techniques are applied (Burke 2003; Dean et al. 2004; Guo 2004; Lovich and Bainbridge 1999).

For this reason, water management and environmental impact assessment in deserts deserve great attention by policy makers and national environmental agencies (Giordano and Villholth 2007; McGlynn and Okin 2006). Mining and oil exploitation are common practices in desert ecosystems due to the abundance of minerals and fuel reserves, which attracts investors from all over the world (Ezcurra 2006; Gitelson et al. 2006). An important aspect of water management is the water balance or water budget, which allows policy makers to understand inflows, outflows and water stocks of watersheds (Riedemann et al. 2006). A good understanding of the water budget makes it possible to manage water resources in order to supply water to human activities minimizing environmental impacts (McGlynn and Okin 2006). Deserts have high evaporation rates (outflow) and scarce precipitation (inflows), hence a negative water balance is likely to occur due to water extraction (Houston 2006; Shibayama et al. 1993). In this context, water stress assessment of natural vegetation and crops plays a key role in water management. It allows scientists and managers to relate water extraction rates to

changes in vegetation water condition, and consequently, to define safe water extraction rates for maintaining a healthy ecosystem.

1.3. Importance of deserts for biodiversity conservation

Deserts, covering almost 20% of the terrestrial surface of the planet (Figure 1.2), are unique and highly adapted ecosystems providing relevant services to support wildlife and human population (Ezcurra 2006). Vegetation is scarce and distributed in patches or belts where water sources become available: sporadic streams and rivers, shallow groundwater or small superficial water bodies. Although deserts are characterized by high aridity and salinity in soils and water, they show a considerable diversity of plant and animal species (Briones 1985; Moran et al. 1994; Penuelas et al. 1994; Richardson and Berlyn 2002). Desert ecosystems frequently are geographically isolated from other ecosystems, thus most of the plant species have evolved into distinct taxonomic groups (Burke 2005). For this reason, deserts are particularly important for conservation of rare and endangered species, and conservation efforts become relevant considering the current pressure for water consumption in arid regions (Dobrowski et al. 2005; Jong and Meer 2005).

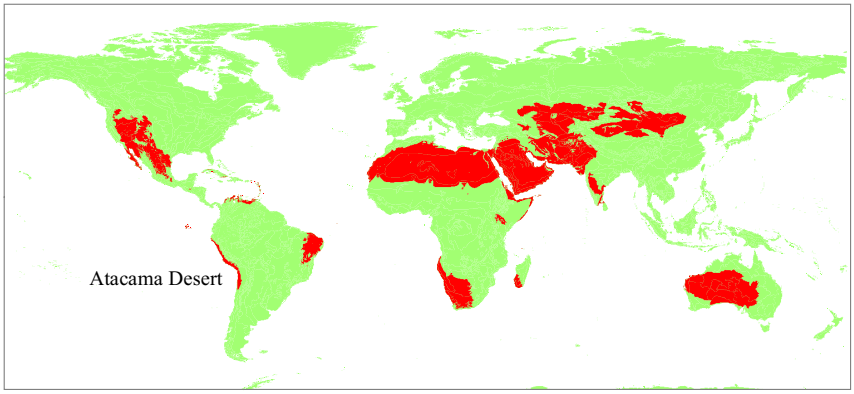

Figure 1.2. Desert and xeric shrublands biome in the world (Olson et al. 2001).

Longer and more severe droughts are presently the most challenging environmental effects of climate change (Romm 2011). Expansion of arid areas is expected to occur in the next 20 to 50 years affecting large areas, especially those near the dry subtropics (Dai 2011; Romm 2011). Considering this prospective, the conservation and study of species, which are naturally able to cope with extreme

desert environments, becomes of high interest. Desert species provide alternatives for arid land management, constituting a genetic pool of 'drought resistance solutions' to deal with the more abundant arid landscapes (Alpert and Oliver 2002).

1.4. Remote sensing for assessing vegetation water stress

Remote sensing allows estimation of important parameters related to plant water conditions, such as evapotranspiration rate, biomass amount, plant pigment concentration and foliage water content (Bowman 1989; Clevers et al. 2001; Govender et al. 2009; Leinonen and Jones 2004; Yu et al. 2000). Its usefulness is based on the basic principle that water stress produces visible (and nonvisible) symptoms in the vegetation canopy, for instance, changes in color or temperature. These changes can be successfully registered by satellite images, providing a unique source of spatial and quantitative data over large areas of vegetation (Karnieli and Dall'Olmo 2003).

The desiccation process begins when water flows out of the soil, producing a decline in soil water potential. As a consequence, plants react by adjusting several biochemical cell and molecular processes and closing stomata to equilibrate their water content. This regulatory mechanism temporally minimizes water stress but it also produces a decrease in the photosynthetic rate and biomass production. If the water depletion is severe, foliage will gradually lose its water and photosynthetic pigments until leaves die (Suárez et al. 2008). In this process, changes occur in the light reflection and light absorption properties of plants (Chaerle and Van Der Straeten 2000; Gillon et al. 2004; Seelig et al. 2009). Remote sensors operated in airplanes and spacecraft are able to measure this change in reflection (Berni et al. 2009; Leinonen and Jones 2004).

Optical remote sensors have been designed to capture different regions of the electromagnetic spectrum in the 400-2500 nm range. During the dehydration process an increase of canopy spectral reflectance in the 1300-2500 nm range occurs as a result of lower absorption of solar radiation by the water in the leaves (Carter 1991; Zarco-Tejada et al. 2003). As leaves dehydrate, more cell wall−air interfaces are present in the leaf tissues causing an increment of spectral reflectance in the 700-1300 nm range due to internal multiple scattering of radiation (Danson et al. 1992; Feret et al. 2008; Jacquemoud et al. 1996).

Furthermore, a negative effect of dehydration on the absorption properties of pigments causes the spectral reflectance to increase in the 400-720 nm range (Carter 1991). Another effect of water stress on vegetation canopy reflectance is the 'blue shift' of the red-edge towards shorter wavelengths (Boochs et al. 1990; Carter 1993; Filella and Penuelas 1994; Horler et al. 1983). The red-edge is the steep slope of the vegetation spectral signature occurring at about 680-750 nm. Although the spectral reflectance in the near-infrared (NIR) region (700-1300 nm) initially increases as a result of dehydration (Clevers et al. 2010; Hunt Jr and Rock 1989), in late stages of water stress it decreases as a consequence of the deterioration of cell walls (Knipling 1970) and the loss of leaves (Asner 1998).

Recent improvements in water stress detection using remote sensing have enabled the identification of small spectral features related to water stress such as the right slope of the vegetation absorption feature at 970 nm (Clevers et al. 2008, 2010) related to canopy water content or the tiny jump in reflectance around 760 nm due to chlorophyll fluorescence (Pérez-Priego et al. 2005), which is a good indicator of stomatal conductance, CO_2 assimilation (Flexas et al. 2000; Flexas et al. 2002) and water potential (Pérez-Priego et al. 2005). The studies carried out by Baret et al. (2007), Carter and Knapp (2001) and Govender et al. (2009) provide a summary of the sensitivity of different spectral regions to water stress.

1.5. Problem definition: how to use remote sensing to assess water stress of desert vegetation?

Two plant functional types are typically present in desert ecosystems: herbaceous plants and woody plants, which can use available water from different layers in the soil profile (Ogle and Reynolds 2004; Walter and Mueller-Dombois 1971). Sporadic pulses of water play a significant role on the establishment and growth of these two functional types, making herbaceous plants more dependent on rain than perennial woody plants, since this second group of desert plants can survive using deeper groundwater within the soil profile (Noy-Meir 1985; Schwinning and Sala 2004). Therefore, in the most extreme cases of aridity plant communities are dominated by perennial woody plants, except for the communities of Cactaceae and Bromeliaceae in some deserts of the American continent. In this thesis, we will focus on the water status assessment of desert woody vegetation in the Atacama Desert of Chile.

Such desert plants have to cope with two main limiting factors: excessive solar radiation and scarce water. In order to survive the natural aridness of these ecosystems they have evolved different mechanism to avoid excessive transpiration and minimize photoinhibition. A common adaptation among desert plants is heliotropic movement or leaf 'solar tracking', which is the ability of some species to move their leaves to avoid facing direct solar irradiation at the hottest time of the day/season (Ehleringer and Forseth 1980; Koller 1990). These movements, specifically called paraheliotropism (facing away the sun), can have an important effect on canopy spectral reflectance measured by satellites as well as on vegetation indices calculated using canopy spectral features such as the normalized difference vegetation index (NDVI). Besides paraheliotropism, another adaptation of desert plants with potential impacts on canopy spectral reflectance is leaf shedding, occurring for example in the case of Acacia shrubs in the Sahara Desert as the dry season progresses (Ezcurra 2006), and desiccation tolerance, a remarkable adaptation of some species to dry out completely during adverse periods and re-grow when water is again available (Proctor and Pence 2002).

Figure 1.3 shows the relationship between water related variables and processes for a given woody desert species that may be affected by groundwater extraction as well as the response of a given spectral vegetation index as measured by remote sensing.

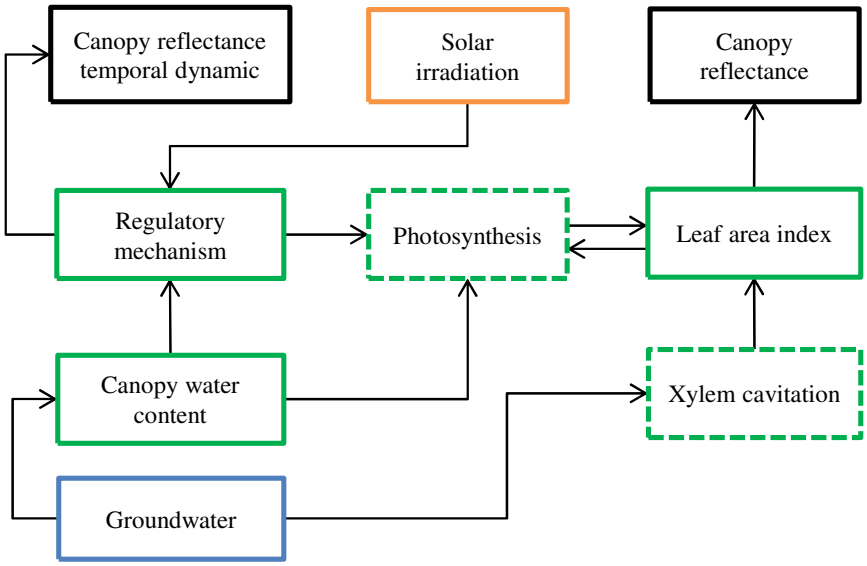

Figure 1.3. Conceptual diagram showing the relationship between variables and processes involved in the water uptake, the mechanism to regulate radiant energy interception by leaves, and the response in canopy reflectance of woody desert vegetation. Dashed boxes correspond to processes/variables not studied in this thesis.

As solar radiation increases during the day and during the season, a regulatory mechanism (e.g. paraheliotropism) at the canopy level is activated to protect the photosynthetic apparatus. This mechanism, for many desert plants unknown, may have an impact on diurnal/seasonal canopy reflectance and spectral vegetation indices derived from it due to partial changes of the canopy structure. Furthermore, the water balance of the soil-plant-air continuum can be negatively affected by external factors such as groundwater pumping. In that case, a lowering of the groundwater table may cause the canopy water content to decrease affecting the natural dynamic of canopy reflectance (or indices derived from it) measured from space. This may also have a negative effect on the photosynthetic capacity of the plant and consequently on the green biomass production. If the water stress persists, some branches may die via xylem cavitation, reducing the above-ground biomass and water loss due to transpiration. This may also have a negative feedback on the photosynthetic capacity of the plant. Since the regulatory mechanisms to protect the photosynthetic apparatus vary between different desert species, the effects of water stress and the response on canopy reflectance and spectral vegetation indices need to be studied for each specific case.

In this thesis, we study the potential of a remote sensing based approach to assess water stress of woody desert vegetation, exemplified by the case of the Tamarugo (*Prosopis tamarugo* Phil.) tree in the Atacama Desert (Northern Chile). We aim to study some of the unknown aspects of Figure 1.3 (e.g. the regulatory mechanism and its effects on canopy spectral reflectance) for this specific species as well as the effects of groundwater overexploitation on its water status (see chapter 6).

The Atacama Desert in Northern Chile is the southern part of the desert close to the coast of the Pacific Ocean in South America (Gajardo 1994). It is characterized by extreme conditions of aridity: almost null precipitation, high temperatures and high potential evapotranspiration (Houston and Hartley 2003). The Atacama Desert has been considered as one of the most extreme environments for life as well as the driest place on Earth (McKay et al. 2003; Navarro-González et al. 2003). The main water resources of this region are aquifers of groundwater and a few rivers and temporary streams, which descend from the Andes to the Pacific Ocean (Aravena 1996). Vegetation spots are scarce, limitedly distributed and closely related to water sources. An exceptional example of adaptation to these extreme environmental conditions is the Tamarugo tree. Tamarugo is an endemic species, adapted to hyper-arid conditions, but with a limited distribution. Most of the Tamarugo population is under official protection and currently belongs to the Pampa del Tamarugal National Reserve, which is administrated by the Chilean National Forest Service (CONAF). However, the pressure for extracting groundwater for human consumption and industry remains and studies regarding the water status of the Tamarugo trees are required for local water management.

Four research questions have been formulated in the framework of this PhD thesis:

Research questions

A. What is the spectral response of the desert Tamarugo tree to water stress?

B. How can we assess the water condition of single Tamarugo trees using modern remote sensing techniques?

C. What is the impact of the regulatory mechanisms of Tamarugo (to avoid excessive transpiration and photoinhibition) on time series of canopy spectral reflectance and vegetation indices with and without water stress?

D. How can we use remote sensing to assess the impact of groundwater extraction on the Tamarugo population at large scale?

1.6. Outline

This thesis consists of four main chapters, each addressing one of the research questions presented in section 1.5.

In **chapter 2**, we addressed research question A by studying the effects of water stress on Tamarugo plants under laboratory conditions and modelling the light-canopy interaction using the Soil-Leaf-Canopy radiative transfer model. In **chapter 3**, we addressed research question B, by checking some specific features of the Tamarugos' light-canopy interaction that were observed in the laboratory (the solar tracking mechanism), but this time under field conditions and by using high spatial resolution images and in-situ data to assess water stress at the tree level. In **chapter 4**, we addressed question C by studying the effect of Tamarugos' leaf solar tracking on NDVI time series from Landsat and MODIS Terra-Aqua satellites with and without water stress. In **chapter 5** we addressed research question D by carrying out a remote sensing based assessment to quantify the spatial and temporal effects of long term (50 years) groundwater extraction on the Tamarugo vegetation at the basin level. This thesis is concluded by **chapter 6**, where the findings for each research question are presented and discussed in a broader context. Chapter 6 concludes with a reflection and outlook based on the results obtained in this PhD research and suggestions for further research.

Chapter

2

Modelling the spectral response of the desert tree *Prosopis tamarugo* to water stress

R.O. Chávez, J.G.P.W. Clevers, M. Herold, M. Ortiz, E. Acevedo

Published in International Journal of Applied Earth Observation and Geoinformation, Volume 21, April 2013, Pages 53-65

In this paper, we carried out a laboratory experiment to study changes in canopy reflectance of Tamarugo plants under controlled water stress. Tamarugo (*Prosopis tamarugo* Phil.) is an endemic and endangered tree species adapted to the hyper-arid conditions of the Atacama Desert, Northern Chile. Observed variation in reflectance during the day (due to leaf movements) as well as changes over the experimental period (due to water stress) were successfully modelled by using the Soil-Leaf-Canopy (SLC) radiative transfer model. Empirical canopy reflectance changes were mostly explained by the parameters leaf area index (LAI), leaf inclination distribution function (LIDF) and equivalent water thickness (EWT) as shown by the SLC simulations. Diurnal leaf movements observed in Tamarugo plants (as adaptation to decrease direct solar irradiation at the hottest time of the day) had an important effect on canopy reflectance and were explained by the LIDF parameter. The results suggest that remote sensing based assessment of this desert tree should consider LAI and canopy water content (CWC) as water stress indicators. Consequently, we tested fifteen different vegetation indices and spectral absorption features proposed in literature for detecting changes of LAI and CWC, considering the effect of LIDF variations. A sensitivity analysis was carried out

using SLC simulations with a broad range of LAI, LIDF and EWT values. The Water Index was the most sensitive remote sensing feature for estimating CWC for values less than 0.036 g/cm^2, while the area under the curve for the spectral range 910-1070 nm was most sensitive for values higher than 0.036 g/cm^2. The red-edge chlorophyll index ($CI_{red\text{-}edge}$) performed the best for estimating LAI. Diurnal leaf movements had an effect on all remote sensing features tested, particularly on those for detecting changes in CWC.

2.1. Introduction

Remote sensing (RS) has become an important tool to quantitatively assess and monitor water stress of vegetation, a key input for water management in arid regions. Water stress in plants activates a series of physiological mechanisms to maintain the water balance of the plant and to keep its vital functions, such as photosynthesis and respiration, while dehydrating (Taiz and Zeiger 2010). Early stages of water stress are often related to loss of foliage water while late stages are related to loss in leaf pigments, loss of biomass (leaves, branches) and finally plants die (Baret et al. 2007; Taiz and Zeiger 2010). These changes modify the light reflection and absorption properties of the vegetation canopy, which can be accurately registered by multispectral and hyperspectral instruments (Karnieli and Dall'Olmo 2003).

Primary effects of water stress (dehydration) on vegetation spectral reflectance are associated with an increment of reflected radiation in the range of 1300-2500 nm solely because of less absorption by water (Carter 1991; Zarco-Tejada et al. 2003). Secondary effects are associated with an increment of spectral reflectance in the range 400-1300 nm due to more cell wall - air interfaces within the leaf tissue as well as the effect of dehydration on the absorption properties of pigments (Carter 1991; Knipling 1970). Another secondary effect of water stress is the “blue shift” of the red edge (the steep slope of the vegetation spectral signature occurring at 680-750 nm) towards shorter wavelengths (Boochs et al. 1990; Carter 1993; Filella and Penuelas 1994; Horler et al. 1983). Although the spectral reflectance in the NIR region (700-1300 nm) initially increases (Clevers et al. 2010; Hunt Jr and Rock 1989), in late stages of water stress it decreases as a consequence of the deterioration of cell walls (Knipling 1970) and loss of leaves (Asner 1998). Furthermore, use of narrow spectral bands has enabled the identification of small spectral features also associated to water stress such as the right slope of the

vegetation absorption feature at 970 nm (Clevers et al. 2008, 2010) related to canopy water content or the tiny jump in reflectance around 760 nm due to chlorophyll fluorescence (Pérez-Priego et al. 2005), which is a good indicator of stomatal conductance, CO_2 assimilation (Flexas et al. 2000; Flexas et al. 2002) and water potential (Pérez-Priego et al. 2005). For a detailed summary of the sensitivity of different spectral regions to water stress and to other stress factors refer to Baret et al. (2007), Carter and Knapp (2001) and Govender et al. (2009).

Based on this knowledge, a considerable number of remote sensing based algorithms have been designed and implemented to quantitatively estimate and map important parameters related to plant water condition, such as leaf area index (LAI), leaf chlorophyll concentration and equivalent water thickness (EWT) (see section 2.2.6).

Nevertheless, the application of remote sensing for assessing water condition of vegetation in hyper-arid ecosystems or "true deserts" is mainly conditioned by (i) the rather small size of the target objects (isolated trees, shrubs or grass patches), (ii) the knowledge on the response of desert species to water stress and potential effects on canopy spectral reflectance that are commonly unknown, and (iii) the species phenological cycles which have an important effect on the proportion of green and brown vegetation material during the year (Asner et al. 2000).

The low vegetation fractional cover and small size of vegetation units in deserts causes a high proportion of mixed pixels in most of the available RS datasets (i.e. Landsat, MODIS, SPOT, MERIS, RapidEye) (Asner and Heidebrecht 2002). Recent improvements in spatial resolution of satellites such as Quickbird2, WorldView2 and GeoEye make it possible to obtain "comparatively pure" pixels of desert small trees and shrubs for more focused analysis on vegetation properties. Spectral resolution has also improved from the four standard bands of sub-metric satellites to up to eight bands in the visible and near infrared regions of WorldView2. All these improvements open new possibilities for remote sensing studies of desert vegetation, but also a need for better understanding of the canopy spectral properties of desert species.

Assessing water stress of vegetation adapted to hyper-arid conditions is not a straightforward process. Desert plant species have developed different mechanisms to tolerate dry conditions, either by controlling water content (via regulation of transpiration rates) or by drying up (partially or completely) and remaining latent

until water supply conditions are again favourable (Alpert and Oliver 2002). Therefore their natural dynamics and responses to external disturbances can significantly vary between different species and sites. These adaptations can radically influence vegetation canopy reflectance and absorption properties, and therefore a good understanding of this interaction is crucial for a reliable remote sensing based assessment.

In this study we aim to improve our understanding of the spectral response of the desert species *Prosopis tamarugo* Phil to water stress. Tamarugo is an endemic tree species, highly adapted to the hyper-arid conditions of the Atacama Desert, Northern Chile. Its geographic distribution is limited to the Atacama Desert and the trees are completely dependent on ground water (Altamirano 2006; Mooney et al. 1980). Although most of the Tamarugo population is under official protection, the species is under threat due to ground water extraction for human consumption and mining (Rojas and Dassargues 2007), and therefore, quantitative tools for assessing the forest water condition are needed for environmental policy making and monitoring.

Tamarugo tree response to water stress and the use of remote sensing to monitor this process have not been studied. In order to provide basic knowledge for a remote sensing based assessment of Tamarugo, we conducted a laboratory experiment to study the response of Tamarugo plants to controlled water stress. Specifically, through this experiment we aim to (1) describe the physiological and spectral response of Tamarugo plants to water stress, (2) define appropriate canopy variables for assessing water stress for this species, (3) model the spectral response of a Tamarugo canopy to water stress using the radiative transfer theory and (4) test the sensitivity of different indices and spectral features to detect water stress using a range of simulated scenarios.

2.2. Material and methods

2.2.1. Species description

Tamarugo (*Prosopis tamarugo* Phil.) is a xerofitic tree species highly adapted to the extreme arid conditions of the Atacama Desert, Northern Chile (Figure 2.1). This hyper-arid environment is characterized by practically null precipitation, high temperatures and high potential evapotranspiration (Houston 2006; Houston and

Hartley 2003) and it is considered one of the most extreme environments for life on Earth (McKay et al. 2003; Navarro-González et al. 2003). The presence of Tamarugo is explained by the existence of a shallow groundwater table (Mooney et al. 1980), occurring in just two hydrological systems: Pampa del Tamarugal aquifer and Llamara aquifer, where practically all remaining Tamarugo population is distributed. Studies have shown that natural and artificial (pumping) discharges in the Pampa del Tamarugal aquifer have been twice as large as natural recharges since 1986 (Rojas and Dassargues 2007). Consequently, groundwater gradually has depleted threatening Tamarugo water supply. Between 1965 and 1970 a big effort for Tamarugo's conservation was promoted by the Chilean government and around 13800 hectares were planted (Aguirre and Wrann 1985; CONAF 1997).

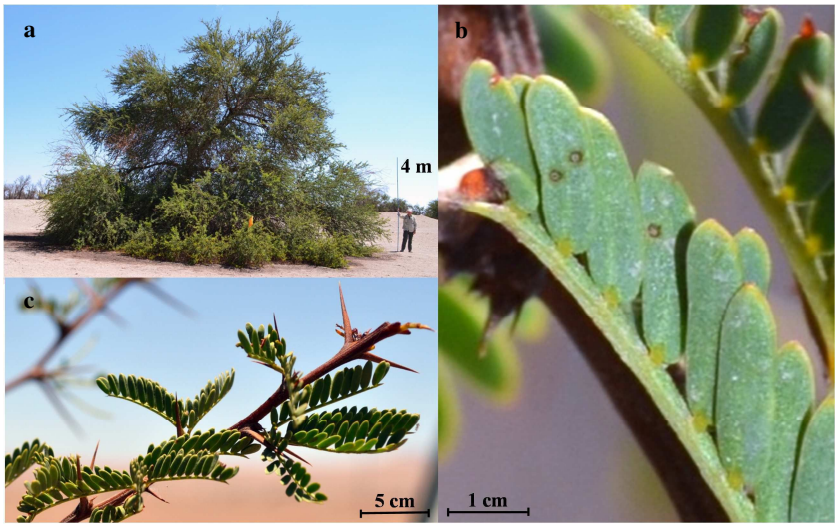

Figure 2.1. Anatomic characteristics of *Prosopis tamarugo* Phil. **(a)** Adult tree; **(b)** Twig; **(c)** Composed bipinnate leaf

Tamarugos are thorny phreatophyc trees and reach heights up to 25 meters, crown size up to 20 meters and stems up to 2 meters in diameter (Altamirano 2006; Riedemann et al. 2006). Tamarugo is a semi-caducifolious tree, keeping a considerable part of its foliage during the winter (Vargas and Bobadilla 2000). Its vegetative period covers all year with a peak occurring between September and December (Acevedo et al. 2007). The branches are arched and gnarled, twigs are flexuose and thorns in pairs are stipular in origin of 0.5-3.8 cm (Kesler et al. 2012). Leaves are often bipinnate with 6-15 pairs of folioles (Figure 2.1b-c).

2.2.2. Experimental setup

A total of nine plants, about 30 cm in height, were placed in a climate chamber with no water supply for 15 days. Plants were grown under greenhouse conditions and kept in the original black containers and substrate during the whole experiment. The plants were arranged in a matrix of 3 by 3 in such a way that a continuous canopy (including leaves, stems and soil) was available for nadir spectral measurements. The climate chamber was deprived of sunlight and artificial light was provided by an ASD Pro lamp. This is a 14.5 Volt 50 Watt lamp especially designed for laboratory diffuse reflectance measurements over the region 400 - 2500 nm. The applied light regimen consisted of 14 hours light from 7:00 hours till 21:00 hours followed by 10 hours of darkness and the temperature was set at 30ºC (+- 5ºC), similar to Tamarugo's natural conditions during summer (Houston 2006; Mooney et al. 1980). A spectroradiometer instrument (ASD FieldSpec Pro) was installed above the plants in order to measure spectral reflectance in the range 400-2500 nm. A foreoptic with instantaneous field of view (IFOV) of 25º was used and placed in nadir position 15 cm above the top of the canopy. This setup gave a circular measurement area of green plants of approximately 35 cm^2. No laboratory background was within the IFOV of the ASD instrument.

2.2.3. Spectral sampling

Spectral sampling was performed hourly, starting at 8:00 hours and ending at 20:00 hours (13 samples per day), in order to study the course of spectral reflectance during the day. This was repeated for 14 days in order to investigate the spectral response to water stress. The last spectral sampling was done on day 15 at 8:00 hours. Each sample corresponded to a spectral signature in the range 400-2500 nm obtained as an average of 50 scans. White reference measurements (spectralon) were used to obtain bi-conical reflectance factor measurements according to the nomenclature proposed by Schaepman-Strub et al. (2006). White reference calibrations were carried out at the beginning of the experiment as well as on day 5 and day 10. Previous tests showed a good stability of the ASD measurements within the chamber, so calibrations were minimized to avoid disturbing the experiment.

2.2.4. Physiological sampling

Physiological sampling was carried out daily at 8:30 hours during 15 days. The physiological measurements included equivalent water thickness (EWT) in g/cm^2, leaf chlorophyll concentration (*a*, *b* and total) in µg/cm^2 and leaf carotenoids concentration in µg/cm^2. Leaves from the lower third of the plants were used for laboratory determinations. No leaf sampling was carried out within the IFOV of the ASD instrument.

Leaf samples for chlorophyll and carotenoid determinations were spectrophotometrically analysed using leaf extracts dissolved in 80% acetone. Absorbance measured at 663 nm was utilised to determine chlorophyll *a*, at 646 nm for chlorophyll *b* and at 479 nm for carotenoids.

Equivalent water thickness (EWT) was measured using the following formula:

$$EWT = \frac{(fresh\ leaf\ weight - dry\ leaf\ weight)}{fresh\ leaf\ area} \qquad (1)$$

The fresh weight was measured immediately after cutting the leaves using a digital balance of 0.0001 g precision. Dry weight was obtained by drying the samples in an oven at 75ºC until getting constant dry weight.

2.2.5. Spectral absorption feature analysis

Continuum removal is a useful spectral processing methodology for studying the relationship between spectral absorption features and the biochemical composition and water content of a vegetation canopy (Huang et al. 2004; Huber et al. 2008; Kokaly and Clark 1999), which both are indicators of water stress. Furthermore, continuum removal minimizes the undesired effects of soil background and atmospheric absorptions on the spectral analysis (Kokaly and Clark 1999). Features of interest in spectral absorption feature analysis are the maximum band depth (MBD), the area under the curve (AUC) and the MBD normalized by the AUC (MBD/AUC) (Curran et al. 2001). An example of continuum removal applied to the canopy spectral signature of Tamarugo is given in Figure 2.2. Typically, the chlorophyll absorption feature in the visible part of the spectrum has been described as occurring approximately between 550 and 750 nm (Curran 1989; Huber et al. 2008; Kokaly et al. 2003). Furthermore, there are two absorption features associated with the presence of water in plant foliage: the first around 970

nm and the second one around 1200 nm (Curran 1989). There are also water absorption features at 1400 and 1900 nm, but they are not of interest for remote sensing applications since they are strongly affected by atmospheric water vapour (Clevers et al. 2008).

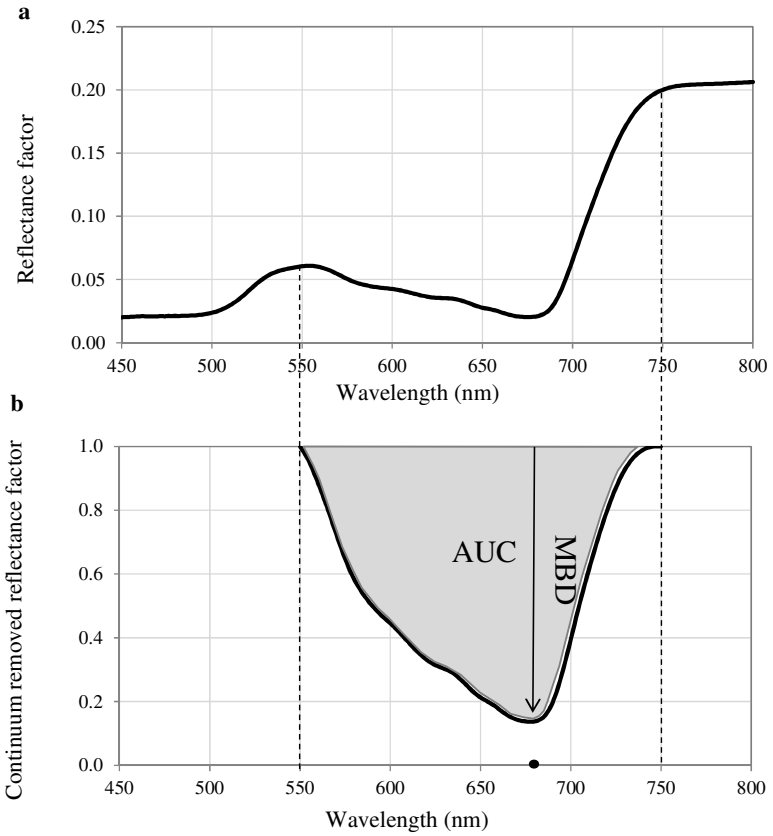

Figure 2.2 Example of continuum removal applied to a Tamarugo spectral signature. **(a)** Original spectrum, **(b)** Continuum removed spectrum, where AUC is the Area Under the Curve and MBD is the Maximum Band Depth.

In this study continuum removal was applied to analyse changes in the chlorophyll absorption feature (at 670 nm) and water absorption features (at 970 and 1200 nm) due to water stress. Spectral signatures measured daily at 8:00 hours during the 15 days of the laboratory experiment were used.

2.2.6. Remote sensing features for assessing water stress

In this study we explore the sensitivity of different RS based approaches to detect water stress in Tamarugos. Empirical models as well as physical models have been used to remotely retrieve LAI, chlorophyll concentration and EWT, main symptoms of plant stress (Baret et al. 2007). Radiative transfer models use physical laws to describe the interaction between light, the vegetation canopy and background (Jacquemoud et al. 2009). They establish an explicit linkage between the canopy reflectance and biochemical and structural properties of the scattering elements of vegetation. Radiative transfer models can be used in the "forward" way to simulate different scenarios of canopy reflectance when vegetation properties vary (this study). They can also be used in the "inverse" way (from canopy reflectance to vegetation properties) to estimate vegetation parameters from remotely sensed or ground measured canopy reflectance (Colombo et al. 2008; Jacquemoud et al. 2009; Laurent et al. 2011a; Vohland et al. 2010; Zarco-Tejada et al. 2003). This inversion process can be complex due to the large amount of parameters involved in the models and therefore the use of prior information or constraints is necessary for a successful estimation (Combal et al. 2003).

Empirical models establish statistical relationships between specific reflectance features of the vegetation spectra and vegetation parameters. Widely used empirical models are the so-called vegetation indices (VIs) which combine a limited amount of spectral information through a numerical indicator that is statistically correlated with specific vegetation parameters. Examples of indices to assess loss in LAI are the Ratio Vegetation Index (RVI) (Jordan 1969), the widely used Normalized Difference Vegetation Index (NDVI) (Tucker 1979) and the Wide Dynamic Range Vegetation Index (WDRVI) (Gitelson 2004). The sharp slope of the vegetation spectral signature occurring at 680-750 nm, the red-edge, has been described to be very sensitive to changes in LAI and leaf chlorophyll (Boochs et al. 1990; Filella and Penuelas 1994) and the Red Edge Position (REP) has been used to retrieve LAI with even better results than using NDVI (Danson and Plummer 1995; Herrmann et al. 2011). Furthermore, VIs like the Red-edge Chlorophyll Index ($CI_{red\text{-}edge}$) and Red-edge Normalized Difference Vegetation Index (Red-edge NDVI) have been developed to retrieve specifically leaf chlorophyll content (Gitelson and Merzlyak 1994; Gitelson et al. 2006), but they also have been utilised for retrieving LAI (Viña et al. 2011). For assessing water stress in terms of EWT or canopy water content (CWC=EWT*LAI), VIs like the

Water Index (WI) (Peñuelas et al. 1997), the Normalized Difference Water Index (NDWI) (Gao 1996) and more recently the Derivative[1015-1050nm] (Clevers et al. 2010) can be used. These indices are based on the water absorption features at 970 nm and 1200 nm and use specific narrow bands.

In this study, the spectral and physiological changes observed during the experiment (sections 2.3.1 and 2.3.2) as well as the spectral absorption feature analysis (section 2.3.3) were used as a base for identifying suitable canopy variables and remote sensing methods to assess water stress of Tamarugo (Table 2.1). A sensitivity analysis was carried out by using a broad range of simulated scenarios using the radiative transfer model Soil-Leaf-Canopy (see section 2.2.7) and the Noise Equivalent (NE) statistic as sensitivity indicator (see section 2.2.8).

Table 2.1. Remote sensing features tested for assessing water stress of Tamarugo plants in terms of LAI and CWC

Remote sensing feature	Formula and spectral regions used in this study	References
For assessing CWC		
Water Index (WI)	R_{900}/R_{970}	(Peñuelas et al. 1997)
Normalized Difference Water Index (NDWI)	$(R_{860}-R_{1240})/(R_{860}+R_{1240})$	(Gao 1996)
Derivative [1015,1050]	$(R_{1015}-R_{1050})/35$	(Clevers et al. 2010)
Water absorption feature [910-1070 nm]		(Clark and Roush 1984)
MBD*		
AUC**		
MBD/AUC		
Water absorption feature [1100-1280 nm]		(Clark and Roush 1984)
MBD*		
AUC**		
MBD/AUC		
For assessing LAI		
Normalized Difference Vegetation Index (NDVI)	$(R_{800}-R_{670})/(R_{800}+R_{670})$	(Tucker 1979)
Red-edge Chlorophyll Index ($CI_{Red-edge}$)	R_{780}/R_{710} -1	(Gitelson et al. 2006)
Red-edge NDVI	$(R_{780}-R_{710})/(R_{780}+R_{710})$	(Gitelson and Merzlyak 1994)
Ratio Vegetation Index (RVI)	R_{800}/R_{670}	(Jordan 1969)
Chlorophyll absorption feature [550-750 nm]		(Clark and Roush 1984)
MBD*		
AUC**		

* Maximum Band Depth
** Area Under the Curve

2.2.7. SLC model calibration and simulations

The Soil-Leaf-Canopy (SLC) model (Verhoef and Bach 2007) simulates top of canopy reflectance using as inputs leaf, canopy and soil parameters (Table 2.2).

The SLC version used in this study is the result of coupling the following models:

- **PROSPECT3** (Jacquemoud and Baret 1990) was modified to include the effects of brown pigments (Verhoef and Bach 2003) and it delivers simulations at 10 nm spectral resolution.
- **4SAIL2** (Verhoef and Bach 2007) is an improved version of the canopy radiative transfer model SAIL (Verhoef 1984). Among the new features, this 2-layer version includes the effects of crown clumping and the effects of the abundance and distribution of green and brown elements within the two canopy layers (Verhoef and Bach 2007), which allows a more realistic representation of the canopy and thus gives improved simulations.
- **SOIL4** (Hapke 1981; Verhoef and Bach 2007) includes the hotspot effect and the soil moisture spectral effect. In this study a measured background was used for calibrations and simulations, and therefore soil reflectance was fixed.

Physiological and spectral measurements carried out on day 1 at 8:00 hours were used to calibrate the SLC model. The parameters LAI, LIDFa, and LIDFb (Table 2.2) were optimized by minimizing the differences between measured and simulated reflectance values. In this optimization procedure, the parameters measured at the laboratory (Cab_{green}, EWT_{green}, Cdm_{green}) were considered fixed. For the other parameters the default values of the SLC model were used as indicated in Table 2.2. The parameters of the 4SAIL2 second layer (brown elements, i.e. stems and twigs) were optimized using the spectral reflectance measured at the end of the experiment, when no green leaves were present. A similar methodology often has been used for assessing radiative transfer model simulations using measured spectra; examples can be found in Darvishzadeh et al. (2011), Laurent et al (2011b) and Laurent et al. (2011a).

Once calibrated, the SLC model was used to simulate spectral reflectance for a wide range of water stress scenarios. These outputs were used to test the sensitivity of RS features indicated in Table 2.1.

Table 2.2. Soil-Leaf-Canopy (SLC) model input parameters.

SLC inputs		Day 1 - 8.00	Day 1 - 20.00	Day 14 - 8.00	Day 14 - 20.00	Source
Leaves (green material)						
Chlorophyll ab content (µg/cm)	Cab_{green}	42	42	42	42	Lab. measurement
Water content (g/cm^2)	**EWT_{green}**	**0.023**	**0.023**	**0.013**	**0.013**	**Lab. measurement**
Dry matter content (g/cm^2)	Cdm_{green}	0.0003	0.0003	0.0003	0.0003	Lab. measurement
Senescent material (no units)	Cs_{green}	0	0	0	0	From experiment
Mesophyll structure (no units)	N_{green}	1.5	1.5	1.5	1.5	SLC default
Twigs and stems (brown material)						
Chlorophyll ab content (µg/cm)	Cab_{brown}	5	5	5	5	SLC default
Water content (g/cm^2)	EWT_{brown}	0.01	0.01	0.01	0.01	Optimized
Dry matter content (g/cm^2)	Cdm_{brown}	0.005	0.005	0.005	0.005	SLC default
Senescent material (no units)	Cs_{brown}	1	1	1	1	SLC default
Mesophyll structure (no units)	N_{brown}	2	2	2	2	SLC default
Canopy						
Plant area index[(a)] (m^2/m^2)	PAI	1.27	1.27	1.12	1.12	Optimized
Leaf area index (m^2/m^2)	**LAI**	**1.00**	**1.00**	**0.85**	**0.85**	**Optimized**
Brown area index (m^2/m^2)	BAI	0.27	0.27	0.27	0.27	Optimized
Leaf inclination distribution function a[(b)] [-1, +1]	**LIDF a**	**-0.30**	**-0.45**	**0.10**	**0.02**	**Optimized**

SLC inputs		**Day 1 - 8.00**	**Day 1 - 20.00**	**Day 14 - 8.00**	**Day 14 - 20.00**	**Source**
Canopy (continuation)						
Leaf inclination distribution function b[(c)] [-1, +1]	LIDF b	-0.15	-0.15	-0.15	-0.15	SLC default
Hot spot effect parameter[(d)]	hot	0.05	0.05	0.05	0.05	SLC default
Fraction brown PAI [0,1]	fb	0.21	0.21	0.24	0.24	Optimized
Dissociation factor [0,1]	D	0.8	0.8	0.8	0.8	SLC default
Vertical crown coverage [0,1]	Cv%	100	100	100	100	From experiment
Tree shape factor[(e)]	zeta	0.5	0.5	0.5	0.5	From experiment
Solar zenith angle (degrees)	sza	30	30	30	30	From experiment
Viewing zenith angle (degrees)	vza	0	0	0	0	From experiment
Sun-view azimuth difference (degrees)	azi	0	0	0	0	From experiment
Soil						
Soil background		Measured values	Measured values	Measured values	Measured values	Lab. measurement

[(a)] PAI = LAI+BAI. PAI and fb change because LAI change
[(b)] Leaf slope indicator
[(c)] Bimodality parameter
[(d)] Estimated as the ratio of the average leaf width and the canopy height
[(e)] Diameter/height

2.2.8. Sensitivity of remote sensing features for assessing water stress

For the sensitivity analysis a total of 528 simulations were carried out by varying the equivalent water thickness (EWT), leaf area index (LAI) and the parameter *a* (slope parameter) of the leaf inclination distribution function (LIDF) as shown in Table 2.3. The whole range of observed water stress conditions was simulated. LAI values ranging from 0 to 2 were used for the simulations considering LAI measurements made by the authors in the field.

Table 2.3. Soil-Leaf-Canopy (SLC) parameter range and intervals used for simulations

SLC Parameters	Min	Max	Step	# values
Cw_{green}	0.005	0.03	0.005	6
LAI	0	2	0.20	11
LIDFa	-0.50	0.20	0.10	8

Using this simulated dataset, the relationship between the RS features and CWC or LAI was analysed by using the best-fit functions. CWC was calculated as follow:

$$CWC = EWT \times LAI \quad (2)$$

In order to compare the different RS features, which present different scales and dynamic ranges, the absolute value of the Noise Equivalent (NE) ΔCWC and NEΔLAI were used (Viña and Gitelson 2005).

$$NE\Delta CWC = \frac{RMSE\ \{RSfeature\ vs\ CWC\}}{Abs\left\{\frac{\partial(RSfeature)}{\partial(CWC)}\right\}} \quad (3)$$

$$NE\Delta LAI = \frac{RMSE\{RSfeature\ vs\ LAI\}}{Abs\left\{\frac{\partial(RSfeature)}{\partial(LAI)}\right\}} \quad (4)$$

Where RMSE is the root mean squared error of the best-fit function of the relationship between the RS feature and LAI or CWC, respectively, and $\partial(RSfeature)/\partial(CWC)$ and $\partial(RSfeature)/\partial(LAI)$ are the corresponding first derivatives of the best-fit functions. Small values for NEΔCWC and NEΔLAI indicate strong sensitivity for CWC and LAI, respectively.

2.3. Results

2.3.1. Physiological response of Tamarugo plants under water stress

The results of the physiological sampling in terms of equivalent water thickness, leaf chlorophyll and leaf carotenoid concentration are depicted in Figure 2.3.

No evident symptoms of stress were observed in the leaf samples until day 11 when the EWT started to drop from values of 0.025 g/cm^2 down to values of 0.005 g/cm^2 on day 15 (Figure 2.3a). Average EWT during the first ten days was 0.023 g/cm^2. There was not a clear trend in the observed values of leaf chlorophyll concentration and carotenoid concentration. During the experiment, it was observed that the plants were gradually drying some leaves while keeping the remaining leaves healthy. From day 10 onwards the amount of dry leaves increased rapidly. However, due to the absence of natural disturbances (like wind) most of the dry leaves remained on the twigs. At day 15 there were few remaining green leaves.

Average values of leaf chlorophyll concentrations for the whole period were 15.9 µg/cm^2 for chlorophyll *a*, 26.0 µg/cm^2 for chlorophyll *b* and 42 µg/cm^2 for total chlorophyll. Leaf carotenoid concentration was rather constant with an average value of 1529 µg/cm^2.

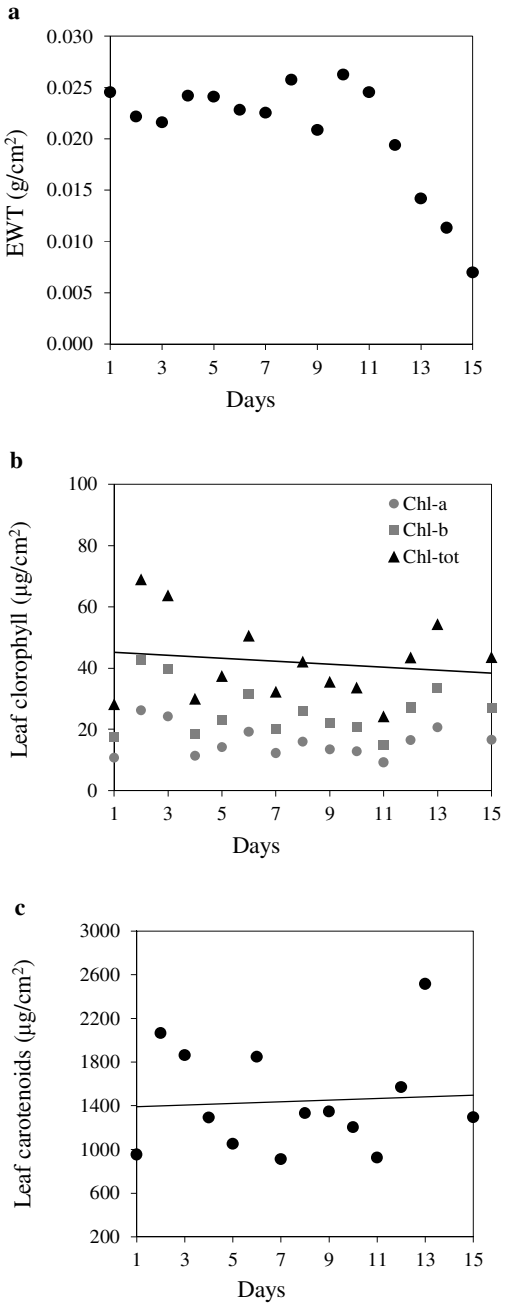

Figure 2.3. Physiological parameters measured during the experiment. **(a)** Equivalent water thickness, **(b)** leaf chlorophyll concentration, and **(c)** leaf carotenoids concentration.

2.3.2. Spectral response of Tamarugo plants under water stress

2.3.2.1. Changes in diurnal reflectance

In the absence of water stress, it was observed that plants modified the incidence angle of light on the leaves by changing the orientation of the folioles (Figure 2.4). As a matter of fact, the orientation of the folioles changed towards a more erectophile leaf distribution (parallel to incoming light rays) after midday. This means leaves avoided to face direct irradiation past noon.

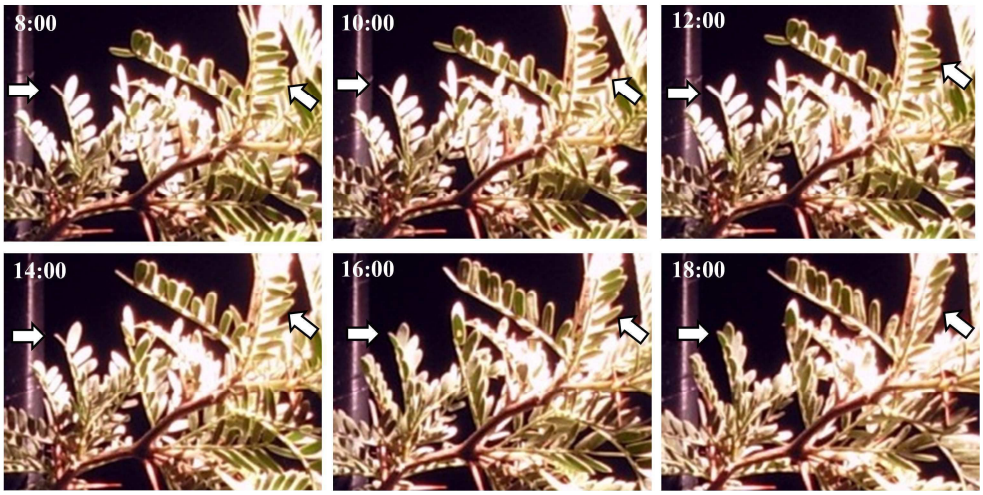

Figure 2.4. Folioles orientation changing throughout day 1.

Consequently, reflectance decreased from midday onwards (Figure 2.5a). Changes occurred despite the angle of illumination (ASD lamp) was fixed at 30º from nadir. Observations made on Tamarugo leaves suggest the presence of a pulvinus, a thickening in the leaf base, which often is the structure responsible for leaf movements (Figure 2.1c). Pulvinar movements have been described for other species with composed leaves (Barchuk and Valiente-Banuet 2006; Ezcurra et al. 1992; Liu et al. 2007) and they are associated with contraction-expansion mechanisms driven by cell turgor changes (Taiz and Zeiger 2010). Therefore, Tamarugo leaf movement can be affected by water stress. Under water stress, leaf cells may have run out of water and, as a consequence, folioles were less able to change the leaf angle. Hence, reflection became more constant throughout the day and the difference between morning and afternoon became smaller (Figures 2.5b-c). The ability of Tamarugo plants to adjust the leaf angle is a good example of

how some adaptations of desert species can influence reflectance properties. For this reason, remote sensing approaches should take into account the biology of arid species to accurately assess the water condition of vegetation in arid environments. More insight is needed to understand the influence of leaf movement of the Tamarugo plant on canopy reflectance under natural conditions, where the incoming solar irradiation is changing (position and intensity) throughout the day. This will be subject for further research.

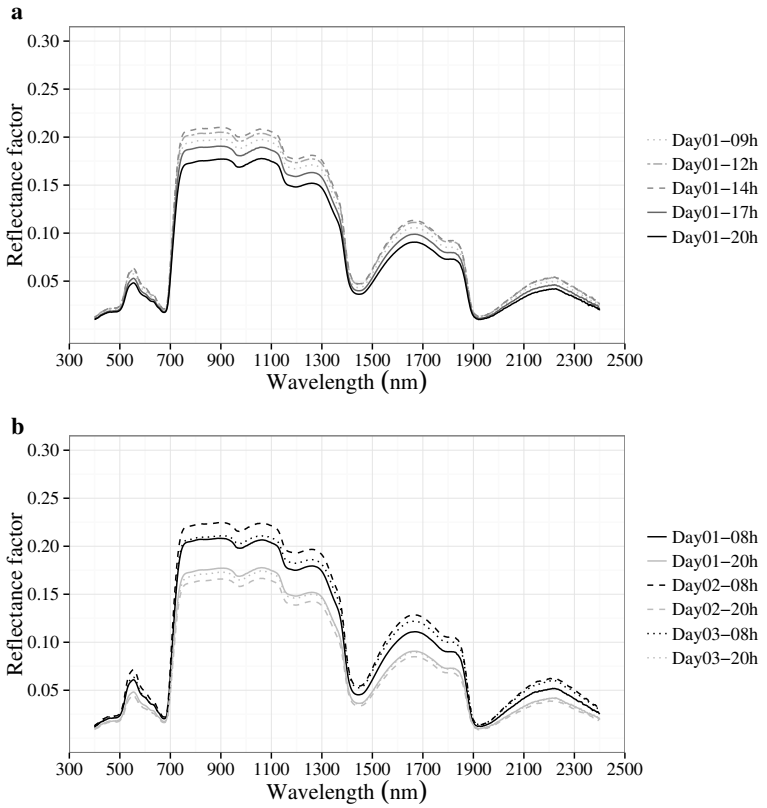

Figure 2.5. Canopy spectral reflectance measured under laboratory conditions. **(a)** Diurnal changes from 9:00 till 20:00 hours of day 1, **(b)** morning - evening differences for days 1 to 3 (no water stress), **(c)** morning - evening differences for days 12-14 (under water stress), and **(d)** Changes due to defoliation**.**

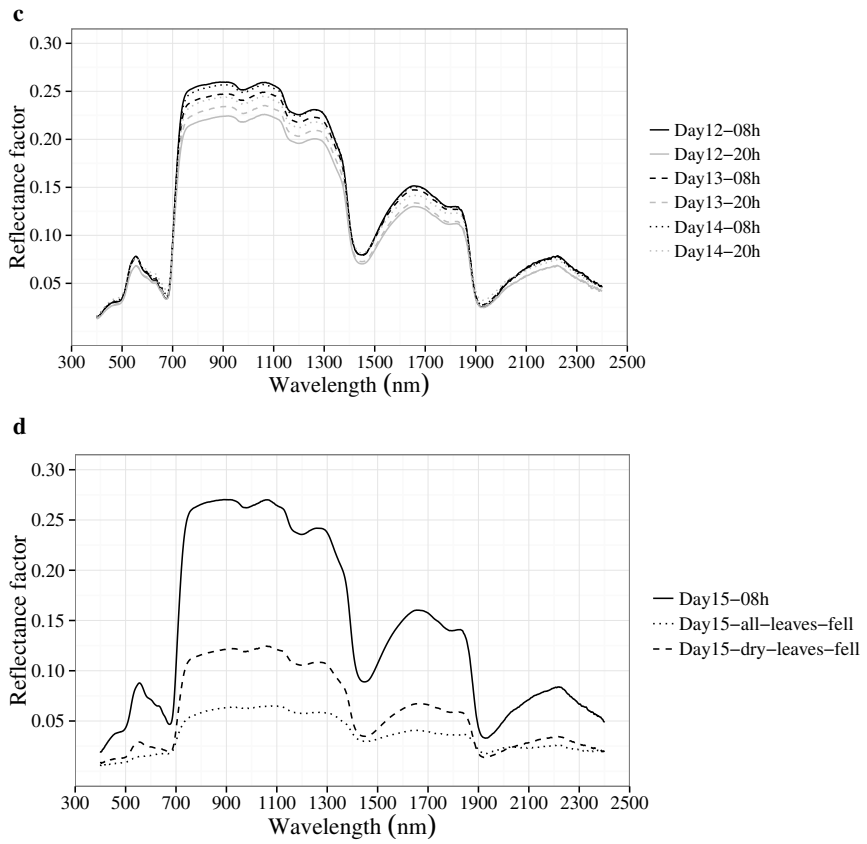

Figure 2.5 (cont.). Canopy spectral reflectance measured under laboratory conditions. **(a)** Diurnal changes from 9:00 till 20:00 hours of day 1, **(b)** morning - evening differences for days 1 to 3 (no water stress), **(c)** morning - evening differences for days 12-14 (under water stress), and **(d)** changes due to defoliation**.**

2.3.2.2. Reflectance changes over the experimental period

Besides the morning-evening changes in spectral reflectance, more changes can be observed when comparing the spectra of days 1 to 3 (Figure 2.5b, no stress) with, e.g., days 12 to 14 (Figure 2.5c, under stress). Reflectance over the infrared region increased as a consequence of the dehydration process. This is due to the larger number of cell wall – air interfaces within the leaf tissue, caused by the absence of water, which produces an increment of internal multiple reflections of NIR radiation (Carter 1991; Knipling 1970).

Furthermore, the water absorption at 1400 and 1900 nm decreased, which is a clear indication of the dehydration process (Carter 1991; Hunt Jr and Rock 1989). The water absorption features at 970 and 1200 nm were too small for visual inspection and for this reason continual removal was applied to quantitatively study changes due to water stress (Section 2.3.3).

Despite senescence, leaves hardly fell during the experiment because within the climate chamber there were no natural disturbances such as wind and decrease in LAI was limited. After measuring spectral and physiological variables on day 15 at 8:00 hours, plants were shaken and dry leaves immediately fell down. Then the spectral reflectance was measured. Subsequently, all green leaves were cut off and the spectral signature was measured again. This way the effects of losing dry and green leaves on spectral reflectance were registered as shown in Figure 2.5d.

2.3.3. Chlorophyll and water absorption features

The continuum removal analysis carried out for the *chlorophyll absorption feature* showed that both MBD and AUC were progressively decreasing over the days (Figure 2.6a-b), while the ratio MBD/AUC was slightly increasing in time (Figure 2.6c). These results differ from the chlorophyll measurements for single leaves (Figure 2.3), which showed slight differences of chlorophyll concentration over time. Therefore, it can be inferred that changes in the chlorophyll absorption feature are due to LAI decrease rather than degradation or relocation of leaf chlorophyll. This is in line with the SLC simulations performed and described in section 2.3.4. The fact that the MBD decreased in time suggests that ratio vegetation indices using the NIR spectral region (760-900 nm) and the Red (630-690 nm) or the NIR and the Red-edge region (680-750 nm) can be used for assessing water stress in terms of LAI loss. MBD, AUC and MBD/AUC also can be used for estimating changes in LAI.

Water absorption features of healthy Tamarugo plants occurred at 973 nm and 1165 nm. MBD, AUC and MBD/AUC of both absorption features decreased over the days, showing a linear trend (Figure 2.6). This differs from the trend observed for EWT measurements for single leaves (Figure 2.3a), where the effects of water stress were observed from day 11 onwards, and could be explained by the fact that the ASD instrument is measuring a surface of stacked leaves rather than single leaves. Therefore, the measured spectral signature is an integrative measure of the water status of the complete canopy within the ASD IFOV. For this reason, the

variable canopy water content (CWC) defined as the product between LAI and EWT is often used in vegetation studies.

These results suggest that ratio vegetation indices using the spectral regions where the water absorption features occur, such as WI and NDWI, can be used for estimating changes in CWC (Table 2.1). Another interesting feature is the change on the right slope of the absorption feature at 973 nm, which recently has been proposed and tested as a good indicator of canopy water content (Clevers et al. 2008, 2010).

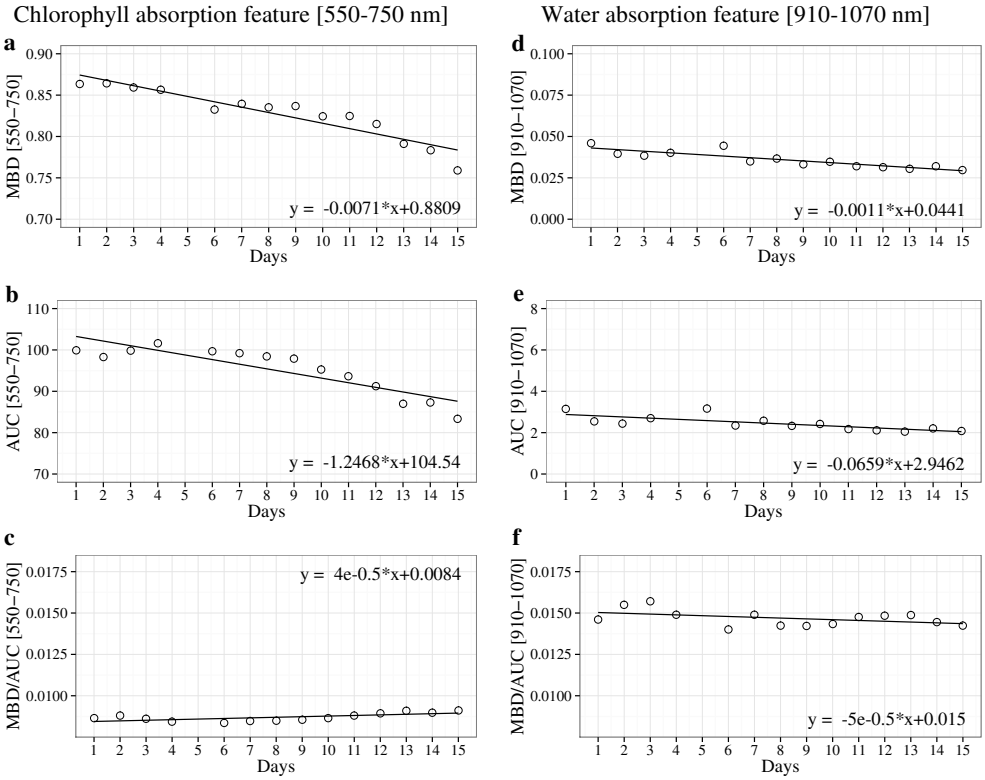

Figure 2.6. Evolution of the chlorophyll [550-750 nm] and water absorption features [910-1070 nm], [1100-1280 nm] during the experimental period. Absorption features are shown in terms of maximum band depth (MBD), area under the curve (AUC) and the ratio MBD/AUC.

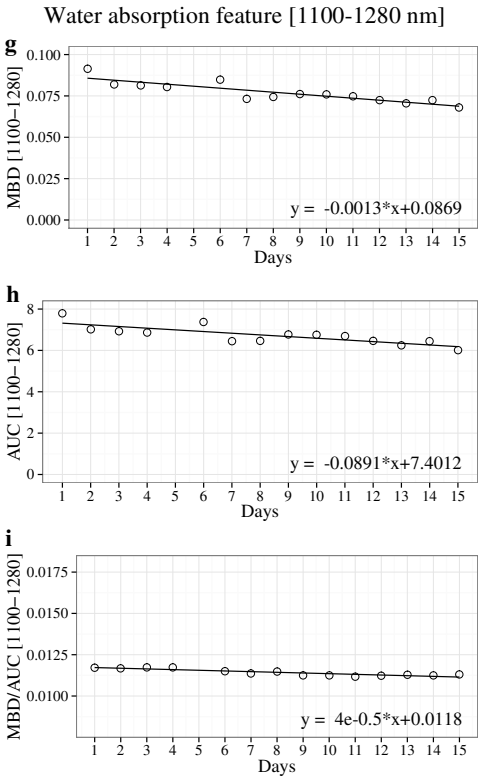

Figure 2.6 (cont.). Evolution of the chlorophyll [550-750 nm] and water absorption features [910-1070 nm], [1100-1280 nm] during the experimental period. Absorption features are shown in terms of maximum band depth (MBD), area under the curve (AUC) and the ratio MBD/AUC.

2.3.4. SLC calibration and simulations

The calibration of the SLC model was performed using the spectral values measured on day 1 at 8:00 hours and physiological values measured during the experiment. The correspondence between simulated and measured spectra was good over the full spectral range (Figure 2.7a) with an RMSE of 0.006 when comparing simulated and measured spectral reflectance.

Subsequently, the slope parameter of the leaf angle distribution function (LIDF*a*) was optimized to fit the measured spectrum at 20:00 hrs. This parameter controls the average leaf slope and ranges from -1 to 1 (Verhoef and Bach 2007). Values of LIDF*a* close to 1 correspond to a planophile distribution, values close to 0 to a

uniform (random) distribution and values close to -1 to an erectophile distribution (Verhoef and Bach 2007). Results of the optimization procedure showed that the LIDF*a* parameter by itself explained the changes in reflectance observed during the day (Figure 2.7a). Matching simulated reflectance curves were obtained by varying the LIDF*a* parameter from -0.30 at 8:00 hours to -0.45 at 20:00 hours. So, changing this parameter towards more negative values is reproducing the leaf movement observed during the experiment: leaves changing towards a more erectophile leaf distribution after midday (Figure 2.4).

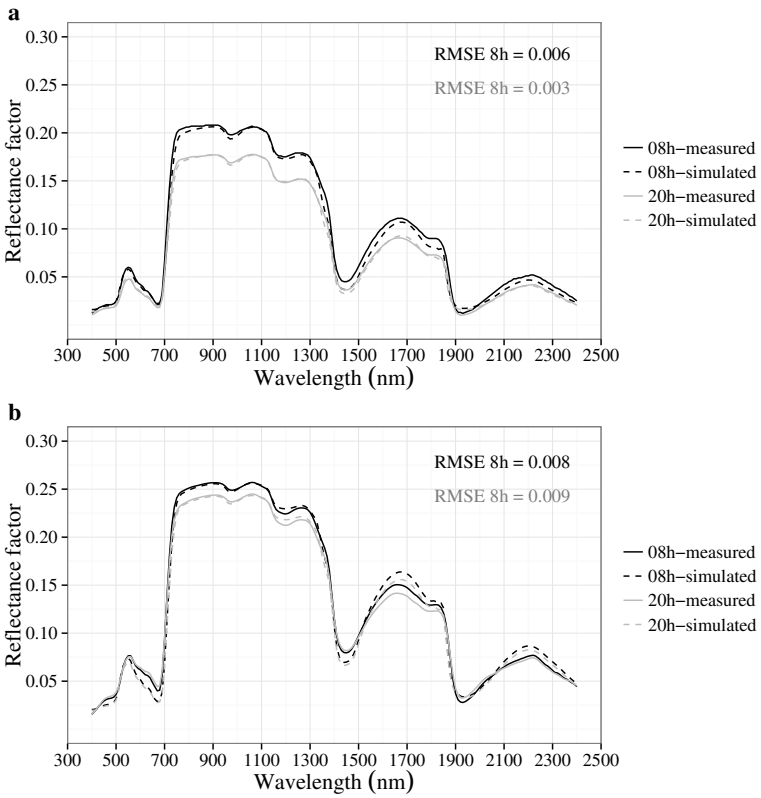

Figure 2.7. Canopy spectral reflectance of **(a)** day 1 (no water stress) and **(b)** day 14 (under water stress). Continuous lines correspond to ASD measurements and dashed lines to SLC simulations.

The SLC parameters LAI and LIDF*a* were then tuned to fit the measured reflectance spectrum of day 14 when the plants were under water stress (measured EWT value of 0.013 was used, see Table 2.2). Correspondence between simulated

and measured spectra was good (Figure 2.7b) with an RMSE of 0.008 for the spectral reflectance at 8:00 hours and 0.009 for the spectral reflectance at 20:00 hours. Once again, reflectance changes between morning and evening on day 14 were explained by the LIDF*a* parameter, while changes from day 1 to 14 were explained mainly by decreasing LAI and EWT (Table 2.2, bold values). This time LIDF*a* values for both morning and evening were close to zero (0.10 and 0.02), which corresponds to a more uniform distribution, resembling a canopy where leaf slope is randomly distributed. This change in LIDF can be interpreted as an effect of water stress on the pulvinar movement of Tamarugo plants, and consequently, on their ability to move the leaves over the day.

2.3.5. Evaluation of remote sensing features for assessing water stress

2.3.5.1. Remote sensing features for detecting changes in canopy water content

Figure 2.8 summarizes the relationship between nine remote sensing features analysed and canopy water content (CWC). The analysis showed an asymptotic relationship for all ratio RS features, i.e. WI, NDWI, MBD/AUC[910-1070] and MBD/AUC[1100-1280], which means they become less sensitive for high values of CWC. The derivative[1015-1050], MBD and AUC for both [910-1070 nm] and [1015-1050 nm] water absorption features showed a linear relationship, but different scatter around the fitted line. The derivative[1015-1050] showed the largest scatter, which is increasing concurrently with CWC values. Daily changes of leaf slope (LIDF*a*) observed for Tamarugo plants (Figure 2.4) induced changes in the right slope of the water absorption feature at 970 nm affecting the prediction capability of this RS feature.

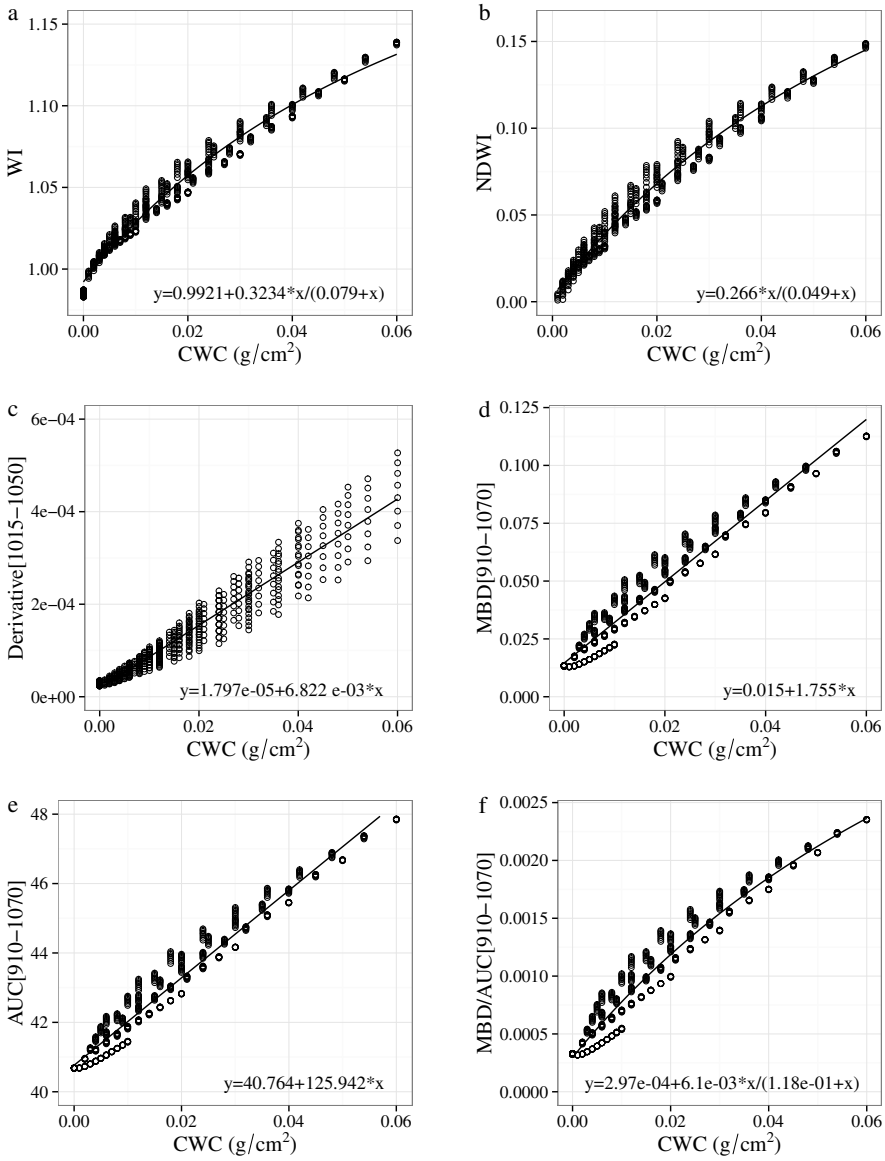

Figure 2.8. Relationship between different remote sensing features and canopy water content (CWC). Lines correspond to the best fit functions.

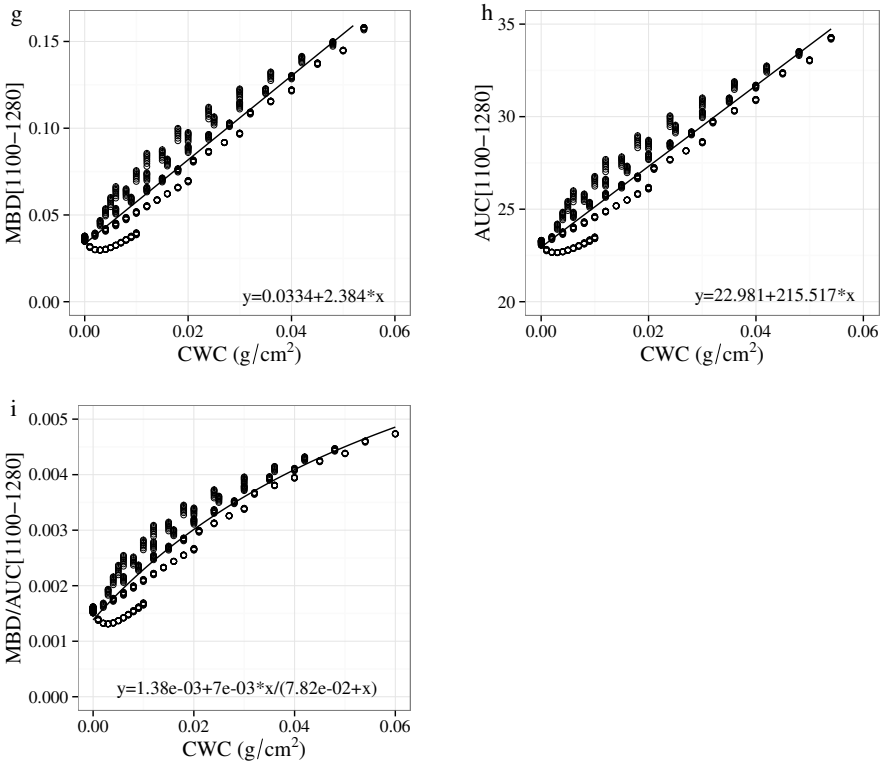

Figure 2.8 (cont.). Relationship between different remote sensing features and canopy water content (CWC). Lines correspond to the best fit functions.

A comparison of the tested RS features for estimating changes in CWC was performed by means of the NEΔCWC (Equation 3). Low values of NEΔCWC indicate high sensitivity to changes in CWC. The sensitivity analysis (Figure 2.9) showed that most of the indices lose sensitivity when CWC increases, especially the MBD/AUC[1100-1280]. The most sensitive RS feature for detecting changes in CWC was the WI for the CWC range from 0.01 to 0.036 g/cm^2. For estimating CWC values larger than 0.036 g/cm^2 the AUC[910-1070] was the most sensitive feature while for values lower than 0.01 the NDWI was the most sensitive.

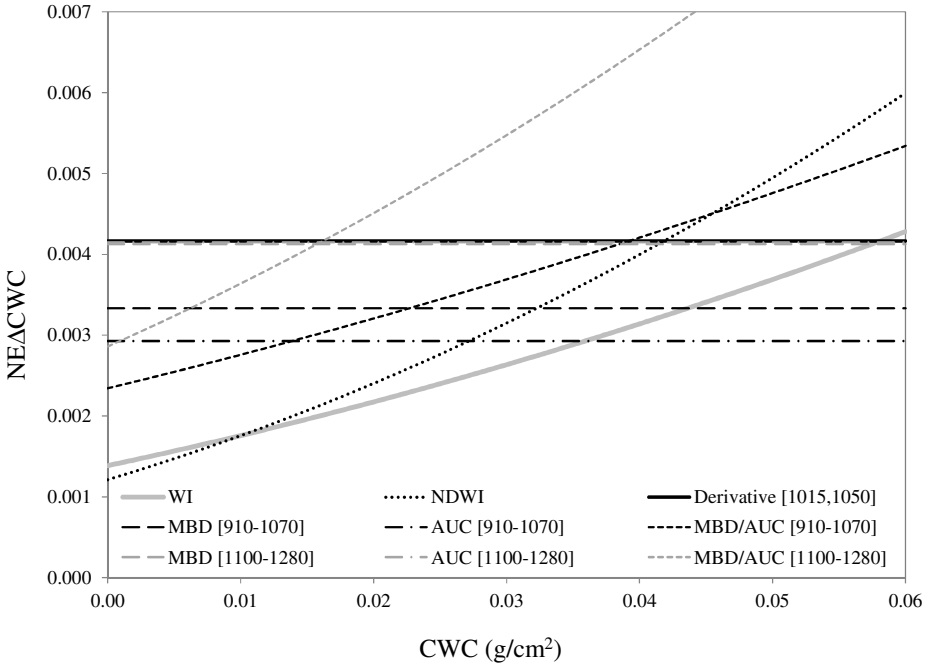

Figure 2.9. Sensitivity analysis of different remote sensing features for detecting water stress in terms of changes in canopy water content (ΔCWC). The sensitivity analysis was performed using the NEΔCWC (Eq. 3). Low values indicate high sensitivity to changes in CWC.

2.3.5.2. Remote sensing features for detecting changes in leaf area index

Figure 2.10 summarizes the relationship between six remote sensing features analysed and leaf area index (LAI). The indices NDVI, Red-edge NDVI as well as the MBD[550-750] and AUC[550-750] showed an asymptotic relationship with LAI with high sensitivities for LAI values less than 1. In the case of RVI the relationship was linear; however, it exhibited increasing scatter for high LAI values. This can be explained by the error introduced by varying the LIDF*a* parameter in the SLC simulation, which is simulating the observed changes in the leaf slope. $CI_{red\text{-}edge}$ showed a relationship with LAI close to linear showing a high sensitivity to changes in LAI for the whole range.

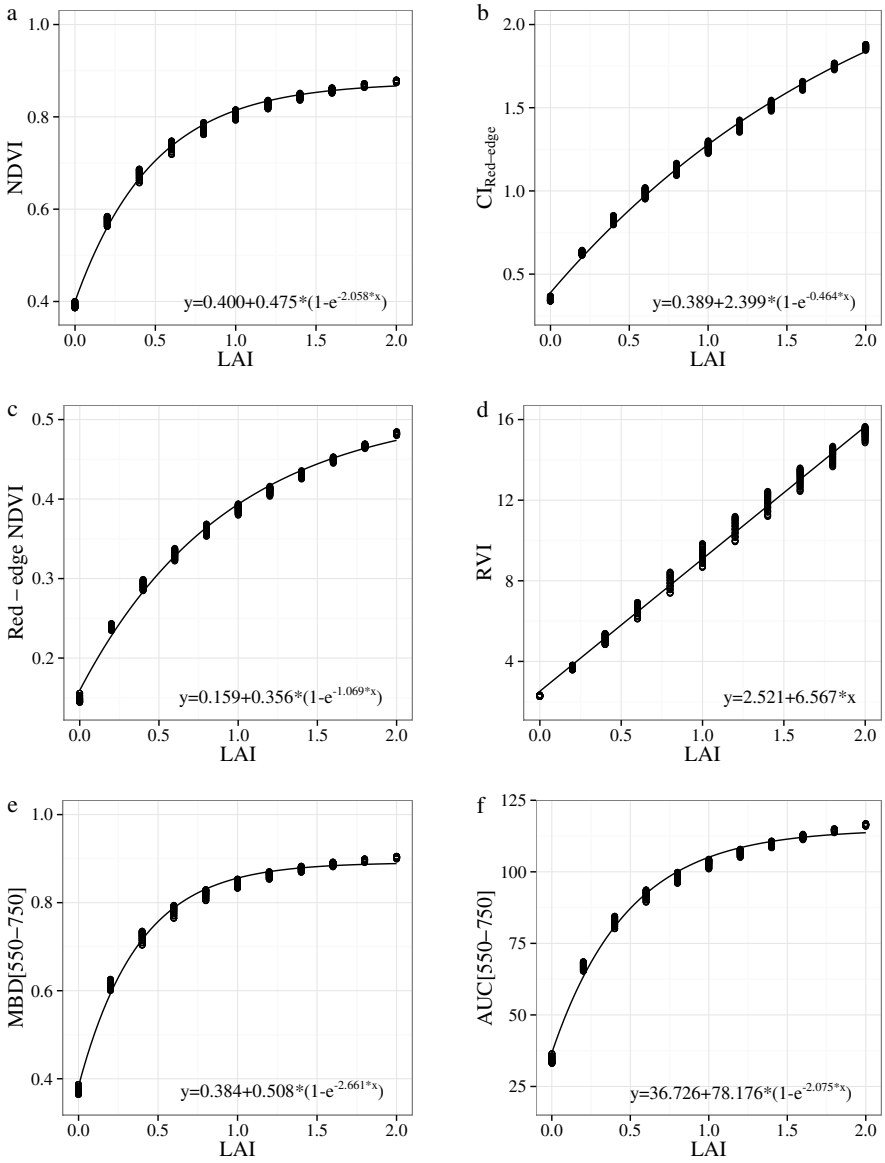

Figure 2.10. Relationship between different remote sensing features and LAI. Lines correspond to the best fit functions.

Finally, a multiple comparison of all RS features is presented in Figure 2.11 by means of the NEΔLAI. Except for the Ratio Vegetation Index (RVI), all the tested RS features were very sensitive (low NEΔLAI values) to changes in LAI in the

range from 0 to 0.5. From this value onwards, the sensitivity of MBD[550-750], AUC[550-750] and NDVI decreased exponentially. The sensitivity of the RVI was constant over the whole LAI range, constituting a good predictor for LAI in the range from 1 to 2 and the most sensitive for values >1.6. Overall, the most sensitive RS feature considering the whole range of LAI values was the $CI_{red\text{-}edge}$.

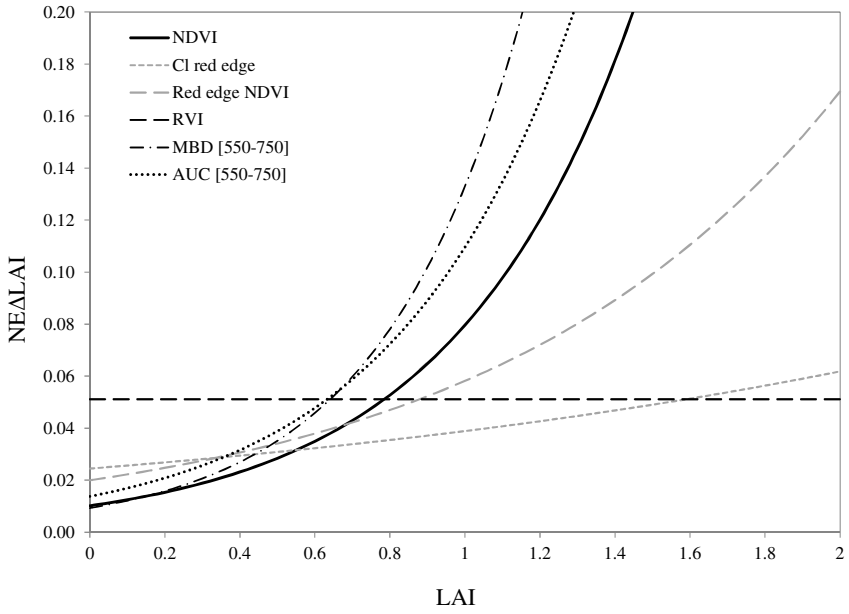

Figure 2.11. Sensitivity analysis of different remote sensing features for detecting water stress in terms of changes in LAI. The sensitivity analysis was performed using the NEΔLAI (Eq. 4). Low values indicate high sensitivity to changes in LAI.

2.4. Discussion and conclusions

This experiment showed that Tamarugo plants are able to adjust the leaf slope to avoid direct irradiation past noon, an adaptation which has an important effect on the spectral reflectance over the whole 400-2500 nm range. This leaf movement, technically known as heliotropism or sun tracking (Raven et al. 2005), is most likely controlled by a pulvinar structure present on the folioles base of Tamarugo plants (Figure 2.1-c) and it is known as a common ability of the Leguminosae plants to avoid photoinhibition (Liu et al. 2007; Pastenes et al. 2005; Pastenes et al.

2004). Measurements done with an ASD spectroradiometer showed that daily canopy reflectance, under the non-stress scenario, decreased from midday onwards as a consequence of this leaf movement. This is likely to be a process controlled by changes in cell turgor of the pulvinus and therefore can be affected by water stress. Under water stress, leaves dehydrated and consequently folioles were not able to change the incidence angle of light on their leaves anymore. Therefore, reflection during the day became more constant and the difference between morning and afternoon smaller. From day 11 onwards, plants responded to water stress by drying out some leaves while keeping the remaining leaves green. When this occurred, dry leaves have a bigger chance to fall down (dehiscent). As a consequence of the resulting loss in water content, spectral reflectance increased over the whole spectrum and the chlorophyll absorption feature at 670 nm as well as the water absorption features at 970 nm and 1200 nm decreased.

Changes in reflectance during the day as well as changes along the experimental period were successfully modelled by using the SLC model. Simulations using SLC showed that changes in canopy reflectance due to water stress were mostly explained by leaf area index (LAI), leaf slope (LIDF*a*) and equivalent water thickness (EWT). We conclude that suitable target variables for remote sensing based assessment of water stress are LAI and canopy water content (CWC), which is defined as EWT*LAI.

Once calibrated, we used the SLC model to analyse the sensitivity of different indices and spectral absorption features to detect water stress in Tamarugo, six for detecting changes in LAI (ΔLAI) and nine for detecting changes in canopy water content (ΔCWC). The sensitivity analysis showed that the Water Index was the most sensitive RS feature to ΔCWC for low values of CWC (<0.036 g/cm^2), but its sensitivity decreased towards higher CWC values. From 0.036 g/cm^2 onwards AUC[910-1070] was the most sensitive. Derivative[1015,1050] was the most influenced RS feature by changes in LIDF*a*, presenting an increasing scatter around the fitted curve for high values of CWC. RS features for detecting changes in LAI were generally asymptotic, showing a decreasing sensitivity to ΔLAI for LAI values higher than 1. The RVI showed a linear relationship with LAI, but also the highest sensitivity to changes in leaf slope. Considering the whole range of LAI, the $CI_{Red\text{-}edge}$ performed the best, which is in agreement with results obtained by Herman et al. (2011) in wheat and Viña et al. (2011) in maize and soybean.

This study proved that the adaptation of Tamarugo to adjust the incidence angle for light by leaf movement can influence the results of RS based assessments. The diurnal patterns of leaf movement must be taken into consideration when using remote sensing tools for water stress assessments of this species.

Remote sensing approaches for detecting CWC changes in Tamarugo trees are limited to the hyperspectral domain, since narrow bands are needed to calculate most of the spectral features and indices proposed in literature and tested in this study. Such data can be obtained from satellite sensors like Hyperion, and airborne sensors like AVIRIS and HyMap, which are hardly ever available for this geographic area. The exception is the NDWI which can be calculated using the broad bands of the MODIS sensor at 860 and 1240 nm. However, the spatial resolution of these bands are very low (500 meters), making an assessments at tree level impossible.

The new generation of very high spatial resolution (VHSR) satellites seems to be very promising for detecting LAI changes in single Tamarugo trees, since they include a red-edge band at 2 meters pixel resolution (WorldView2) or less (1.2 meters pixel resolution for the WorldView3 satellite, expected to be launched in 2014), allowing the calculation of red-edge based vegetation indices. The WorldView3 sensor is expected to deliver also 8 bands in the SWIR region at 3.7 meters pixel resolution (1195-2365 nm), opening new perspectives for canopy water estimations.

Nevertheless, due to the high cost of VHSR imagery, sensors with moderate spatial resolution like Landsat (30 meters) and low spatial resolution like MODIS (250/500 meters) are also a good alternative and indices like NDVI and RVI can be used considering the above mentioned limitations and scale constraints. These sensors are also interesting since they provide a long and consistent time series of images to study temporal dynamics and trends of vegetation. A key issue for assessing arid vegetation using moderate to low spatial resolution imagery is to estimate the spectral contribution of non-photosynthetic material and bare soil to the mixed pixel, since foliar spectral properties of desert plants seem to be very stable along environmental gradients (Asner et al. 2000). Therefore, species like Tamarugo would resolve water scarcity via controlling biomass production rather than adjusting foliar properties, thus the green canopy fraction would be a good water stress indicator at the stand level. This would be matter for further research.

Acknowledgements

This work has been supported by CONICYT-Chile and Wageningen University. The authors would like to thank CONAF-Chile for the donation of plants for the experiment; to P. Silva, C. Pastenes and U. Arriagada (Universidad de Chile); S. Estay and E. Gayó (PUC); N. Gutiérrez (CONAF); C. Chávez and C. Baeza for providing logistical support and equipment; and to V. Laurent (WUR) for advising on the SLC simulations.

Chapter

3

Assessing water stress of desert Tamarugo trees using in situ data and very high spatial resolution remote sensing

R. O. Chávez, J. G. P. W. Clevers, M. Herold, E. Acevedo and M. Ortiz

Published in Remote Sensing, Volume 5, October 2013, Pages 5064-5088

The hyper-arid Atacama Desert is one of the most extreme environments for life and only few species have evolved to survive its aridness. One such species is the tree *Prosopis tamarugo* Phil. Because Tamarugo completely depends on groundwater, it is being threatened by the high water demand from the Chilean mining industry and the human consumption. In this paper, we identified the most important biophysical variables to assess the water status of Tamarugo trees and tested the potential of WorldView2 satellite images to retrieve these variables. We propose green canopy fraction (GCF) and green drip line leaf area index ($DLLAI_{green}$) as best variables and a value of 0.25 GCF as a critical threshold for Tamarugo survival. Using the WorldView2 spectral bands and an object-based image analysis, we showed that the NDVI and the Red-edge Chlorophyll Index ($CI_{Red\text{-}edge}$) have good potential to retrieve GCF and $DLLAI_{green}$. The NDVI performed best for $DLLAI_{green}$ (RMSE = 0.4) while the $CI_{Red\text{-}edge}$ was best for GCF (RMSE = 0.1). However, both indices were affected by Tamarugo leaf movements (leaves avoid facing direct solar radiation at the hottest time of the day). Thus, monitoring systems based on these indices should consider the time of the day and the season of the year at which the satellite images are acquired.

Keywords: arid ecosystems; water stress; groundwater depletion; LAI; green canopy fraction; satellite images; vegetation indices; pulvinar movement

3.1. Introduction

The conservation of arid vegetation is difficult to address by managers and policy makers since vegetation dots (trees and shrubs) or patches (small grasslands or limited groups of shrubs and trees) are frequently immersed into a large matrix of bare land. Therefore, its identification and assessment is costly and hard to implement. Furthermore, these dots are always closely related to the few water sources that are also required by industry and human consumption (Ezcurra 2006). This dependency makes arid plant species susceptible to water stress although they are well adapted to survive water scarcity. Even the most resistant plant has limits, and thresholds for environmentally safe operations need to be determined in order to preserve the vegetation in deserts.

The new generation of very high spatial resolution (VHSR) satellites, starting with IKONOS in 1999 and followed by QuickBird2 in 2001, GeoEye1 in 2008 and WorldView2 in 2009, has become a real option to approach the problem of assessing the water condition of desert vegetation. Satellite images from these sensors allow identification of small dots such as individual trees, shrubs or small grass patches (Blaschke 2010). Since vegetation structure and composition of most arid regions is rather simple, the identification of vegetation objects using high spatial resolution remote sensing has been carried out successfully (Gibbes et al. 2010; Laliberte et al. 2004). Nevertheless, the estimation of biophysical properties such as canopy water content, chlorophyll content or leaf area index for small vegetation objects has not been sufficiently studied yet due to the limited spectral information of VHSR satellites (Asner et al. 2000; Borzuchowski and Schulz 2010). These sensors typically have only three bands in the visible region and one band in the near infra-red region (IKONOS, QuickBird2 and Geo-Eye). This spectral constraint has changed since 2009, when the WorldView2 satellite was launched, providing VHSR images with six bands in the visible region and two bands in the near infra-red region. In the near future (2014), the WorldView3 will provide images with the same eight bands of WorldView2 plus eight additional bands in the short-wave-infra-red region, opening new opportunities for the retrieval of biophysical properties of small desert features (Chávez et al. 2013b).

Besides spatial and spectral constraints, the assessment of arid vegetation has also temporal constraints. Desert species have developed different adaptations to cope with water scarcity and these adaptations can affect remote sensing based retrievals of biophysical parameters. A good example is the Tamarugo tree in the Atacama Desert (Northern Chile), which adjusts the leaf angle to avoid facing direct solar radiation at the hottest time of the day (midday) (Chávez et al. 2013b). These leaf movements, known as pulvinar movements, are controlled by changes in cellular turgor pressure of a structure located in the base of the leaves and folioles (the pulvinus) (Taiz and Zeiger 2010), and they can have an important impact on canopy spectral reflectance (Chávez et al. 2013b; Moran et al. 1989; Taiz and Zeiger 2010). Furthermore, in a previous study we analyzed the effects of water stress on Tamarugo plants under laboratory conditions by measuring a set of biophysical variables as well as the spectral reflectance response (Chávez et al. 2013b). Using a modeling approach (SLC radiative transfer model (Verhoef and Bach 2007)), we found that the indices to retrieve canopy water content were more affected by leaf movements than those used to retrieve leaf area index (LAI). Good estimators of LAI were the Red-Edge Chlorophyll Index and the NDVI. However, our previous study (Chávez et al. 2013b) was conducted under laboratory conditions and no research has been carried out to test these vegetation indices under field conditions, where the solar angle and intensity are changing during the day.

In this paper, we measured and analyzed a complete dataset of biophysical and structural variables of Tamarugo trees as well as their canopy spectral reflectance response under different field conditions and water stress scenarios. Furthermore, we studied the suitability of using an up-to-date VHSR satellite image (WorldView2) to retrieve biophysical parameters of single Tamarugo trees, considering the spatial, spectral and temporal constraints previously discussed. Water condition assessment of the Tamarugo forest is urgently needed since this endemic species is currently threatened by groundwater extraction (Rojas and Dassargues 2007; Romero et al. 2012). The Tamarugo forest is practically the only ecosystem of the Absolute Desert eco-region in Northern Chile (CONAMA 2008; Gajardo 1994). It sustains a biodiversity of about 10 plant species and 30 animal species (CONAF 1997), some of which are endemic for the Atacama Desert (e.g., the bird C. tamarugense (Estades 1996) and the reptile M. theresioides (Ramírez-Leyton and Pincheira-Donoso 2005)). The Pampa del Tamarugal (local name of

the Tamarugo forest) is distributed into two hydrological systems: Pampa del Tamarugal basin and Llamara basin (Figure 3.1). The most important one is the Pampa del Tamarugal basin, comprising all the plantations at the Zapiga, Pintados and Bellavista salt flats, and one small sector with natural forest (Pintados), all of which have been officially protected since 1987, and which constitute the Pampa del Tamarugal National Reserve. The second hydrological system is the Llamara basin, enclosing a well preserved natural forest located at the Llamara salt flat, which is not under official protection.

The Atacama Desert is rich in mineral resources such as copper and lithium and the mining sector is by far the most important one for the Chilean economy. Mining has created a lot of pressure to extract groundwater not only to provide drinking water to workers and the population nearby, but also as input to many industrial processes (Oyarzún and Oyarzún 2011; Romero et al. 2012). Currently the water extraction at the Pampa del Tamarugal basin is twice as large as natural recharges, causing a progressive groundwater depletion (Rojas and Dassargues 2007). The Llamara basin was not exploited until 2006, when the Chilean environmental agencies (DGA and SEIA) authorized water extraction up to a maximum of 120 L/s. A new extraction up to 244 L/s was authorized on October 2011.

Chilean environmental agencies, the academic world and the private sector have extensively debated about how to define groundwater extraction thresholds to preserve the Tamarugo forest. To achieve this, a clear understanding of the relationship between the extraction rates and the water condition of the trees needs to be established. In this paper, we focus on the first part of this relationship, i.e., the assessment of the water condition of the Tamarugo trees. The study of the effects of groundwater depletion (or depth) on the water status of Tamarugo at a large scale (basin) will be matter for further research. Currently, the water condition of Tamarugo trees is assessed using qualitative descriptors and an expert-knowledge approach. Several industrial projects in the area have to report about the Tamarugo forest to continue their operations. For this reason, quantitative and reliable estimations of the Tamarugo forest status are needed for water management and environmental monitoring. In order to provide such estimations, in this paper we aim specifically to:

1. Test the water stress indicators proposed by (Chávez et al. 2013b) for Tamarugo plants under laboratory conditions, namely canopy water

content and leaf area index, on single Tamarugo trees under different field water stress scenarios.

2. Test the vegetation indices proposed by (Chávez et al. 2013b) to assess water condition of single Tamarugo trees by using the spectral bands of WorldView2 images and in situ measurements.
3. Study Tamarugo leaf movements during the day in the field and their implications for remote sensing based estimations of water stress.

3.2. Material and methods

3.2.1. Species description

The genus *Prosopis* belongs to the family Leguminoseae, subfamily Mimosaceae and comprises 44 species (Burkart 1976). As other species of this genus, Tamarugo (*Prosopis tamarugo* Phil.) shows a variety of shapes and sizes, depending on genetics and growing conditions. They can reach up to 25 m height, 2 m stem diameter and 20 m crown diameter (Altamirano 2006; Riedemann et al. 2006). Tamarugos are thorny phreatophytic trees, often multi-stem, with a semi-circular crown and branches reaching the ground (Altamirano 2006). It is a semi-deciduous species with a vegetative period covering the whole year and a peak occurring between September and December (Acevedo et al. 2007; Sudzuki 1985a).

3.2.2. Study area

In this study, we considered two sampling sites and two field campaigns as shown in Table 3.1. In the first campaign (summer 2011), we measured foliar and canopy properties of 32 Tamarugo trees at two sampling sites (Figure 3.1): 16 trees in the natural forest located in the northern part of the Llamara basin and 16 trees in the Pintados plantation near the center of the Pampa del Tamarugal basin. Basins' borders depicted in Figure 3.1 were obtained from (DICTUC 2008)). During the second campaign (summer 2012), we studied Tamarugo leaf movements and their potential effect on the canopy spectral signature and on vegetation indices for three trees in the Llamara site. Details of the two field campaigns are given in Section 3.2.4. A description of the two sampling sites is given as follows.

Table 3.1. Field campaigns and WorldView2 images used in this study.

Field campaign / WorldView2 image	**Variables**	**Sample and location**	**Dates**
Field campaign summer 2011	Hydraulic, biochemical and structural variables	32 trees (16 Llamara, 16 Pintados)	24–28/01/2011
	Canopy spectral reflectance at midday (FieldSpec)	32 trees (16 Llamara, 16 Pintados) × 4 quarters per tree = 128 measurements	24–28/01/2011
Field campaign summer 2012	Diurnal leaf movements and canopy spectral reflectance (FieldSpec)	3 trees (Llamara)	13–15/01/2012
WorldView2 image winter 2011	Top-of-atmosphere (TOA) spectral reflectance	1 scene (Pintados)	13/07/2011
WorldView2 image spring 2011	Top-of-atmosphere (TOA) spectral reflectance	1 scene (Llamara)	25/09/2011

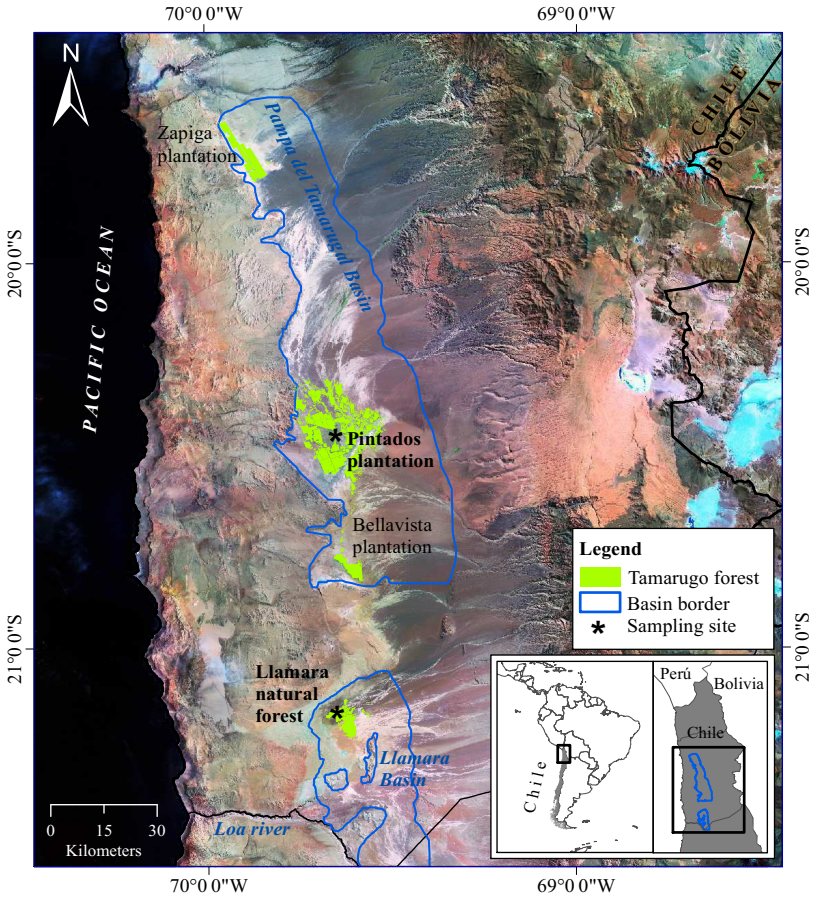

Figure 3.1. Satellite image (Landsat mosaic, USGS) of Pampa del Tamarugal in the Atacama Desert, Chile. Asterisks show the two sampling sites in the Pintados plantation and Llamara natural forest.

3.2.2.1. Llamara site

In the Llamara forest, all trees are native, sparsely distributed (isolated trees or small groups) and at an advanced growing stage (adult or senescent trees) since regeneration is almost absent. A pumping station, operating since 2006, is located at the basin's north border. The tree sampling was performed on a north-south linear transect going from trees close to the pumping station towards the south.

Since trees close to the pumping station were sparse, we selected all the available trees on the transect (eight in total). Towards the south and after a gap with no trees, we selected eight more trees on the transect from an area with more abundant trees. This way we completed a sample along the whole groundwater depletion gradient in the Llamara basin, with trees close to the pumping area facing a depletion of around 6–7 m after five years of pumping whereas trees 1500 m or more away were facing little or null depletion (Figure 3.2). This sample of 16 trees is part of an environmental monitoring system operated in the Llamara basin and its relevance lies in the fact that *in situ* groundwater data are provided on a monthly basis (Geohidrología-SQM 2012). Groundwater and ground level depicted in Figure 3.2 were obtained from Geohidrología-SQM (Geohidrología-SQM 2012).

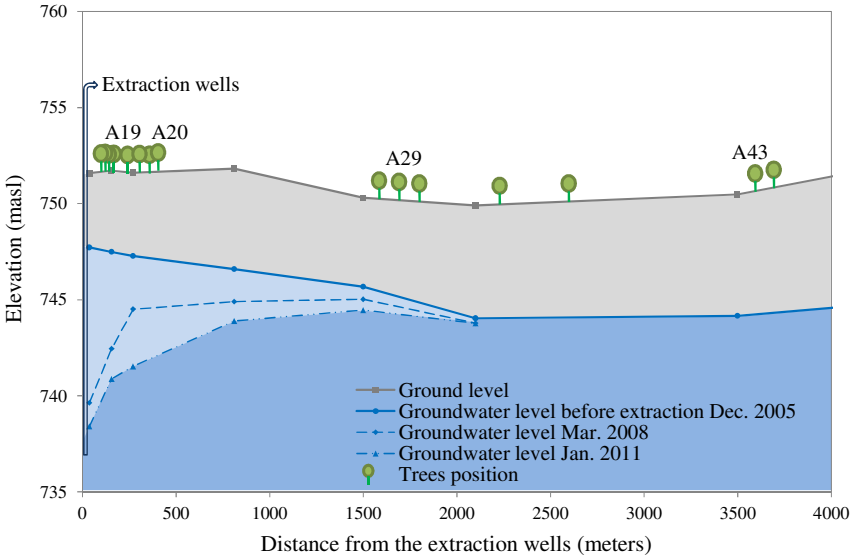

Figure 3.2. Vertical profile showing the distance of the Tamarugo trees from the extraction wells in the Llamara forest and ground water level in 2005 (before extraction), 2008 and 2011. Pictures of representative trees (A19, A20, A29 and A43) are provided in Figure 3.5.

3.2.2.2. Pintados site

The plantation stands in Pintados were established between 1969 and 1973 (CONAF 1997). Monitoring of groundwater depletion started in the 1980s and has currently reached all plantation sectors in the Pampa del Tamarugal basin (Rojas

and Dassargues 2007). At the sampling site, the depth of the groundwater table was about 9 m in 1986 and the total depletion for the period 1986–2006 was estimated at 1.1 m (DICTUC 2008). The sampled trees were selected from contiguous plantation lines in a matrix of 12 × 12 m. Despite having the same groundwater depletion regimen, they visually showed a wide range in tree condition with one tree totally dry and the rest with different levels of water stress. The trees had a similar height (7 m) and about the same age (around 40 years old).

3.2.3. Groundwater depletion scenarios

In this study, we aim to find suitable remote sensing methods to estimate the water condition of Tamarugo trees for a wide range of field situations. To achieve this, we selected trees under different groundwater depletion regimens and origins (natural forest and plantations). We classified the trees as follows:

1. *Null water depletion (Dep1-null):* trees located in the Llamara site at a distance >1500 m from the pumping area (nine trees). Ground water depth was between 5 and 6 m in January 2011 (Figure 3.2).
2. *Short-term intensive water depletion (Dep2-int)*: trees located at the Llamara site at a distance <500 m from the pumping area with depletions of around 6–7 m in five years (seven trees). Ground water depth was between 10 and 12 m in January 2011 (Figure 3.2).
3. *Long-term gradual water depletion (Dep3-grad)*: trees located at the Pintados site with depletions of around 1 meter in 20 years (16 trees). At this site groundwater depth was about 11 m in 2011 according to the records of the closest DGA (Chilean Water Service) monitoring well (about 1 km away from this site).

3.2.4. In situ measurements

In the first field campaign (summer 2011), we studied foliar and canopy variables of Tamarugo trees growing under the three groundwater depletion scenarios (section 3.2.3) and considering three levels of information: (1) hydraulic, to study the actual water supply at the root system (predawn water potential); (2) biochemical, to study effects at leaf level in terms of foliar water loss and pigment degradation; and (3) structural, to study effects at the canopy level in terms of green foliage loss. Details of the procedures and sampling schemes are given in Table 3.2.

For each tree, the crown was divided in four quarters following the cardinal points. Hydraulic and biochemical variables were sampled in green branches, one branch per quarter. Thus, four samples per tree were taken in the case of fully green trees. We measured predawn leaf water potential (closed stomata) using a Scholander chamber (Meyer and Ritchie 1980; Scholander et al. 1965) and collected leaf samples for laboratory determinations of equivalent water thickness (EWT), chlorophyll (a + b) and carotenoids. Chlorophyll and carotenoids were determined spectrophotometrically (Lichtenthaler and Wellburn 1983). Canopy water content (CWC) was calculated as EWT*$DLLAI_{green}$. For more details refer to Table 3.2.

Structural information at the canopy level was quantified by the drip line leaf area index (DLLAI), the green canopy fraction (GCF) and the combination of these two variables. First, a visual estimation of the GCF of each tree was carried out in the field (GCF_{vis}) using five categories: 0.0, 0.01–0.25, 0.25–0.50, 0.50–0.75 and 0.75–1.0. We also performed estimations of GCF from digital pictures (GCF_{pics}) taken from the four cardinal points at a fixed 10 meter distance from the tree. To do this, we developed an object based algorithm using the eCognition software to first segment the digital pictures into small tree-objects, and secondly to classify the tree-objects into brown canopy and green canopy (Figure 3.3b). To classify the segments we used the green ratio and red ratio calculated by rationing the red, green and blue bands of the digital pictures as shown in Table 3.2. Only the two pictures with full solar illumination were considered. Finally, the GCF_{pics} of each tree was obtained from the simple average of the partial results.

DLLAI was measured using a LI-COR LAI-2000 instrument (Figure 3.3a), which derives these quantities from gap fraction measurements. Gap fraction is the fraction of solar radiation which is not blocked by foliage and reaches the ground, in other words it is the amount of 'blue sky' that the sensor "sees" from beneath the canopy (Jonckheere et al. 2004; LI-COR 1992; Peper and McPherson 2003). The sensor has a hemispherical lens, which records blue radiation under diffuse illumination conditions at five distinct angular intervals, with central zenith angles of 7, 23, 38, 53 and 68° (Figure 3.3a). Gap fraction is obtained by rationing a below canopy and an above canopy reading. All blocking elements are considered in the gap fraction reading, thus the instrument does not discriminate between green and brown foliage.

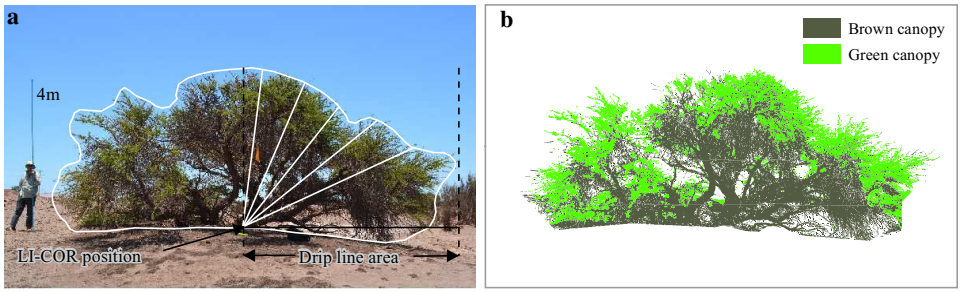

Figure 3.3. (a) Procedure for measuring DLLAI of a Tamarugo tree using the LI-COR instrument. Path lengths at the five viewing angles of the instrument were corrected by the tree profile. **(b)** GCF_{pics} was estimated from digital pictures using object-based image analysis.

Table 3.2. Hydraulic, biochemical and structural variables measured for the 32 Tamarugo trees between January 24 and 28, 2011.

Variables	Units	Sampling time	Sampling scheme	Instrument/procedure	Reference/formula
Hydraulic					
Leaf water potential	MPa	Predawn	4 twigs per tree	Scholander chamber	(Meyer and Ritchie 1980; Scholander et al. 1965)
			Foliar biochemistry		
Equivalent water thickness (EWT)	g/cm^2	Midday	4 twigs per tree	Precision weight (0.0001g) and oven	$EWT = \frac{\text{fresh leaf weight-dry leaf weight}}{\text{fresh leaf area}}$
Canopy water content (CWC)	g/cm^2				$CWC = EWT \times DLLAI_{green}$
Chlorophyll (a + b) and Carotenoids	$\mu g/cm^2$	Midday	4 twigs per tree	Spectro-photometric analysis of extracts dissolved in 80% acetone	(Lichtenthaler 1983)
			Canopy structure		
Green canopy fraction visual estimation(GCF_{vis})		Any time	2 times, 2 surveyors	Visual estimation, using five categories: 0; 0.01–0.25; 0.25–0.50; 0.50–0.75; 0.75–1.0	$GCFvis = \frac{\text{vol. green canopy}}{\text{vol. total canopy}}$

Table 3.2. (cont.) Hydraulic, biochemical and structural variables measured for the 32 Tamarugo trees between January 24 and 28, 2011.

Variables	Units	Sampling time	Sampling scheme	Instrument/procedure	Reference/formula
Green canopy fraction from digital pictures (GCF_{pics})		Any time	2 digital color pictures (RGB) per tree	Object-based image analysis. Segmentation: multiresolution (scale: 10, shape: 0.5, compactness: 0.1). Classification: objects with [G/(R + G + B) > 0.34] as green canopy; objects with [R/(R + G + B) > 0.37] as brown canopy.	$GCFpics = \frac{\text{Green canopy}}{\text{(Green+Brown canopy)}}$
Drip line leaf area index (DLLAI) (green + brown)	m^2/m^2	Dawn or sunset	4 partial records (at each tree quarters)	LI-COR LAI-2000 instrument. Measurements corrected by the tree profile	$DLLAI = \frac{\text{leaf area}}{\text{drip line area}}$ (Jonckheere et al. 2004; LI-COR 1992; Peper and McPherson 2003)
Green drip line leaf area index ($DLLAI_{green}$)	m^2/m^2				$DLLAI_{green} = DLLAI \times GCF_{pics}$

One of the assumptions of the LI-COR instrument is that vegetation has a homogeneous height, which is not correct in the case of individual trees. Nevertheless, it is possible to derive the correct LAI for single trees by correcting the LI-COR readings for the tree profile (Figure 3.3a), obtaining as a result DLLAI, which is the LAI for the projected (to the ground) crown area or drip line area. Partial path lengths at the five angles of the LI-COR instrument were recalculated from the vertical profile of the tree on digital pictures as shown in Figure 3.3a. Partial DLLAI values were taken at the four quarters of the trees by covering the hemispherical lens with a 270° cap. The final DLLAI value of each tree was obtained from the average of the partial values weighted by their partial crown volumes. Partial crown volumes were calculated internally by the LI-COR software using the corrected path lengths (Figure 3.3a). Because the LI-COR instrument provides values of DLLAI considering brown and green material, we multiply the DLLAI of each tree with the green canopy factor obtained from digital pictures (GCF_{pics}) obtaining as a result $DLLAI_{green.}$

During the timeframe of performing the hydraulic, biochemical and structural sampling, we also measured the canopy spectral reflectance at the same four points of the crown for all 32 trees. We measured spectral signatures in the 400–1300 nm range with a spectroradiometer instrument (ASD FieldSpec Pro) and using a foreoptic with instantaneous field of view (IFOV) of 25° placed in nadir position 30 cm above the canopy. We sampled reachable parts of the canopy at the same four quarters where the hydraulic and biochemical measurements were carried out. The spectral measurements were performed at 13.00 h +/− 1 h. White reference measurements (spectralon) were used to calibrate the ASD instrument before every canopy reflectance measurement.

In the second field campaign (summer 2012), we studied diurnal leaf movements of three Tamarugo trees on three consecutive days in the Llamara natural forest. These leaf movements were originally reported by (Chávez et al. 2013b) under laboratory conditions and showed an important effect on the canopy spectral reflectance of small Tamarugo plants. In this study, we registered diurnal leaf movements of the Tamarugo trees using a digital camera mounted on a tripod and measured canopy spectral reflectance with the FieldSpec instrument simultaneously. To perform the spectral measurements, we set the spectroradiometer instrument in nadir position 30 cm above the top of the canopy (TOC) of the Tamarugo trees. Since the solar angle changes during the day, a strict

TOC position for the FieldSpec instrument is needed to minimize internal shadowing within the IFOV. Most trees are too tall to perform such measurements, and for this reason we searched for trees partially covered by sand-dunes, which allowed reaching the TOC position with a tripod. Only three trees with the above-mentioned condition were found and measured. Measurements were performed on an hourly basis from 9:00 to 18:00 hours and only interrupted at 13.00 when the instrument was shadowing the sampling area and occasionally during sand-storms.

3.2.5. Calculation of spectral vegetation indices using object-based analysis and WorldView2 images

3.2.5.1. The WorldView2 sensor

Before the WorldView2 satellite was launched in 2009, the available VHSR imagery was limited to four broad spectral bands, typically blue (450–520 nm), green (520–600 nm), red (630–690 nm) and NIR (760–900 nm) at spatial resolution of 4 m (IKONOS) to 2.4 m (QuickBird2). The WorldView2 sensor incorporated four extra bands: coastal (401–453 nm), yellow (589–627 nm), red-edge (704–744 nm) and NIR2 (862–954) and slightly modified the bands blue (448–508 nm), green (511–581 nm) and NIR (772–890 nm), which, combined with an increased spatial resolution of 0.5 m for the panchromatic channel and 2 m for the multispectral channels, enables spectral analysis of spatial features at a very high spatial resolution. In this study, we used two WorldView2 scenes to assess water stress of Tamarugo trees: the first, acquired on 13 July 2011, is covering the plantation stand of Pintados (16 trees) and the second, acquired on 25 September 2011, is covering the natural forest of Llamara (16 trees). The catalogue of WorldView2 is limited to a restricted number of dates and areas and we selected the ones closest to the field campaign date (January 2011).

The date difference between the fieldwork and the satellite image acquisitions constitutes a limitation to this study. It is a problem that users usually face when using VHSR imagery since the image catalogues are limited and ordering specific acquisition dates is very expensive. Nevertheless, Tamarugo has a vegetative period covering the whole year with a partial recession occurring between May and August and a new regrowth starting in September (Ortiz et al. 2010). In other words, the trees remain green during the year and we do not expect a big seasonal effect. In order to check for this time difference, we compared the spectral vegetation

indices obtained from the FieldSpec measurements (January) and the satellite images (July and September, respectively) in Section 3.3 and discussed our findings in Section 3.4.

3.2.5.2. Crown delineation

Crown area was automatically delineated on the WorldView2 panchromatic images and cross-checked with *in situ* measurements of crown diameter performed at two azimuthal positions (N-S and E-W). We used a simple quad-tree object-based segmentation and classification of the mean object values in the panchromatic band (Figure 3.4). The algorithm was implemented in the eCognition-Developer 8TM software and it produced polygons for the crown area of all 32 single trees. Shadows next to the trees were present only in the scene acquired in winter (Figure 3.4b) and were manually subtracted considering the crown diameters measured in the field.

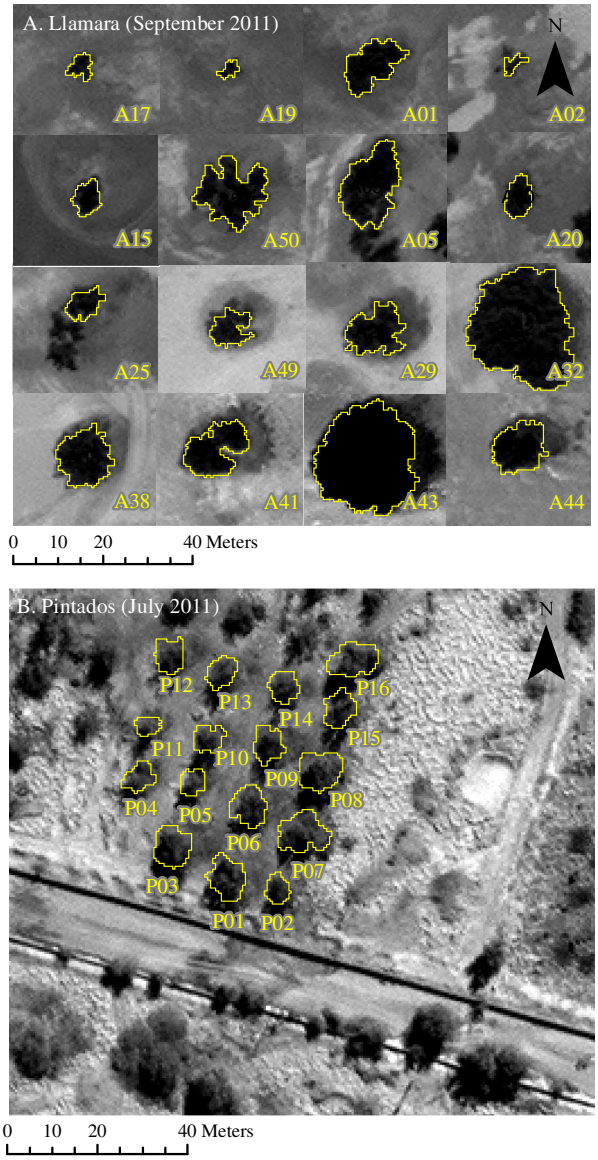

Figure 3.4. WorldView2 satellite images of the two sampling sites: **(a)** Llamara natural forest and **(b)** Pintados plantation. Delineated in yellow the crown of the trees identified using object-based image analysis.

3.2.5.3. Vegetation indices

We calculated the average top of atmosphere (TOA) reflectance of the pixels located inside the crown polygons for each of the eight bands of the WorldView2 multispectral image. To obtain TOA reflectance (per band), we converted the digital numbers of the original spectral bands into TOA spectral reflectance by using the absolute calibration factors as well as the solar and sensor geometry given with the scene (for details see (Updike and Comp 2010)). Finally, we used the TOA reflectance values to calculate the Normalized Difference Vegetation Index (NDVI) (Tucker 1979) and Red-edge Chlorophyll Index ($CI_{Red\text{-}edge}$) (Gitelson et al. 2006) as shown in Table 3.3. The selection of these indices was based on the results obtained by (Chávez et al. 2013b) and the best target field indicators found in this study (GCF and $DLLAI_{green}$).

Table 3.3. Remote sensing vegetation indices used to estimate GCF_{pics} and $DLLAI_{green}$ of single Tamarugo trees

Remote sensing feature	Formula using the position of the WorldView2 spectral bands (nm)
Normalized Difference Vegetation Index (NDVI) (Tucker 1979)	$(R_{831} - R_{659})/(R_{831} + R_{659})$
Red-edge Chlorophyll Index ($CI_{Red\text{-}edge}$) (Gitelson et al. 2006)	$R_{831}/R_{724} - 1$

3.2.6. Data analysis

In order to meet the three specific objectives defined in section 3.1, we performed the following data analysis:

Objective 1. Test the variables CWC and LAI as water stress indicators for single Tamarugo trees under different field water stress scenarios. We tested first for significant differences in predawn water potential between trees under the three depletion scenarios to check if they were facing different levels of water stress. Then we tested for significant differences in selected foliar and canopy variables between trees under different depletion scenarios. Additionally, we analyzed whether trees with a different GCF_{vis} were significantly different in terms of predawn water potential, foliar biochemistry and other canopy variables.

Significance was tested with the Tukey-Kramer multiple comparison test for unbalanced samples with a significance level α of 0.05.

Objective 2. Test the $CI_{Red\text{-}edge}$ and NDVI to assess water condition of single Tamarugo trees by using WorldView2 images and *in situ* measurements. We tested the capability of these two vegetation indices as best field water stress indicators using the root mean squared errors (RMSE) between estimated values and the *in situ* measurements. We compared the fitted curves and RMSE for the indices calculated using FieldSpec data, which were obtained during the field campaign, and the indices calculated from satellite data to check for seasonal effects in the remote sensing estimations.

Objective 3. Study Tamarugo leaf movements during the day in the field and their implications for remote sensing based estimations of water stress. The photographic recording of diurnal leaf movements was carried out simultaneously with the FieldSpec measurements, and therefore, diurnal changes in canopy reflection can be associated to these movements. Using the hourly FieldSpec data, we obtained hourly values of $CI_{Red\text{-}edge}$ and NDVI and calculated the correlation coefficient (R) between these values and hourly values of solar radiation. We hypothesize that solar radiation is the main environmental variable driving the leaf movements of Tamarugo trees since this has been shown for other Leguminosae plants (Liu et al. 2007; Pastenes et al. 2005; Pastenes et al. 2004). Solar radiation data were obtained from the meteorological station Canchones of the Universidad Arturo Prat (20°26′36″S, 69°41′43″W). A potential correlation between spectral vegetation indices and solar radiation would imply that not only diurnal but also seasonal changes of this variable would have an impact on biophysical retrievals from remote sensing data. This is especially relevant for hyper-arid ecosystems such as the Atacama Desert, where the solar radiation can be extremely high with high fluctuations between summer and winter (Julio Hirschmann 1973; Ortega et al. 2010).

3.3. Results

3.3.1. Biophysical response of the Tamarugo trees under different water depletion scenarios

In the previous study of (Chávez et al. 2013b), best indicators of induced water stress on small Tamarugo plants were LAI and canopy water content (CWC). This laboratory experiment also showed that leaf pigments concentrations did not change during the 15 days that plants were deprived from water. In this paper, we study whether these conclusions are also valid for adult trees in the field and under different depletion scenarios.

3.3.1.1. Differences between depletion scenarios

According to the visual assessment of green canopy fraction (GCF_{vis}), all trees with null groundwater depletion (Dep1-null) corresponded to the class 0.75–1.0 GCF_{vis} (see trees A43 and A29 in Figure 3.5 for examples). For the short-term intensive depletion scenario (Dep2-int), five out of eight trees corresponded to the class 0.50–0.75 (see trees A19 and A20 in Figure 3.5 for examples), two trees belonged to 0.25–0.50 and one to 0.75–1.0. Finally, trees under long-term gradual depletion (Dep3-grad) corresponded to different GCF_{vis} classes (see Figure 3.6 for examples), where the class 0.01–0.25 was the most represented with six trees and one tree was completely dry (0.0 GCF_{vis}). The other classes were represented by three trees each. The result of this assessment indicated that the effects of groundwater depletion on foliage loss were more severe in Scenario 3 than in Scenario 2 despite the similar final water depth (about 11 m).

Table 3.4 shows the mean values and standard deviations of the quantitative variables measured for Tamarugo trees in the three depletion scenarios. Significant differences between mean values of the scenarios are indicated.

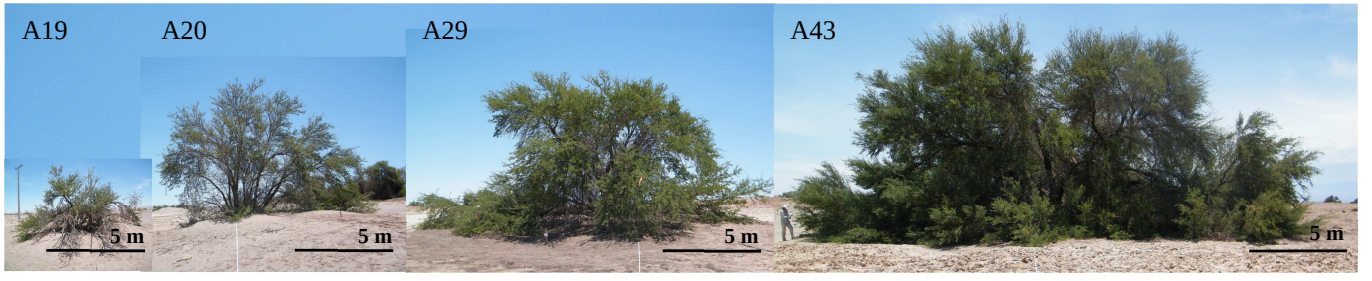

Figure 3.5. Examples of Tamarugo trees at the Llamara site. Tamarugos are sorted according to the proximity to the pumping area (left one, the closest).

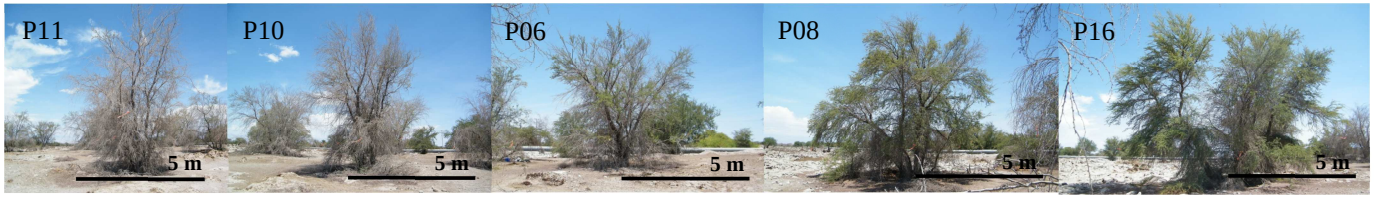

Figure 3.6. Tamarugo trees at the Pintados site sorted by GCF_{vis}. From left to right: 0, 0.01–0.25, 0.25–0.50, 0.50–0.75 and 0.75–1.0.

Pre-dawn water potential was significantly lower for trees under long-term gradual depletion (Dep3-grad), implying that the water surrounding the root system was less available for these trees (Richter 1997; Schmidhalter 1997; Veste et al. 2008), and consequently, they were facing higher water stress than Dep1-null and Dep2-int. Additionally, the biochemical analysis showed that only trees with no groundwater depletion (Dep1-null) had higher values of EWT than trees under Dep2-int and Dep3-grad. Trees with no water depletion (Dep1-null) showed higher concentrations than Dep2-int and Dep3-grad in terms of foliar pigments (chlorophyll and carotenoids), but only Dep1-null and Dep3-grad were significantly different. At the crown level, trees under Dep2-int and Dep3-grad showed a significantly lower DLLAI, GCF_{pics} and $DLLAI_{green}$ than trees with no ground water depletion (Dep1-null). Overall, we observed significant differences between depletion scenarios Dep1-null and Dep3-grad for all measured variables. These differences suggest that the duration of the depletion (20 years for Dep3-grad *versus* five years for Dep2-int) had a higher impact on the Tamarugo water status than the intensity of the depletion (1 meter for Dep3-grad *versus* 6–7 m for Dep2-int).

Table 3.4. Means and standard deviations (in brackets) of the hydraulic, biochemical and structural variables for Tamarugo trees under different groundwater depletion scenarios.

Variables	Depletion scenarios		
	Dep1-null	**Dep2-intensive** (6–7 m in 5 years)	**Dep3-gradual** (1 m in 20 years)
Hydraulic			
Predawn leaf water potential (MPa)	−2.061 (0.199) [a]	−2.194 (0.164) [a]	−2.588 (0.316) [b]
Biochemistry			
EWT (g/cm^2)	0.021 (0.002) [a]	0.019 (0.002) [b]	0.018 (0.002) [b]
Chlorophyll (a + b) (µg/cm^2)	12.28 (4.08) [a]	18.55 (2.05) [a/b]	19.23 (7.31) [b]
Carotenoids (µg/cm^2)	475.9 (115.9) [a]	620.7 (46.5) [a/b]	761.7 (236.8) [b]
Structure			
DLLAI (m^2/m^2)	2.486 (0.718) [a]	1.482 (0.664) [b]	1.658 (0.677) [b]
GCF_{pics}	0.755 (0.064) [a]	0.517(0.086) [b]	0.405 (0.253) [b]
$DLLAI_{green}$	1.887 (0.576) [a]	0.743 (0.286) [b]	0.797 (0.671) [b]
Crown area (m^2)	200.7 (175.0) [a]	69.6 (65.2) [b]	46.0 (17.13) [b]

Note: Mean values with different letters (a, b) are significantly different (α = 0.05) according to the Tukey–Kramer multiple comparison test (after ANOVA).

3.3.1.2. Differences between GCF_{vis} classes

In addition to sharing equal depletion conditions, trees under the Dep3-grad scenario had large differences in GCF_{vis} (Figure 3.6). Thus, not all trees reacted equally to long-term groundwater depletion. The GCF_{vis} class of 0.01–0.25 constituted a critical threshold for the water status of Tamarugo trees, since these trees showed significantly lower values of predawn water potential (the actual direct measure of water stress) in comparison to trees of higher GCF_{vis} classes (Figure 3.7a). Therefore, this variable (GCF) and this threshold (<0.25) were related to high water stress.

Although results showed that foliar biochemical variables as well as crown area did not significantly differ for the different green GCF_{vis} categories, the variables GCF_{pics}, DLLAI and $DLLAI_{green}$ showed significant differences as well as a positive correlation with GCF_{vis} (Figure 3.7). In the case of EWT, only trees at the extreme GCF_{vis} classes (0.01–0.25 and 0.75–1.0) showed significant differences.

For this reason, canopy water content (CWC = EWT × LAI) estimations depended more on the LAI factor, which is $DLLAI_{green}$ in the case of individual trees.

3.3.2. Remote sensing based estimations of Tamarugo water status

In the previous section, we showed that the structural variables GCF, DLLAI, and $DLLAI_{green}$ were good field indicators of the Tamarugo water status at tree level. Thus, in this section we present our findings on the suitability to use the WorldView2 spatial and spectral characteristics to retrieve these variables for single Tamarugo trees. First, we analyzed the spectral signature of trees with different GCF, and second, we studied the relationship between vegetation indices (NDVI and $CI_{Red\text{-}edge}$) and GCF and $DLLAI_{green}$, considering the spectral bands of the WorldView2 sensor. We focus our analysis on $DLLAI_{green}$ since DLLAI considers the brown and green elements of the canopy, but water stress had an impact only on the green fraction of the canopy.

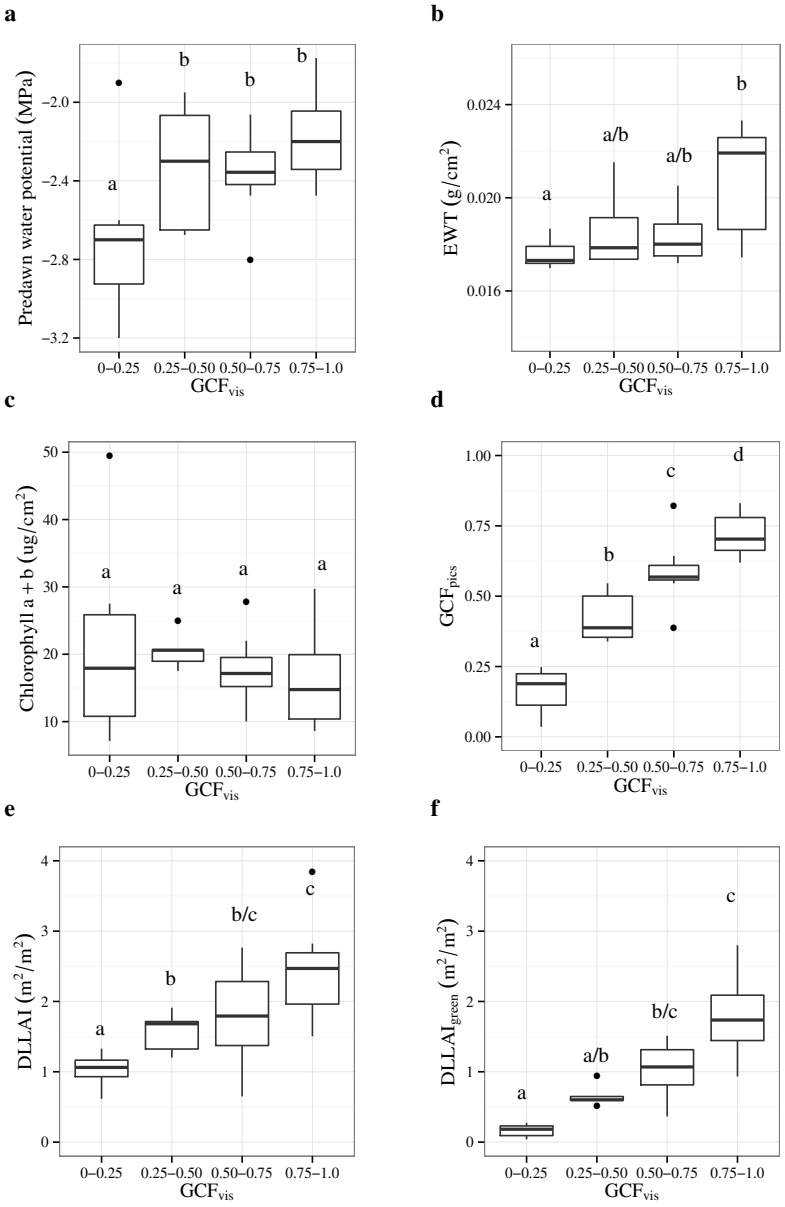

Figure 3.7. Box plots of different hydraulic, biochemical and structural variables measured for the 32 Tamarugo trees grouped by GCF_{vis}: **(a)** predawn water potential, **(b)** EWT, **(c)** chlorophyll (a + b), **(d)** GCF_{pics}, **(e)** DLLAI, and **(f)** $DLLAI_{green}$.

3.3.2.1. Spectral response to green foliage loss

Figure 3.8 shows the average canopy spectral signatures of the 32 Tamarugo trees grouped in five classes of green canopy fraction (GCF_{vis}) as measured with the FieldSpec instrument. From this figure, we can observe that reflectance over the near-infrared (NIR) region (760–900 nm) was higher for trees with a GCF_{vis} of 0.50–0.75 than for the trees with values of 0.75–1.0. Trees with GCF_{vis} of 0.25–0.50 showed a lower reflectance in the NIR than trees with a GCF_{vis} larger than 0.5, showing a spectral signature similar to a dead tree (GCF_{vis} = 0.0), where the brown material (branches and trunk) is dominant. In the visible region (400–700 nm) we observed similar changes to the ones observed in the NIR region, although reflectance values for trees with GCF_{vis} values of 0.75–1.0 were always reflecting less (or absorbing more) radiation than the other trees. Another interesting spectral feature useful for water stress detection is the red-edge (Boochs et al. 1990; Filella and Penuelas 1994), which is the sharp slope of the vegetation spectral signature at 680–750 nm (Figure 3.8). Studies have shown that foliage loss cause the red-edge to shift towards shorter wavelengths, a phenomenon also known as "blue shift" [46–49]. In the case of Tamarugo trees the "blue shift" is not (visually) clear when comparing trees with different GCF_{vis} (Figure 3.8), although between the GCF_{vis} classes 0.75–1.0 and 0.50–075 the shift is slightly noticeable.

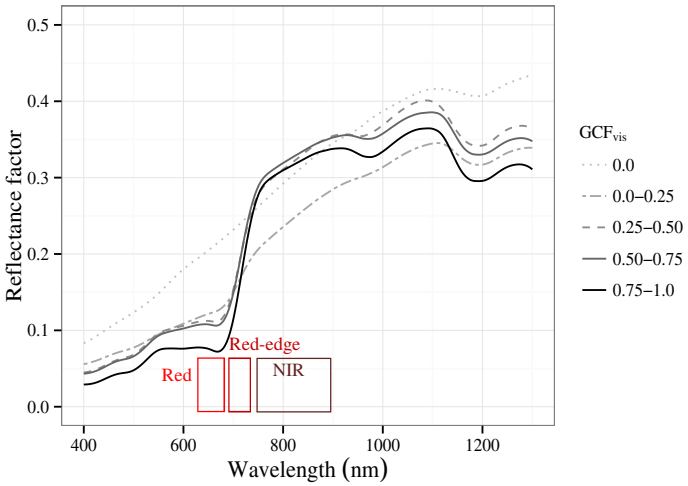

Figure 3.8. Canopy spectral signature (average) of the 32 Tamarugo trees grouped by GCF_{vis} measured on 24–28 January, 2011. The 50% band pass of the WorldView2 red, red-edge and NIR1 spectral bands are displayed as reference.

3.3.2.2. Vegetation indices for GCF and $DLLAI_{green}$ estimations

Normalized Difference Vegetation Index (NDVI)

In the previous section, we showed that the reflectance difference between the NIR and visible region decreased when trees get dry. This is clearly noticeable in Figure 3.9a, where the NDVI is displayed for trees with different GCF_{pics} and $DLLAI_{green}$ values. Figure 3.9a shows the NDVI calculated using the narrow bands of the FieldSpec instrument (1 nm band width) at the wavelengths defined in literature, *i.e.*, 670 nm for the red band and 780 nm for the NIR band (Tucker 1979), while Figure 3.9b shows the NDVI calculated using the FieldSpec bands at 659 nm and 831 nm, wavelengths where the WorldView2 red and NIR1 spectral bands are centered (see Figure 3.8 for a reference). Despite this shift in the spectral position, the R^2 for the linear relationship between NDVI and GCF_{pics} was high in both cases (0.80 and 0.78, respectively) and the RMSE similar (0.10 and 0.11, respectively). Moreover, the relationship between NDVI and $DLLAI_{green}$ was asymptotic, showing a lower sensitivity of NDVI for high values of DLLAI and similar RMSE values when using the spectral position defined in literature (Figure 3.9d) and the WorldView2 bands position (Figure 3.9e) with values of 0.35 and 0.36, respectively.

Figure 3.9c shows the relationship between NDVI and GCF_{pics} with NDVI values calculated using the broad bands of the WorldView2. In this case, the Red and NIR values were obtained by averaging the spectral values of the pixels inside the canopy polygons of each tree in the WorldView2 images (Figure 3.4). The NDVI values calculated this way were twice as small as values calculated using FieldSpec data. This can be explained because the FieldSpec data relate to reflectance measurements at the branch level, whereas reflectances derived from WorldView2 data relate to the canopy level. Clumping effects and internal shadowing inside the tree canopy cause lower NDVI values at the canopy level (Malenovský et al. 2007; Moorthy et al. 2008). In spite of this, NDVI was linearly correlated to GCF showing an R^2 of 0.7 and a RMSE of 0.12. The relationship between NDVI-WV2 and DLLAI was more linear than between NDVI-FieldSpec and DLLAI, but the RMSE increased from 0.36 to 0.40 (Figure 3.9f). Besides the differences between the acquisition date of the images covering scenarios Dep1-null/Dep2-int (September 2011), Dep3-grad (July 2011) and the FieldSpec measurements (January 2011), the R^2 and RMSE for the relationship between NDVI-GCF using FieldSpec data (Figure 3.9b) was similar to the relationship

GCF-NDVI using WorldView2 data (Figure 3.9c). For the NDVI-$DLLAI_{green}$ relationship, the RMSE was higher when using WorldView2 data (Figure 3.9f) than when using FieldSpec data (Figure 3.9e), which can be attributed to the different acquisition dates.

Red-edge Chlorophyll Index ($CI_{Red-edge}$)

The relationship between the $CI_{Red-edge}$ and GCF was asymptotic with a lower sensitivity for low GCF values and a RMSE of 0.1 (Figure 3.10a). On the contrary, the $CI_{Red-edge}$-$DLLAI_{green}$ relationship was linear with an R^2 of 0.72 and a RMSE of 0.38. However, in both cases the RMSE values increased when changing from the wavelengths defined in literature (670 nm for the red band and 710 nm for the red-edge band (Gitelson et al. 2006)) to the positions where the red and red-edge bands of the WorldView2 sensor are centered (659 nm and 724 nm, respectively). The $CI_{Red-edge}$ showed similar RMSE as NDVI for retrieving GCF (0.1) and an asymptotic relationship when using the wavelengths from literature, but this is not the case anymore when using the spectral band positions of WorldView2 (Figure 3.10b).

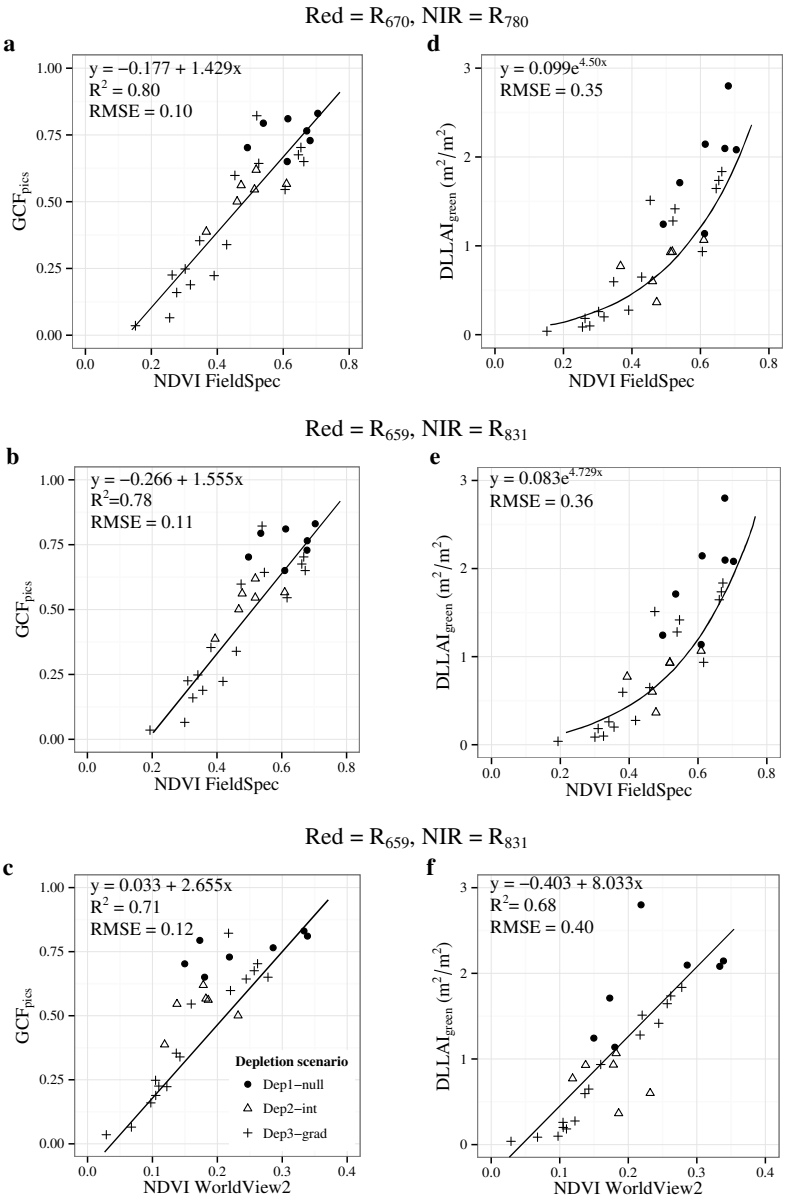

Figure 3.9. Relationships between NDVI *vs.* GCF_{pics} **(a**, **b**, **c)** and NDVI *vs.* $DLLAI_{green}$ **(d**, **e** and **f)** for 32 Tamarugo trees. NDVI was calculated using specific FieldSpec bands (first two rows) and the WorldView2 broad bands (third row).

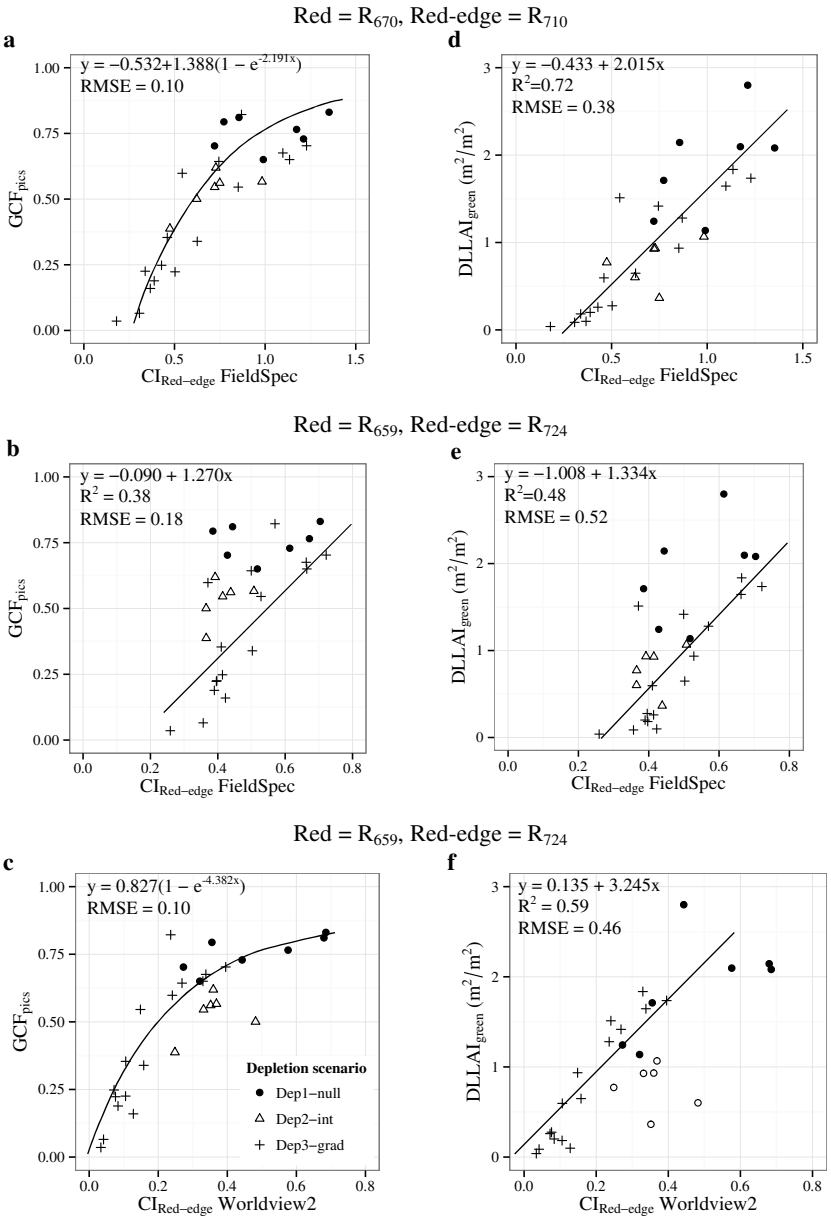

Figure 3.10. Relationships between $CI_{Red\text{-}edge}$ *vs.* GCF_{pics} **(a**, **b**, **c)** and $CI_{Red\text{-}edge}$ *vs.* $DLLAI_{green}$ **(d**, **e** and **f)** for 32 Tamarugo trees. $CI_{Red\text{-}edge}$ was calculated using specific FieldSpec bands (first two rows) and the WorldView2 broad bands (third row).

When using the broad bands of the WorldView2 sensor (Figure 3.10c), the relationship turns into asymptotic again and the RMSE was comparable to the one observed for FieldSpec data at the wavelengths suggested in literature. For $DLLAI_{green}$ estimations using the $CI_{Red\text{-}edge}$ and the WorldView2 sensor, the RMSE (0.46) was between the value observed for FieldSpec data using literature band positions (0.38) and using the WorldView2 band positions (0.52). Differences between the WorldView2 image acquisition dates and the FieldSpec measurements seem to have little effect on the R2 and RMSE for the $CI_{Red\text{-}edge}$-GCF relationship (Figures 3.9b1 and 3.9b3), while for the $CI_{Red\text{-}edge}$–$DLLAI_{green}$ relationship the RMSE increased when using WorldView2 data (Figures 3.10d and 3.10f). Overall, the NDVI constituted the best estimator for $DLLAI_{green}$ while the $CI_{Red\text{-}edge}$ was the best for estimating GCF for tree objects extracted from WorldView2 imagery.

3.3.3. Effects of Tamarugo pulvinar movements on spectral reflectance

Figure 3.11 shows pulvinar movements of Tamarugo trees under field conditions and Figure 3.12a shows the canopy spectral reflectance changes throughout the day. From 9.00 hours onwards leaves were changing gradually from a planophile leaf distribution (parallel to the leveled horizon) to a more erectophile distribution (perpendicular to the leveled horizon), making canopy reflectance to drop during the day. In Figure 3.12b, we depicted the NDVI and $CI_{Red\text{-}edge}$ as well as solar radiation recorded hourly during three days of the summer 2012 campaign. Both indices were calculated using FieldSpec 1 nm bands at the wavelengths where the WorldView2 bands are centered. This figure shows that the lowest values for both vegetation indices were around 13.00 h when the solar radiation was reaching its maximum. The correlation coefficient (R) between NDVI and solar radiation was negative and higher ($R = -0.52$) than in case of the R between $CI_{Red\text{-}edge}$ and solar radiation ($R = -0.24$).

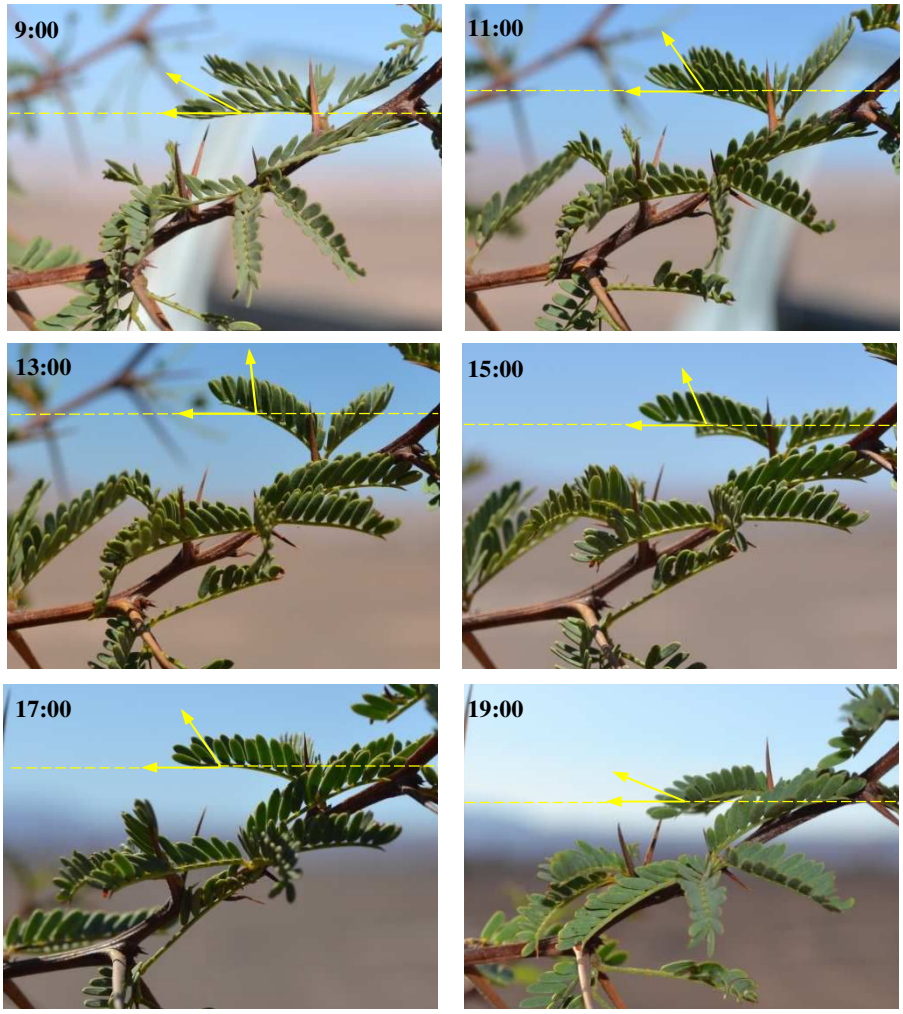

Figure 3.11. Pulvinar movement of Tamarugo leaves recorded on 13 January 2012.

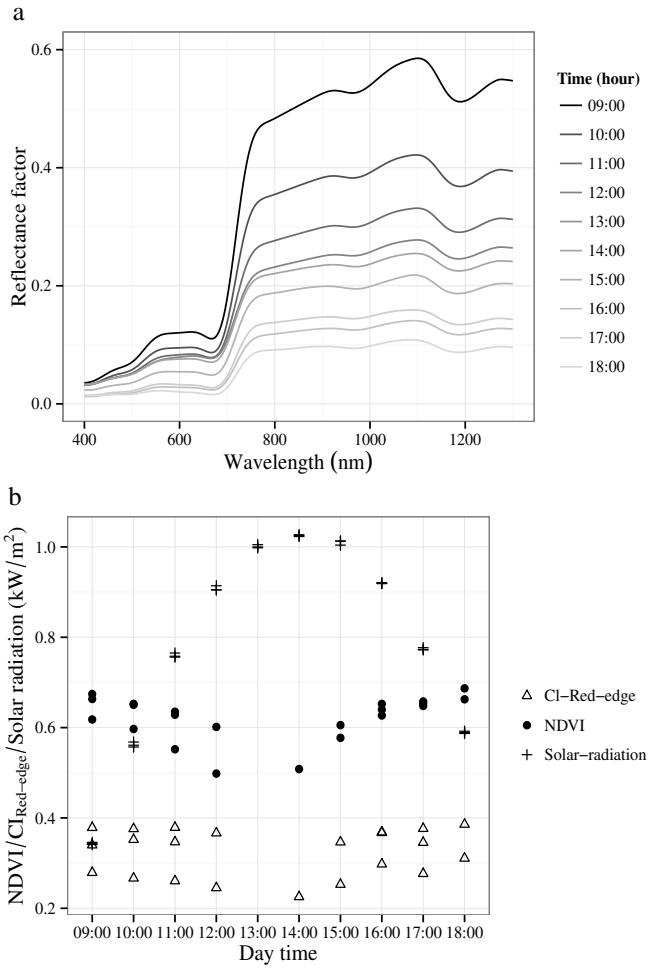

Figure 3.12. (a) Hourly changes on Tamarugo canopy spectral signature measured on 13 January 2012 (summer), **(b)** Hourly values of NDVI and $CI_{Red\text{-}edge}$ (FieldSpec data) for three Tamarugo trees and solar radiation measured on three consecutive days: 13–15 January 2012.

3.4. Discussion

The analysis of the biophysical variables of trees under different depletion scenarios in this study showed no clear trends (Table 3.4). Scenarios Dep2-int and Dep3-grad did not show significant differences for the biochemical and structural variables, although trees for Dep3-grad were facing a higher water stress (as shown

by the predawn leaf water potential). Besides, trees sharing equal depletion conditions reacted differently to changes in groundwater supply. This is well illustrated in Figure 3.6, where we can observe trees for scenario Dep3-grad with large differences in GCF_{vis}. This variability in the response of Tamarugo to water stress implies that water extraction on a large scale may not affect the Tamarugo population homogeneously in space, and therefore, an assessment of water condition at the tree level is necessary to understand the impact of groundwater extraction.

Although a clear trend in the biophysical variables for the three depletion scenarios was absent, we observed significant differences between the null depletion scenario and the two water stress scenarios for the biochemical and structural variables (Table 3.4), which means that trees under water stress had (a) lower water concentration, (b) higher pigment concentration, and (c) lower green foliage fraction. Another interesting finding from Table 3.4 is that Dep3-grad may induce higher water stress than Dep2-int. In other words, Tamarugo trees would be more sensitive to the duration of the water stress rather than to the intensity of the water stress. However, this hypothesis needs to be tested using more trees and more information on the groundwater depth and depletion for the whole aquifer. The goal of the current study was not to estimate the extent of the water depletion or different levels of depletion, but to define useful indicators for tree condition and to test whether remote sensing based indices can be used to estimate these indicators. Therefore, potential autocorrelation of trees within one depletion scenario may exist, but no conclusions on the depletion scenarios themselves have been made.

After studying differences in the biophysical variables for different water scenarios, we analyzed trees with different green canopy fraction, that was visually assessed (GCF_{vis}). Although Tamarugo trees are defined as semi-deciduous species (Acevedo et al. 2007; Ortiz et al. 2010; Sudzuki 1985a), healthy trees look green during the whole year and this is the reason why current water condition assessments use GCF_{vis} estimations. When grouping the 32 trees into four categories of GCF_{vis}, we found that trees with 0.01–0.25 GCF_{vis} presented a significantly lower predawn water potential than trees from the other three higher GCF_{vis} classes, which means that Tamarugo is able to keep its water status at normal ranges till losing about 75% of green foliage. This value (GCF = 0.25) is therefore critical for Tamarugo's water balance and can be used as a threshold for

conservation purposes. Furthermore, we did not observe significant differences between the GCF_{vis} classes for the foliar biochemical variables, except for EWT and only when comparing the 0.01–0.25 and 0.75–1.0 classes. This is an indication that Tamarugo trees cope with water stress by adjusting their water balance at the canopy level rather than adjusting their foliage properties. This is in line with research conducted by (Asner et al. 2000) in the Chihuahuan desert (New Mexico) where they found that foliar spectral properties of desert plants were very stable along environmental gradients in comparison with canopy variables, which were very variable.

In this study, we implemented a quantitative method to estimate the green canopy fraction of single Tamarugo trees using digital pictures (GCF_{pics}), which showed a good correspondence with the visual method GCF_{vis} (Figure 3.7d). This quantitative approach, based on segmentation of the digital pictures using the red-green-blue (RGB) bands has been successfully used before for retrieving the green fraction of crops (Baret et al. 2010; Liu et al. 2013). The use of the green ratio and red ratio to discriminate green and brown segments of the trees within the pictures allowed us to use images with different illumination conditions and with different radiometric resolutions (different cameras), providing an observer-independent indicator of water stress. GCF_{pics} can be used for assessing green foliage loss for single trees regardless of the tree size. This variable is also easy to interpret for policy makers since it gives a direct value of the percentage of the remaining foliage. If the purpose of the assessment is to study the effects of groundwater depletion on the biomass of Tamarugo trees, $DLLAI_{green}$ is more suitable than GCF since it gives a quantitative estimation of the amount of green material available.

WorldView2 satellite imagery provided a unique source of detailed spatial and spectral data, allowing single tree identification and calculation of the NDVI and the $CI_{Red\text{-}edge}$ per tree. Our results showed that both indices provided accurate estimations of GCF and $DLLAI_{green}$ for single Tamarugo trees. These results demonstrate that an assessment of the condition of single Tamarugo trees is possible at a regional scale, and therefore, a digital inventory and assessment will be the logical next step.

To perform such an assessment, temporal constraints must be taken into account since we have shown that the spectral reflectance varied during the day due to Tamarugo leaf movements. These movements constitute an adaptation of Tamarugo trees to survive the high solar radiation of the Atacama Desert and have

an important impact on remote sensing based vegetation indices. We observed a negative correlation coefficient (R) of about −0.5 between the NDVI and solar radiation during the day, and consequently, we may expect also that NDVI values in summer could be lower than in winter only because of more solar radiation. We hypothesize that this fact could be the explanation why in Figure 3.9c some trees with high GCF at scenario Dep1-null had low NDVI values. The WorldView2 scene corresponding to the scenarios Dep1-null and Dep2-int was acquired in September (spring, high solar radiation), while the image corresponding to the scenario Dep3-grad was acquired in July (winter, low solar radiation). Thus, full green trees would have been able to adjust their leaf angle distribution according to the solar radiation, showing lower values of NDVI in spring. Although we cannot discard Tamarugo's phenological cycle as a cause of seasonal changes in vegetation indices, we believe that pulvinar movements play a major role. Nevertheless, this hypothesis needs to be tested in more detail and it will be subject for further research.

3.5. Conclusions and recommendations

Green canopy fraction (GCF), estimated with object based image analysis on digital pictures, and green drip line leaf area index ($DLLAI_{green}$), measured with a LI-COR instrument, are good field estimators of the condition of single Tamarugo trees. We recommend using GCF for environmental monitoring and DLLAI for biomass studies. We suggest a critical GCF value of 0.25 for Tamarugo survival, below which the trees are facing leaf water potentials (predawn) significantly below normal ranges.

Single tree identification, crown size delineation and estimations of $DLLAI_{green}$ and GCF were successfully performed using WorldView2 high spatial resolution satellite images and an object based image analysis approach. This methodology constitutes a powerful tool for assessing and monitoring the effects of groundwater depletion on Tamarugo trees at a large regional scale since it copes with the spatial heterogeneity in the forest. The NDVI constituted the best estimator for $DLLAI_{green}$, while the Red-edge Chlorophyll Index was the best one for estimating GCF for tree objects extracted from WorldView2 imagery.

Tamarugo pulvinar movements, an adaptation to survive the extreme conditions of the Atacama Desert, affected vegetation indices calculated from canopy spectral

reflectance. Therefore, they can only be used for monitoring purposes if they (a) have been measured at the same time during the day and at the same season, or (b) they have been corrected for this temporal effect. No research has been carried out so far to cope with the second option and it will be subject for further research.

Acknowledgements

This work has been supported by CONICYT-Chile and Wageningen University. The authors would like to thank Digital Globe for providing the WorldView2 imagery, to CONAF-Chile and SQM-S.A. for supporting the logistics during the field campaigns, and UNAP for providing the meteorological data. Special thanks to X. Aravena (SQM), C. Squella, M. Garrido (SAP-UCH), and M. Decuyper (WUR) for assisting the harsh fieldwork.

Chapter

4

Detecting leaf pulvinar movements on NDVI time series of desert trees: a new approach for water stress detection

R.O. Chávez, J.G.P.W. Clevers, J. Verbesselt, P.I. Naulin, M. Herold

Accepted for PLOS One (after revision).

Heliotropic leaf movement or leaf 'solar tracking' occurs for a wide variety of plants, including many desert species and some crops. This has an important effect on the canopy spectral reflectance as measured from satellites. For this reason, monitoring systems based on spectral vegetation indices, such as the normalized difference vegetation index (NDVI), should account for heliotropic movements when evaluating the health condition of such species. In the hyper-arid Atacama Desert, Northern Chile, we studied seasonal and diurnal variations of MODIS and Landsat NDVI time series of plantation stands of the endemic species *Prosopis tamarugo* Phil., subject to different levels of groundwater depletion. As solar irradiation increased during the day and also during the summer, the paraheliotropic leaves of Tamarugo moved to an erectophile position (parallel to the sun rays) making the NDVI signal to drop. This way, Tamarugo stands with no water stress showed a positive NDVI difference between morning and midday ($\Delta NDVI_{mo-mi}$) and between winter and summer ($\Delta NDVI_{W-S}$). In this paper, we showed that the $\Delta NDVI_{mo-mi}$ of Tamarugo stands can be detected using MODIS Terra and Aqua images, and the $\Delta NDVI_{W-S}$ using Landsat or MODIS Terra images. Because pulvinar movement is triggered by changes in cell turgor, the

effects of water stress caused by groundwater depletion can be assessed and monitored using $\Delta NDVI_{mo-mi}$ and $\Delta NDVI_{W-S}$. For an 11-year time series without rainfall events, Landsat $\Delta NDVI_{W-S}$ of Tamarugo stands showed a negative linear relationship with cumulative groundwater depletion. We conclude that both $\Delta NDVI_{mo-mi}$ and $\Delta NDVI_{W-S}$ have potential to detect early water stress of paraheliotropic vegetation.

Keywords

Solar tracking; water stress; phenology; normalized difference vegetation index; Landsat; MODIS; arid ecosystems; Tamarugo; Atacama

4.1. Introduction

Heliotropism or 'solar tracking' is the ability of many desert species and crops to move leaves and flowers as a response to changes in the position of the sun throughout the day (Ehleringer and Forseth 1980). There are two types of heliotropic movements: diaheliotropic movements in which leaves adjust the leaf lamina to face direct solar irradiation, and paraheliotropic movements, in which leaves adjust to avoid facing incoming radiation by contraction of pulvinar structures located at the base of leaves (Ehleringer and Forseth 1980; Koller 1990; Moran et al. 1989). Paraheliotropic movements are triggered by directional solar irradiation and allow partial regulation of the incident irradiance on the leaves. For desert species, the regulation of the solar irradiation intensity on the leaves is an important adaptation to avoid photosynthesis saturation (photoinhibition) and to enhance the water use efficiency (Koller 2001; Pastenes et al. 2005; Pastenes et al. 2004).

Diurnal paraheliotropic movements have a direct impact on the canopy reflectance properties of vegetation (Chávez et al. 2013a; Chávez et al. 2013b; Kimes and Kirchner 1983). Therefore, spectral vegetation indices derived from remote sensing data, like the normalized difference vegetation index (NDVI), can significantly vary during the day and during the year due to leaf movement as solar irradiation changes. Nevertheless, no studies have quantified the effects of solar tracking by plants on the NDVI signal recorded from satellites. Diurnal leaf movements of Tamarugo plants (*Prosopis tamarugo* Phil.) were first described by Chávez et al. (2013b) under laboratory conditions, and later by Chávez et al.

(2013a) for adult trees in the field. These diurnal leaf movements corresponded to paraheliotropic movements since the leaves moved to an erectophyle leaf distribution (facing away from the sun) around midday when solar irradiation was maximum. The paper of Chávez et al. (2013a) showed that leaf pulvinar movements caused diurnal changes of Tamarugo's canopy spectral reflectance and NDVI signal, which was negatively correlated to diurnal solar irradiation values.

In the present study, we hypothesize that the effects of Tamarugo's diurnal leaf pulvinar movements on the NDVI can also be recorded by remote sensors from space, since the acquisition time of the different sensors differ. A high solar irradiation at midday is assumed to cause a lower NDVI than in the morning as indicated in Figure 4.1a. In this context the MODIS (Moderate Resolution Imaging Spectroradiometer) sensor seems to be especially suitable to capture this difference in NDVI between morning (low solar irradiation, high NDVI) and midday (high solar irradiation, low NDVI), since the MODIS sensor on board of the Terra satellite acquires data for the study site at 10 a.m. (local time) and the MODIS sensor on board of the Aqua satellite acquires data at 1.30 p.m. (local time). Thus, the NDVI difference between morning and midday ($\Delta NDVI_{mo\text{-}mi}$) can be calculated as the difference between the NDVI MODIS Terra and the NDVI MODIS Aqua.

Considering the negative correlation between diurnal NDVI measurements and solar irradiation reported by Chávez et al. (2013a), we expect also seasonal NDVI variations associated with seasonal changes in solar irradiation with peaks in winter when the solar irradiation is the lowest. We hypothesize that this effect can also be recorded by sensors from space as indicated in Figure 4.1b. In this case, the Landsat TM (Thematic Mapper) and ETM (Enhanced Thematic Mapper) catalogue seems to be very suitable for studying NDVI seasonal variations since it offers one of the longest existing time series of systematically recorded satellite data worldwide (Williams et al. 2006). Besides, the Landsat catalogue is considered the most relevant satellite dataset for ecological applications and environmental monitoring (Birdsey et al. 2013; Cohen and Goward 2004). MODIS data might also be used to study seasonal effects of the pulvinar movements on the NDVI signal, providing images with a coarser spatial resolution (250 meters vs the 30 meters of Landsat), but with a higher temporal resolution (daily) enabling near real time vegetation monitoring (Verbesselt et al. 2012). However, the MODIS time series is considerably shorter than the Landsat time series (only since 2000).

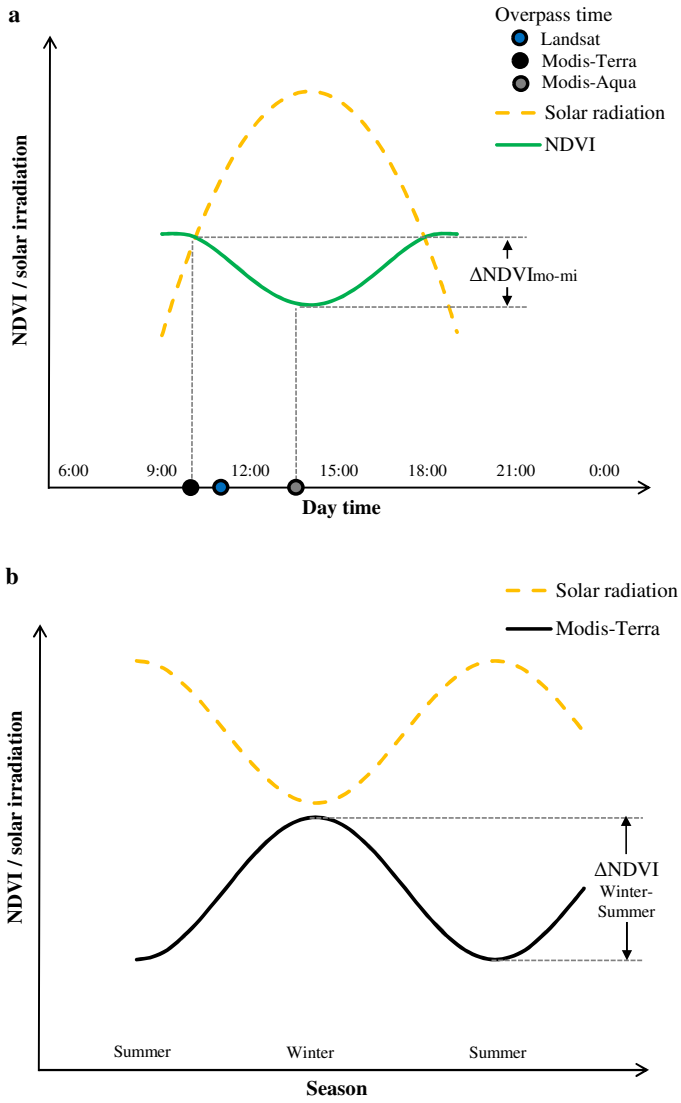

Figure 4.1. Conceptual diagram of the effect of leaf pulvinar movement on the NDVI signal. **(a)** NDVI difference between morning and midday ($\Delta NDVI_{mo\text{-}mi}$) occuring as solar irradiation changes during the day, and **(b)** NDVI difference between winter and summer ($\Delta NDVI_{W\text{-}S}$) occuring as solar irradiation varies between seasons. The time at which the Landsat (5-7), MODIS-Terra, and MODIS-Aqua satellites acquire data is displayed to illustrate the impact of pulvinar movements on the NDVI retrieved from these platforms.

Tamarugo is an endemic tree of the hyper-arid Atacama Desert, Northern Chile, a location considered among the most extreme environments for life (McKay et al. 2003; Navarro-González et al. 2003). The Tamarugo forest, locally known as Pampa del Tamarugal, sustains a biodiversity of about 40 species of plants and animals, some of them endemic for this particular ecosystem (CONAMA 2008; Estades 1996; Gajardo 1994; Ramírez-Leyton and Pincheira-Donoso 2005). Precipitation events are very rare and the only source of water supply for vegetation is the groundwater (GW), from which Tamarugo is completely dependent. However, not only Tamarugo trees are demanding water: the main economic activity in Atacama is mining, which is also demanding water for human consumption and for many industrial processes. This has led to an overexploitation of the GW sources and a progressive depletion of the GW over the whole Pampa del Tamarugal (Rojas and Dassargues 2007).

The natural Tamarugo forest was almost extinct in the 19th century and during the 1970's an enormous reforestation effort was carried out by the Chilean government and 13,000 hectares of Tamarugo were planted in the Pampa del Tamarugal basin (Zelada 1986). Currently, the Pampa del Tamarugal is under threat due to GW overexploitation. Chilean policy makers, scientists and private companies have debated intensively about defining environmentally safe GW extractions. To achieve this, good indicators of the Tamarugo water condition are needed and remote sensing, and specifically the NDVI, has proved to be useful for assessing Tamarugo's water condition (Chávez et al. 2013a; Chávez et al. 2013b). Nevertheless, time series of NDVI have not been directly related to GW depletion yet and to do so, the effect of the leaf pulvinar movements must be considered to understand a) the natural NDVI dynamic in the absence of water stress, and b) how this dynamic may be altered by GW depletion. In this paper, we use MODIS and Landsat NDVI time series to study both the natural and the altered NDVI dynamics of Tamarugo stands located in the Pampa del Tamarugal basin. Furthermore, we explore other biological (phenology) and environmental factors (precipitation) with potential effects on the NDVI signal.

4.2. Material and methods

4.2.1. Species description

Tamarugo is a phreatophytic desert tree that is highly specialized to survive the hyper-arid conditions of the Atacama Desert. This species belongs to the Leguminoseae family, Mimosaceae subfamily and it can reach up to 25 meters height, 20-30 meters crown size and 2 meters stem diameter (Altamirano 2006; Riedemann et al. 2006). The branches are arched and twigs flexuous with composite leaves, often bipinnate with 6-15 pairs of folioles (Figure 4.2b,c,f) (Trobok 1985). The Tamarugo petioles have a distinctive structure of motor cells in the pulvinus, responsible for the leaf paraheliotropic movements (Figure 4.2d,e,f). Differential turgor changes of the pulvinus cells make the leaves to stand up and orientate the leaf lamina parallel to the incoming sun rays. The composite leaves of Tamarugo have three levels of pulvinar structures: the first at the base of the bipinna, the second at the base of each pinna, and the third at the base of each of the folioles. This pulvinar mechanism at the three levels allows the Tamarugo canopy to adjust its internal structure to avoid facing excessive solar irradiation.

Figure 4.2. Pulvinar structures of *Prosopis tamarugo* Phil. leaves. **(a)** Tamarugo trees, **(b)** leaf angle randomly distributed during the morning when the solar radiation is low, **(c)** leaf angle in erectophyle position to avoid facing high solar irradiation at midday, **(d)** transversal section of a closed pulvinus (empty of water) during the morning, **(e)** transversal section of an open pulvinus (filled with water), which allows leaves to stand up and reach the erectophyle position, and **(f)** detail of the base of a Tamarugo pinna showing the three levels of pulvinar structures (at the base of the bipinna, of each pinna and each foliole).

4.2.2. Study area

The study area is located in the Atacama Desert (Northern Chile), specifically in the southern part of the Pampa del Tamarugal basin, where most of the remaining Tamarugo population is concentrated (Figure 4.3). The Tamarugo forest is practically the only ecosystem of the Absolute Desert eco-region (Gajardo 1994), and it is characterized by almost null precipitation, high day-night temperature oscillation, and high potential evapotranspiration (Houston 2006; Houston and Hartley 2003). Most of the plantation stands (Pintados and Bellavista) are in the southern part of the basin and within the study area. Just little natural patches of Tamarugo remain in the northern portion of the Pintados plantation (Figure 4.3). Although the oldest plantation stands were established as early as 1936, most of the existing plantation stands were planted between 1968 and 1972 (CONAF 1997). The plantation scheme consisted of squared 1×1 kilometres stands and trees separated 10×10 meters. Besides Tamarugo plantations, there are plantations of other *Prosopis* species, sometimes mixed with Tamarugo. Only pure Tamarugo plantation stands and some natural forest patches were considered in this study and they can be identified in Figure 4.3 as the green areas highlighted in black.

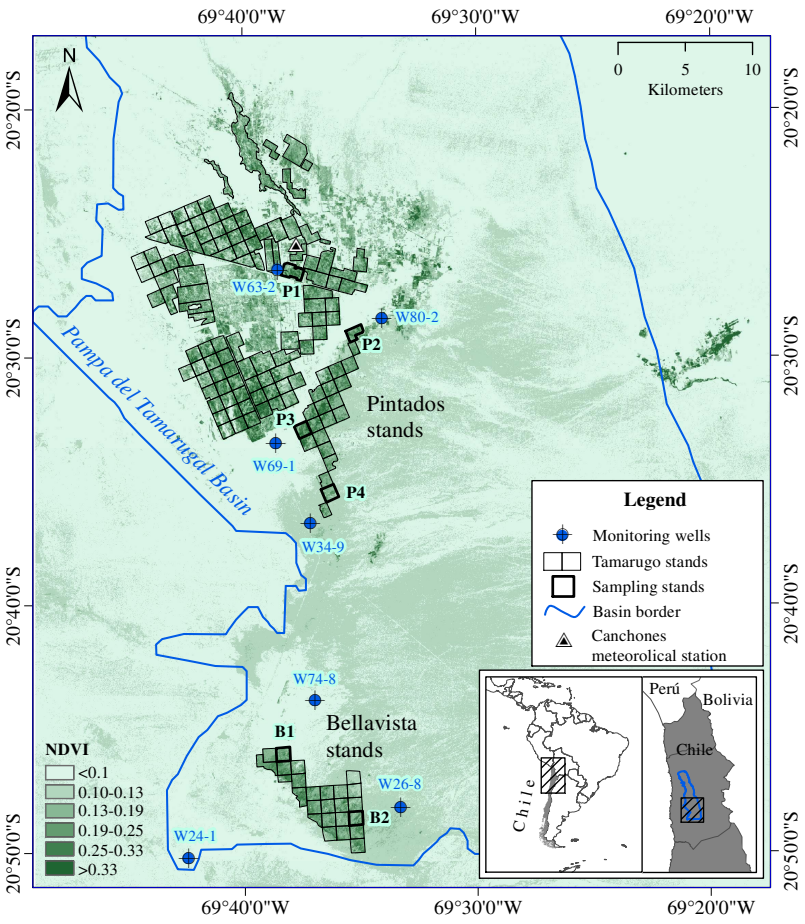

Figure 4.3. Landsat NDVI image (Winter 2007) showing the location of the Tamarugo stands in the Pampa del Tamarugal basin.

4.2.3. Landsat and MODIS NDVI time series

We used all available Landsat 5 TM and Landsat 7 ETM data (referred from here onwards in the text as 'Landsat' data) as well as MODIS-Terra and MODIS-Aqua data of the study area covering the period 1989-2012. We selected this time frame since this is the period of time with available GW depth records for most of the monitoring wells located in the study area (Figure 4.3). For the Landsat NDVI time series we used cloud free L1T images of 30 meters pixel resolution (471 scenes) corresponding to path 1 and row 34 and pre-processed using the Landsat

Ecosystem Disturbance Adaptive Processing System (LEDAPS) to obtain surface reflectance values for all spectral bands (Masek et al. 2006). Finally, we used the surface reflectance values of red and NIR to compute the NDVI for each date as follows: NDVI = (NIR-Red)/(NIR+Red). For the MODIS-Terra and MODIS-Aqua NDVI time series we used the MODIS 16-day composites at 250 meters pixel resolution (MOD13Q1 and MYD13Q1 data products). MODIS pixel reliability showed that 85% of the observations can be used with confidence (reliability = 0) and 15% were considered useful (reliability=1) of which MODIS vegetation index quality indicated average aerosol quantity. MODIS pixels with reliability 0 and 1 were considered in this study and showed consistent values for the NDVI time series of all forest stands. Both MODIS and Landsat data were downloaded from the USGS Earth Explorer website. Complementary, we used a panchromatic WorldView2 image of 0.6 meters pixel resolution to quantify the tree coverage of each plantation stand. This was carried out by using object-based image classification and the eCognition software following the procedure used by Chávez et al. (2013a).

4.2.4. Groundwater and climatic data

GW records were obtained from the monitoring network of the Dirección General de Aguas (DGA), the Chilean Water Service. From this network, seven wells were close to the Tamarugo stands and had enough records to establish a direct relationship between the groundwater table and the forest status (Figure 4.3). We averaged the (three to twelve) records of each year to obtain annual values of groundwater depth for the seven monitoring wells. Table 4.1 and Figure 4.3 show the location and details of the monitoring wells used in this study as well as the forest stands located close to each well. This way we obtained representative groundwater data for six Tamarugo stands for the period 1989-2012. In the case of stands B1 and B2, the groundwater depth was estimated using an inverse distance weighted interpolation of records from three wells (see Table 4.1).

Table 4.1. Plantation stands close to monitoring wells in the Pampa del Tamarugal basin.

Stand	Plantation year	Canopy coverage (%)	Closest monitoring well (DGA code)	Distance to well (km)	Groundwater depth (m) 1989	1997	2007	2012
B1	1968-1969	17	017000-74-8, 017000-26-8, 017000-24-1	4.7 9.5 10.4	10.99*	11.19*	11.64*	11.90*
B2	1968-1969	21	017000-74-8, 017000-26-8, 017000-24-1	9.3 3.4 12.8	14.75*	14.87*	15.45*	15.82*
P1	unknown	22	017000-63-2	0.4	7.97	9.03	9.93	10.26
P2	1972	25	017000-80-2	1.6	9.90	11.91	12.97	13.11
P3	1972	27	017000-69-1	1.7	5.70	6.26	6.87	6.89
P4	1972	11	017000-34-9	1.9	7.93	8.65	9.54	9.55

(*) Groundwater depth and depletion estimated using inverse distance weighted interpolation of 3 neighbouring wells.

Although groundwater is the main water source of the Tamarugo forest, sporadic precipitation may occur in the Atacama Desert, having a positive impact on the water status of the trees and the NDVI signal. For this reason, we included in our analysis precipitation records from the DGA meteorological station Huara en Fuerte Baquedano (20°07'51"S, 69°44'59"W) located about 30 km north from the study area and at a similar altitude (1,100 m). Solar irradiation records were obtained from the Canchones Experimental Station of the Universidad Arturo Prat (Chile), located next to the Tamarugo stand P1 in the northern part of the study area (Figure 4.3).

4.2.5. Data analysis

4.2.5.1. NDVI signal in the absence of water stress (natural dynamic)

Finding Tamarugo vegetation without nearby GW depletion in the Atacama Desert was a difficult task. We identified a Tamarugo forest stand (B1) and a time frame (2005-2008) with almost null GW depletion and no precipitation events in the southern part of the study area (see Figure 4.3, Bellavista stand). We assumed the NDVI time series of this three year period was not strongly influenced by the growth of trees. The Landsat, MODIS-Terra and MODIS-Aqua NDVI time series for the stand B1 were calculated using the median value of the pixels inside the

1×1 km stand. In the case of the Landsat time series we excluded pixels with NDVI values lower than 0.13, which were considered as no forest pixels. This threshold was set by considering the NDVI values observed outside the plantation stands, which correspond to completely bare areas (Figure 4.3). We first analysed the time series without any level of temporal aggregation, and then we aggregated the values to monthly averages in order to study the relationship between the NDVI and the monthly mean solar irradiation. For the latter purpose we used simple linear regression.

4.2.5.2. NDVI signal under water stress

After studying the natural dynamic of the NDVI time series for the three satellite sensors, we analysed the relationship between the average annual records of GW depletion and different metrics derived from the NDVI signal. To achieve this we used simple linear regression between the cumulative GW depletion and the NDVI derived metrics of the period between 1997 and 2007 with no precipitation. For the Landsat NDVI time series, these metrics were: annual NDVI average ($NDVI_{av}$), NDVI in winter ($NDVI_W$), and the NDVI difference between winter and summer ($\Delta NDVI_{W\text{-}S}$). For MODIS NDVI time series, these metrics were the $\Delta NDVI_{W\text{-}S}$ and the NDVI difference between morning and midday ($\Delta NDVI_{mo\text{-}mi}$). We calculated $\Delta NDVI_{W\text{-}S}$ and $\Delta NDVI_{mo\text{-}mi}$ for each year as follows:

(1) MODIS $\Delta NDVI_{W\text{-}S}$ = MODIS-Terra $NDVI_W$ – MODIS-Terra $NDVI_S$,
(2) Landsat $\Delta NDVI_{W\text{-}S}$ = Landsat $NDVI_W$ – Landsat $NDVI_S$, and
(3) $\Delta NDVI_{mo\text{-}mi}$ = MODIS-Terra $NDVI_W$ – MODIS-Aqua $NDVI_W$

Where:

$NDVI_W$ = average of all NDVI scenes from the months May, June and July (winter).

$NDVI_S$ = average of all NDVI scenes from the months November, December and January (summer).

In the case of the Landsat NDVI time series, we considered a minimum of three scenes for the summer and winter period to obtain a representative value of the respective season.

4.3. Results

4.3.1. Leaf pulvinar movement and the NDVI natural dynamic

In the absence of water disturbances (meaning GW extraction or precipitation events), the NDVI signal of the Tamarugo stand B1 presented a strong seasonal variation for the period 2005-2008, mainly explained by the seasonal variation of the monthly average solar irradiation (Figure 4.4). The R^2 for the linear relationship between NDVI and solar irradiation was 0.66 for the Landsat NDVI time series, 0.65 for the MODIS-Terra NDVI, and 0.41 for the MODIS-Aqua NDVI. We believe that the Tamarugo canopy reacted to the high solar irradiation in summer by having a predominantly erectophyle leaf angle distribution during daytime in order to minimize photoinhibition, similar to the diurnal mechanism reported by Chávez et al. (2013a). As a result, the canopy spectral reflectance decreased causing the NDVI to drop in summer. On the other hand, the lower solar irradiation in winter made the leaf pulvinar adjustment less necessary, resulting in a more random leaf angle distribution and in a higher NDVI. Partial foliage loss during the period May-September and the peak of the vegetative period occurring around October seemed to have only a marginal effect on the NDVI time series, noticeable as a small drop followed by a peak around October (green arrows in Figure 4.4). Overall, the seasonal variation is the main feature of the annual NDVI signal, and therefore the $\Delta NDVI_{W\text{-}S}$ may be used to detect the leaf pulvinar movement occurring in the Tamarugo canopy under natural conditions.

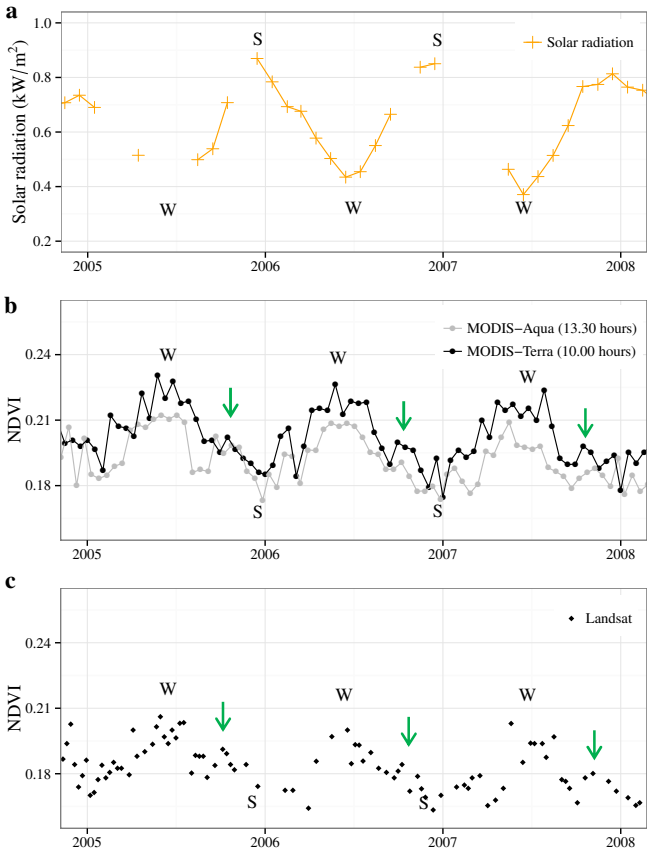

Figure 4.4. **(a)** Solar irradiation, **(b)** MODIS 16 days composite NDVI, and **(c)** Landsat NDVI of the B1 site (low groundwater depletion). Arrows indicate the peak of Tamarugo's vegetative period. S=summer, W=winter.

Besides the seasonal variation, the MODIS-Terra and MODIS-Aqua NDVI time series allowed to identify the $\Delta NDVI_{mo\text{-}mi}$ reported by Chávez et al. (2013a) on single Tamarugo trees, for instance for the Tamarugo stand B1 (Figure 4.4b). Although the $\Delta NDVI_{mo\text{-}mi}$ was clearly noticeable during winter, it was close to zero in summer. This was expected since both the morning and midday solar irradiation in the Atacama Desert are much higher in summer than in winter. For example, the average solar irradiation of June 2007 (winter) was 0.21 kW/m^2 at 10.00 hours and 0.62 kW/m^2 at 13.30 hours while the average of December 2006 (summer) was 0.87 kW/m^2 at 10.00 hours and 0.94 kW/m^2 at 13.30 hours. As a result, in winter the leaves will only have an erectophile position at midday, but in summer this

occurs already half way the morning (yielding a small $\Delta NDVI_{mo\text{-}mi}$). Based on what we observed in Figure 4.4 for a Tamarugo stand without water stress we can expect that it has a positive $\Delta NDVI_{mo\text{-}mi}$ in winter as well as a positive $\Delta NDVI_{W\text{-}S}$. Both NDVI derived metrics can be quantified and mapped using Landsat and MODIS images as shown in Figure 4.5.

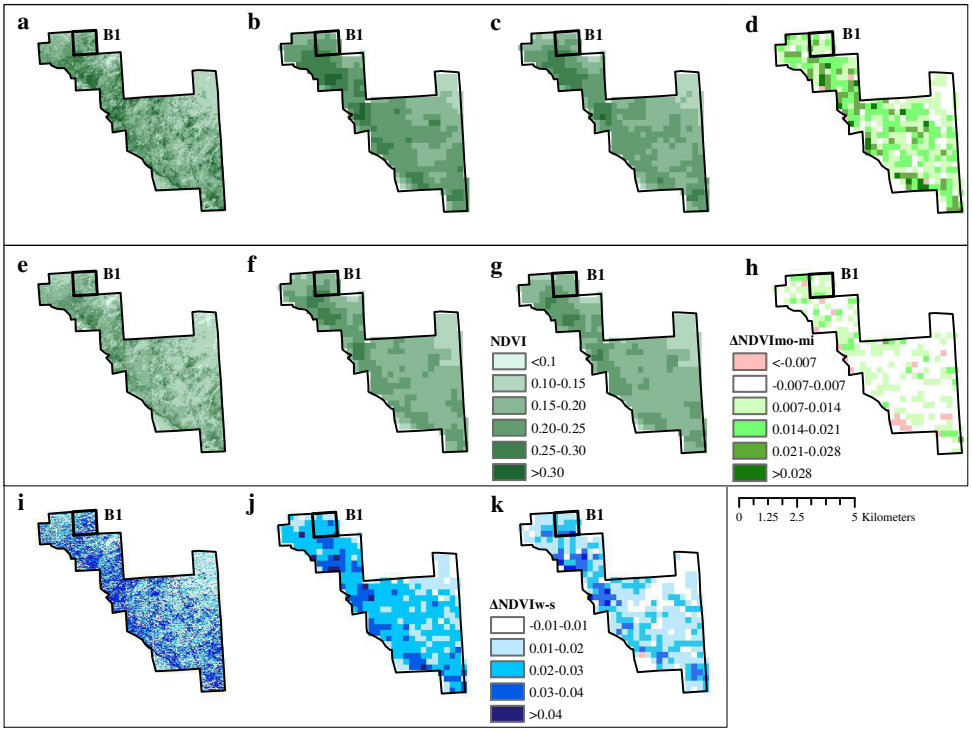

Figure 4.5. MODIS and Landsat NDVI of the Bellavista plantation in the **Winter 2007** with **(a)** Landsat NDVI, **(b)** MODIS-Terra NDVI (morning), **(c)** MODIS-Aqua NDVI (midday), **(d)** $\Delta NDVI_{mo\text{-}mi}$ = b-c, and in **Summer 2006-07** with **(e)** Landsat NDVI, **(f)** MODIS-Terra NDVI (morning), **(g)** MODIS-Aqua NDVI (midday), and **(h)** $\Delta NDVI_{mo\text{-}mi}$ = f-g. Graphs **i**, **j** and **k** display the **$\Delta NDVI_{W\text{-}S}$ 2007**, with (i) Landsat $\Delta NDVI_{W\text{-}S}$ = a-e, (j) MODIS-Terra $\Delta NDVI_{W\text{-}S}$ = b-f, and (k) the MODIS-Terra $\Delta NDVI_{W\text{-}S}$ = c-g.

Figure 4.5 displays the NDVI values at pixel level of all Bellavista plantation stands (including the stand B1) in the winter of 2007 (first row), the summer of 2006-2007 (second row), and the $\Delta NDVI_{W\text{-}S}$ of 2007 (third row) obtained from Landsat images (first column), MODIS-Terra images (second column), and MODIS-Aqua images (third column). The fourth column corresponds to the

$\Delta NDVI_{mo\text{-}mi}$ in winter (Figure 4.5d) and summer (Figure 4.5h) based on Terra (morning) and Aqua (midday). This figure confirms that the $\Delta NDVI_{mo\text{-}mi}$ in winter and the $\Delta NDVI_{W\text{-}S}$ of 2007 was positive for the forested area. On the other hand, the $\Delta NDVI_{mo\text{-}mi}$ in summer was zero or close to zero. In a similar way, and as a consequence of the diurnal pulvinar movements, the $\Delta NDVI_{W\text{-}S}$ was higher when using MODIS-Terra images than when using MODIS-Aqua images. Thus, the more promising indicators of pulvinar movement seemed to be the $\Delta NDVI_{mo\text{-}mi}$ in winter and the $\Delta NDVI_{W\text{-}S}$ in the morning (MODIS-Terra). When using the NDVI as a potential indicator of Tamarugo's water status, the signal in winter was stronger. The canopy coverage can also play an important role in the strength of the NDVI signal and its effect has to be considered when using these NDVI derived metrics for monitoring purposes. We will discuss this issue further in the next section where more Tamarugo stands, with different canopy coverage, were analysed.

4.3.2. Groundwater depletion: the NDVI signal under water stress

Figure 4.6 displays the annual time series of GW depth and the Landsat and MODIS $NDVI_W$, $\Delta NDVI_{W\text{-}S}$, and $\Delta NDVI_{mo\text{-}mi}$ for the six Tamarugo stands analysed in this study. The precipitation events are indicated with arrows. Only four precipitation events were recorded in the 24 years period analysed: 3.0 mm in 1996, 1.8 mm in 2008, 7.9 mm in 2011, and 2.2 mm in 2012, three of them during the last five years. The Landsat $NDVI_W$ signal reacted to the precipitation event of 1996 by showing a short recovering phase (about one year) and quickly returned to the general decreasing trend. For the precipitation events in the last years this effect was difficult to observe since they occurred close to each other in time. These precipitation events did not have any impact on the groundwater table, so we assumed this water was only available for the trees in the superficial soil layers. Apart from the precipitation events, the three analysed NDVI metrics seemed to follow the GW depth trend for all stands. To quantify this relationship, we calculated the multiple R^2 for the linear regression between each of the NDVI metrics and the cumulative GW depletion for the period without precipitation (1997-2007). We also included in this analysis the Landsat annual $NDVI_{av}$ values to check whether the $NDVI_W$ was a better indicator than the simple annual NDVI average. The results are given in Table 4.2.

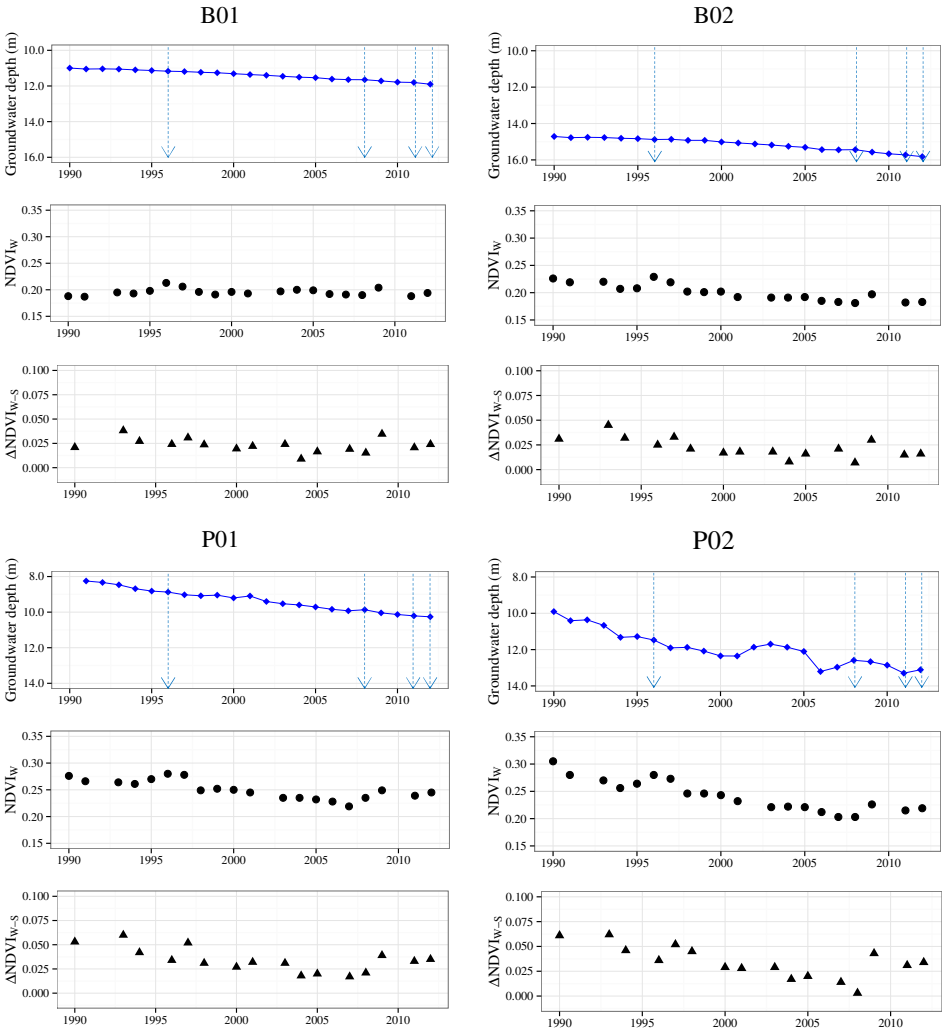

Figure 4.6. Time series of groundwater depth, Landsat $NDVI_W$, and Landsat $\Delta NDVI_{W\text{-}S}$ for six Tamarugo plantation stands in the Pampa del Tamarugal basin. Blue arrows indicate precipitation events.

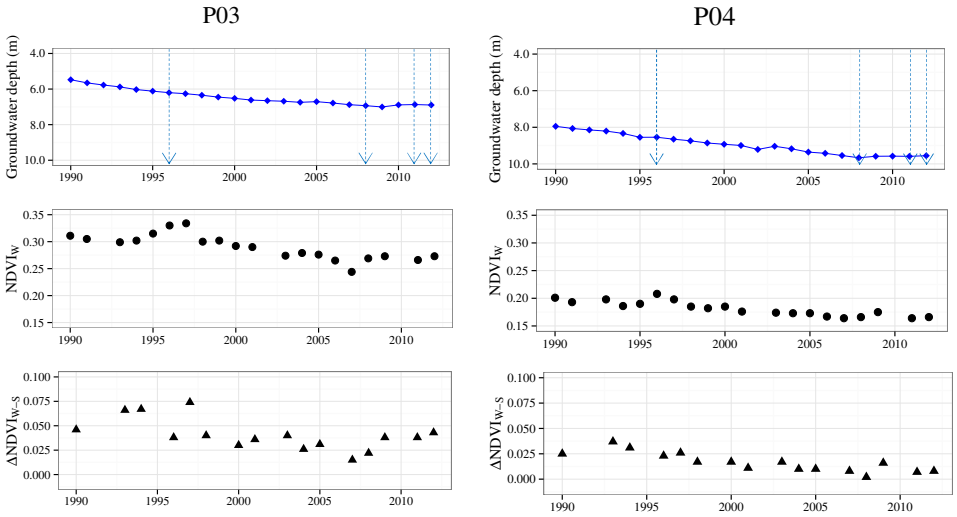

Figure 4.6 (cont.). Time series of groundwater depth, Landsat $NDVI_W$, and Landsat $\Delta NDVI_{W\text{-}S}$ for six Tamarugo plantation stands in the Pampa del Tamarugal basin. Blue arrows indicate precipitation events.

Table 4.2. Multiple R^2 of the linear model of cumulative groundwater depletion v/s $NDVI_{av}$, $NDVI_W$, $\Delta NDVI_{W\text{-}S}$ and $\Delta NDVI_{mo\text{-}mi}$ for the period 1997-2007 (no precipitation events).

Stand	Cumulative GW depletion (1997-2007)	Landsat $NDVI_{av}$ n=11	Landsat $NDVI_W$ n=10	Landsat $\Delta NDVI_{W\text{-}S}$ n=8	MODIS $\Delta NDVI_{W\text{-}S}$ n=4	MODIS $\Delta NDVI_{mo\text{-}mi}$ n=5
B1	0.45	<0.1	0.13	0.44*	0.55	0.29
B2	0.58	0.74***	0.76***	0.26	0.76	0.35
P1	0.90	0.58***	0.75***	0.60**	<0.1	<0.1
P2	1.06	0.27*	0.29	0.24	0.70	0.70
P3	0.61	0.82***	0.90***	0.70***	0.66	0.14
P4	0.89	0.77***	0.85***	0.74***	<0.1	0.52

Significative linear relationship with ***P<0,01; **P<0.05, *P<0.1

The Bellavista Tamarugo stands (B1 and B2) are located in the southern part of the basin and far from the area where the pumping wells are concentrated, which is towards the north and east of the Pintados stands (Figure 4.3). For this reason, the GW depletion in the stands B1 and B2 was less in comparison to the stands of the Pintados sector (P stands), especially in the case of P2. The stand B1 showed the lowest cumulative depletion (0.45 m) for the period 1997-2007 as well as the lowest R^2 (<0.1) for the relationship between Landsat $NDVI_{av}$ and GW depletion.

Furthermore, the R^2 of the GW depletion - Landsat $NDVI_W$ relationship was also the lowest, but higher than the GW depletion - Landsat $NDVI_{av}$ relationship. In fact, this was the case for almost all stands. Thus, the Landsat $NDVI_W$ was more sensitive to changes in GW depth than the Landsat $NDVI_{av}$. This was also the case when comparing Landsat $NDVI_W$ with Landsat $\Delta NDVI_{W-S}$. Only for the stand B1, the R^2 of the Landsat $\Delta NDVI_{W-S}$ - GW depletion relationship was higher than for the $NDVI_W$ - GW depletion relationship.

The rest of the stands showed GW depletions between 0.58 and 1.06 meters between 1997 and 2007 and R^2 values for the Landsat $NDVI_W$ - GW depletion relationship higher than 0.75 except for the stand P2 with an R^2 of 0.29. The stand P2 is located close to the pumping area, and therefore the GW depletion could have been influenced by short-term changes of the pumping rate. If the intra-annual GW values fluctuated too rapidly, the depletion may not have had an effect on the NDVI signal. However, this is difficult to detect in annually averaged records. Overall the Landsat $NDVI_W$ was the most sensitive NDVI derived metric to the 11-year changes in GW depletion.

In the case of the MODIS NDVI derived metrics, the R^2 values presented in Table 4.2 were difficult to interpret since the time series without precipitation events was very short (2003-2007). We found R^2 values as high as 0.70 when using the MODIS $\Delta NDVI_{W-S}$ (stand B2) and the MODIS $\Delta NDVI_{mo-mi}$ (stand P2), but also <0.1 (stands P1 and P4) for $\Delta NDVI_{W-S}$ or $\Delta NDVI_{mo-mi}$ (stand P3).

4.3.3. Mapping water stress using Landsat $\Delta NDVI_{W-S}$

The $NDVI_W$ and $\Delta NDVI_{W-S}$ showed good potential to assess the effect of GW depletion on the water status of Tamarugo trees. We selected the Landsat $\Delta NDVI_{W-S}$ to map this effect in the study area because we believe it senses water stress earlier than $NDVI_W$ (see Discussion section for more details). We mapped the $\Delta NDVI_{W-S}$ for three different years: 1997, 2007, and 2011 as shown in Figure 4.7 averaged to a 1×1 km grid. The $\Delta NDVI_{W-S}$ difference between 1997 and 2007 can be explained by groundwater depletion since no precipitation events occurred in this period. For most of the stands, the $\Delta NDVI_{W-S}$ values in 2011 showed a recovery of the forest after the precipitation event of 2011 (7.9 mm), the most intense rain recorded in the last 25 years in Pampa del Tamarugal. The stands with more stable $\Delta NDVI_{W-S}$ through time were those located at the west border of the Bellavista plantation, close to the well W24-1, which reported very shallow GW

depths in 1997 (2.6 m), 2007 (3.0 m), and 2011 (3.1 m). Furthermore, a $\Delta NDVI_{W-S}$ gradient can be observed in the Bellavista sector from east to west, showing a good spatial agreement with the increasing GW depletion towards the east (GW depth in well W26-8 was about 19.6 m in 1997, 20.3 m in 2007, and 21 m in 2011).

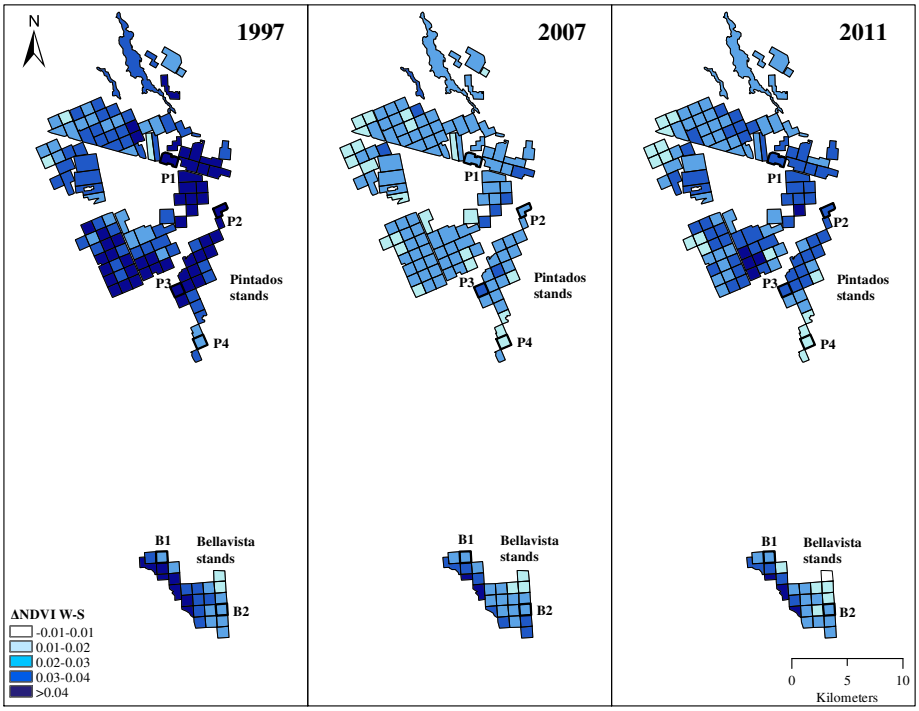

Figure 4.7. Landsat $\Delta NDVI_{W-S}$ of all plantation stands in the southern area of the Pampa del Tamarugal basin in 1997, 2007 (period with no precipitation), and 2011 (after a precipitation event).

4.4. Discussion

Early stages of water stress in plants are associated with a lower leaf water potential, reduction in transpiration rate, and foliage water loss while late stages are associated with pigment degradation, biomass loss, and finally dying plants (Alpert and Oliver 2002; Baret et al. 2007; Taiz and Zeiger 2010). Although Tamarugo trees are naturally adapted to the predominant water scarcity of the Atacama desert, they can be affected by water stress due to GW depletion as

shown in this paper. From previous papers (Chávez et al. 2013a; Chávez et al. 2013b), we know that Tamarugos show the typical water stress symptoms of most plants, but additionally water stress limits the normal functioning of the leaf pulvinar mechanism. These pulvinar movements are typical for heliotropic species. Furthermore, we have shown that leaf pulvinar movement can be remotely sensed by different metrics derived from the NDVI signal, allowing to understand both the temporal natural dynamic of the Tamarugo forest and the effects of GW depletion. In Table 4.3 we give an overview of the water stress symptoms of Tamarugo trees, the temporal scale at which they occur, and the NDVI derived metrics we can use to study these symptoms.

Table 4.3. Water stress stages of Tamarugo desert trees and NDVI based variables to assess their effects using satellite remote sensing.

Water stress			**Remote sensing**	
Stage	**Effects on Tamarugo vegetation**	**Temporal scale to perceive the effects**	**Monitoring variable**	**Sensor useful to retrieve this variable**
Instantaneous	Limitation of the diurnal photoinhibition control via pulvinar movements	Diurnal	$\Delta NDVI_{mo\text{-}mi}$	MODIS Terra and Aqua
Early	Limitation of the seasonal photoinhibition control via pulvinar movements	Seasonal	$\Delta NDVI_{W\text{-}S}$	MODIS Terra, Landsat
Advanced	Foliage loss	More than 1 year	$NDVI_W$	MODIS Terra, Landsat
Irreversible	Partial crown death and tree death	Several years	$NDVI_W$	MODIS Terra, Landsat, combined with very high spatial resolution sensors: Quickbird2, WorldView2 or GeoEye

Diurnal leaf movements can be studied using $\Delta NDVI_{mo\text{-}mi}$ from MODIS Terra and Aqua satellites as shown in this paper. No significant differences have been found for the MODIS NDVI Terra and Aqua for other non-solar tracker vegetation (Wang et al. 2007; Wu et al. 2008). Since these two satellites acquire data on a

daily basis, it would be possible to map the $\Delta NDVI_{mo\text{-}mi}$ of the Pampa del Tamarugal basin every day at a spatial resolution of 250×250 m. This way, the effects of an abrupt GW depletion could be identified using MODIS data if the forest is dense enough to provide a sufficiently strong signal as well as large enough to cover one or more MODIS pixels (Verbesselt et al. 2009; Wolfe et al. 2002). In this paper we analysed averaged $\Delta NDVI_{mo\text{-}mi}$ values for the winter seasons and its relationship with annual records of GW depth. This time series was rather short, sometimes resulting in low R^2 values. Perhaps better results can be achieved when using the full temporal resolution (daily or 16 days) of the MODIS NDVI products and more detailed records of the water availability. This is an interesting topic for further research and not only for Tamarugo plants, but also for detecting short-term water stress in, e.g., bean crops, which also have documented paraheliotropic behaviour (Pastenes et al. 2005; Pastenes et al. 2004).

Seasonal differences of leaf pulvinar adjustments of Tamarugo vegetation can be studied at a large scale using the $\Delta NDVI_{W\text{-}S}$ as measured from Landsat (Figure 4.7) and MODIS Terra satellites. The advantage of using Landsat images is the possibility to map this variable at 30 meters pixel resolution and the disadvantage is that these satellites (Landsat 5, 7 and 8) have a revisit time of 16 days, increasing the chance of missing dates due to cloud cover. Although cloud cover is not such as problem in deserts, missing data can have an important impact on the calculation of the $\Delta NDVI_{W\text{-}S}$ if the NDVI values of winter or summer are not well represented by sufficient images. In this paper, we considered a minimum of three Landsat scenes for calculating a representative value of the summer or winter period. The NDVI signal of Tamarugo showed a strong seasonality (Figure 4.4c) and, for example, a calculation of the $NDVI_W$ using one or two images in May and a calculation of the $NDVI_S$ using one or two images in December may lead to a serious underestimation of the $\Delta NDVI_{W\text{-}S}$. This is not a problem for MODIS 16-day composites, which provide five or six images for the winter and summer period systematically distributed within the three months' timeframe. Therefore, there is a trade-off between temporal and spatial resolution when choosing Landsat or MODIS to detect the $\Delta NDVI_{W\text{-}S}$.

If the water stress persists, Tamarugo trees will react by selectively shutting down leaves, twigs and entire branches to reduce the transpiration surface while keeping the remaining foliage green with hydric parameters within normal ranges (Chávez et al. 2013a). Foliage loss has been successfully assessed using NDVI for a wide

range of vegetation types and it is especially accurate for LAI values <2 (Gamon et al. 1995). Such assessments are usually carried out at the peak of the vegetative period, usually in spring. In the case of Tamarugo the seasonal variation of the NDVI signal is mainly driven by the pulvinar movements, which are primarily driven by seasonal changes in solar irradiation. Thus, the 'pulvinar effect' on the NDVI signal is minimum in winter and therefore this is the best time to retrieve the NDVI for inter annual foliage loss estimations (Table 4.3).

The strong relationship between $NDVI_W$ and cumulative GW depletion observed for most of the Tamarugo stands is an indication that foliage is decreasing in the study area as a consequence of water extraction, in other words, the forest is reaching an advanced stage of water stress (Table 4.3). However, it was not possible to discriminate whether the decreasing $NDVI_W$ signal was because some trees were dying while others remained alive (intra species competition) or all trees were losing foliage gradually. The tree coverage played also an important role in the absolute value of the $NDVI_W$ signal and, therefore, it was not possible to directly compare different stands at a single point in time. In order to better interpret the Landat and MODIS $NDVI_W$ signal, we believe that high spatial resolution remote sensing data can provide complementary information about the actual tree coverage of the forest as well as the water status of single trees. This will be the topic for further research.

4.5. Conclusions

i. Leaf pulvinar movements are the main factor explaining both diurnal and seasonal changes of the NDVI signal measured for Tamarugo plantations in the Atacama Desert. Because leaf pulvinar movement is driven by changes in solar irradiation, there was a negative correlation between the NDVI signal of the forest and the seasonal values of solar irradiation.

ii. The NDVI difference between midday and morning ($\Delta NDVI_{mo\text{-}mi}$), as measured by the difference of the NDVI signal from the MODIS Terra and Aqua satellites, can be used to detect the diurnal leaf pulvinar movement of Tamarugo plantation stands. This has not been reported in literature before, and therefore, this paper constitutes a proof of concept that MODIS images can be used to detect diurnal movements of paraheliotropic vegetation.

iii. Similarly, the NDVI difference between winter and summer ($\Delta NDVI_{W\text{-}S}$), as measured by the Landsat or the MODIS Terra satellites, can be used to detect differences in seasonal pulvinar movements, associated to photoinhibition regulation.

iv. Leaf pulvinar movements are triggered by changes in cell turgor and they can be limited by water stress. Thus, water stress in Tamarugo vegetation caused by groundwater overexploitation can be assessed and monitored using $\Delta NDVI_{mo\text{-}mi}$ and $\Delta NDVI_{W\text{-}S}$. For long time series (more than 10 years), Landsat $\Delta NDVI_{W\text{-}S}$ of Tamarugo stands showed a negative linear relationship with cumulative groundwater depletion.

v. Under water stress, a limitation of the pulvinar movement occurs in Tamarugo trees before they start losing foliage. For this reason, changes in $\Delta NDVI_{mo\text{-}mi}$ and $\Delta NDVI_{W\text{-}S}$ are expected to occur before NDVI decreases due to foliage loss, and therefore, $\Delta NDVI_{mo\text{-}mi}$ and $\Delta NDVI_{W\text{-}S}$ have potential for early water stress detection.

Acknowledgements

The authors would like to thank Digital Globe for providing the WorldView2 imagery and UNAP (Chile) for providing the solar irradiation records. Especial thanks to L. Dutrieux, B. de Vries, M. Schultz, and J. González de Tanago from Wageningen University for the valuable contribution of R code for the time series analysis. Finally, we thank V. Urra and G. Valenzuela from Universidad de Chile for their collaboration on the anatomical description of Tamarugo leaves.

Chapter

5

50 years of groundwater extraction in the Pampa del Tamarugal basin: can Tamarugo trees survive in the hyper-arid Atacama Desert?

R.O. Chávez, J.G.P.W. Clevers, M. Decuyper, S. De Bruin, M. Herold

Ecological Applications (Submitted).

One of the most extreme ecosystems on Earth, the Pampa del Tamarugal in the hyper-arid Atacama Desert, is under threat due to groundwater overexploitation. The Pampa del Tamarugal aquifer is one of the most important sources of fresh water for urban areas and industry in northern Chile. Although there is concern among Chilean environmental agencies about the conservation of this ecosystem, little research has been done so far to quantify the spatio-temporal effects of groundwater depletion on the Tamarugo trees. In this study, we used a dense time series of Landsat images combined with high spatial resolution satellite images and hydrogeological records to provide a quantitative assessment of the water status of Tamarugo trees after 50 years of increasing groundwater extraction. Since Tamarugo trees are solar trackers, canopy spectral reflectance (as measured by satellites) changes on a diurnal and seasonal basis. For this reason, a careful interpretation of remote sensing time series needs to be made for assessing the effects of groundwater depletion on Tamarugo trees. To estimate the water status of the trees, we used three metrics derived from the normalized difference vegetation index (NDVI): the Landsat NDVI in winter ($NDVI_W$), the Landsat NDVI difference between winter and summer ($\Delta NDVI_{W-S}$), and the green canopy

fraction (GCF) of single trees from high spatial resolution images. The results showed that the $NDVI_W$ and $\Delta NDVI_{W-S}$ of the areas with Tamarugo declined 19% and 51% as groundwater depleted (3 m on average) for the period 1989-2013. Both variables were negatively correlated to groundwater depth both temporally and spatially. About 730.000 Tamarugo trees remained in the study area by 2011, from which 5.2% showed a GCF<0.25 to be associated to severe water stress. Based on this spatio-temporal analysis, we suggest a maximum groundwater depth of 20 m as a threshold for survival of Tamarugo trees.

Keywords

Arid ecosystems; water stress; groundwater extraction; time series; remote sensing; normalized difference vegetation index; water management

5.1. Introduction

Water is a limiting resource for wildlife and human activities in arid and semi-arid areas. As national economies develop, the pressure for using the scarce water sources of desert basins to provide water to urban centers and industry increases, becoming a threat for desert ecosystems worldwide (Ezcurra 2006; Le Maitre et al. 1999; Pringle 2001). The main water source in deserts is the groundwater (GW) and several authors have highlighted the importance of assessing the negative impacts of GW extraction on natural vegetation (Elmore et al. 2006; Elmore et al. 2003; Naumburg et al. 2005; Patten et al. 2008). Desert vegetation provides important ecosystem services such as the regulation of the hydrological cycle, the conservation of endemic and rare species, and the provision of an oasis for local settlements, grazing and small scale agriculture (Ezcurra 2006). The expected decrease in available fresh surface water due to global warming together with the future increase of water consumption at global scale, make GW overexploitation likely to occur (Wang et al. 2014). As a result, the main challenge for water managers today is to promote a sustainable exploitation of GW aquifers compatible with the conservation of desert ecosystems (Elmore et al. 2003). Chilean environmental institutions are already facing such a challenge in the Pampa del Tamarugal aquifer, where one of the most extreme desert ecosystems still remains in the heart of the Atacama Desert (Northern Chile).

The Pampa del Tamarugal aquifer is the only source of drinking water for a large area in the Atacama Desert and for more than 50 years GW has been extracted to supply water to urban areas (including important cities like Iquique), the mining industry and agriculture (Figure 5.1). From 1988 onwards the authorized GW extractions have exceeded the natural recharge of the aquifer (Figure 5.1) inducing a depletion of the GW table in the whole aquifer (Rojas et al. 2010; Rojas and Dassargues 2007). This unbalance in the water budget is threatening the Tamarugo ecosystem, which is completely dependent on GW and limited to the areas with shallow GW. The main species of this ecosystem is the Tamarugo tree: an endemic tree species of the Atacama Desert. The 'Pampa del Tamarugal' formation provides habitat to about 40 other plant and animal species, some of them endangered and/or endemic species (CONAMA 2008; Estades and López-Calleja 1995; Ramírez-Leyton and Pincheira-Donoso 2005). Currently, most of the Tamarugo ecosystem is under protection in the Pampa del Tamarugal National Reserve, administrated by the Chilean Forest Service (CONAF), but question is whether CONAF can protect this ecosystem from the impact of GW extraction occurring in the whole aquifer.

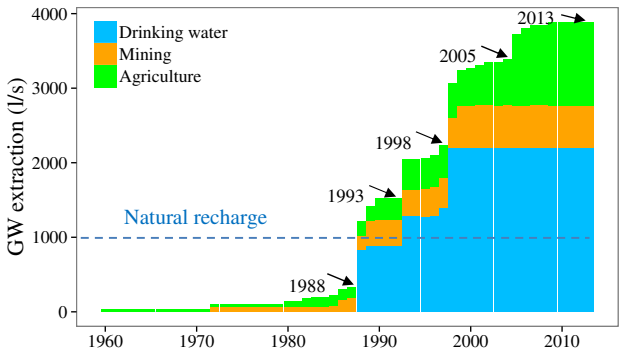

Figure 5.1. Legally authorized groundwater extraction and estimated natural recharge for the Pampa del Tamarugal aquifer in the period 1960-2013 (Source: DGA, 2011)

Considering the cumulated GW depletion after 50 years of extractions, the Chilean Water Service (the Dirección General de Aguas, DGA) officially declared the Pampa del Tamarugal aquifer as 'restricted area' (Res. DGA Number 245) in 2009. Hence, no new GW extraction will be authorized from 2009 onwards. Although this is a positive action towards the conservation of the Tamarugo ecosystem, still the question remains whether this restraint is enough to consider the Tamarugo

trees as safe in the future. There is consensus among environmental authorities on the decline of the Tamarugo trees due to GW depletion. However, there is a lack of studies quantifying the magnitude and extent of the impacts on the water status of the trees. Furthermore, there is no clear definition of a groundwater depth (GWD) threshold under which the water status of Tamarugo trees can be considered as below normal conditions. These three aspects: the magnitude of the impacts, the extent and the thresholds for Tamarugo's survival are required for environmental impact assessment and water management. In this paper, we attempt to approach these aspects by analyzing different remote sensing datasets and hydrogeological data.

Although previous studies have shown the usefulness of remote sensing for assessing water stress of Tamarugo (Chávez et al. 2013a; Chávez et al. 2013b; Chávez et al. 2014), these findings have not been applied on a large scale yet. In these studies, the normalized difference vegetation index (NDVI) has proved useful to assess the water stress of Tamarugo from the tree level (using high spatial resolution satellites) to the stand level (using satellites with coarser sensors such as Landsat or MODIS). NDVI is a well-known estimator of the green biomass of vegetation, widely utilized to assess the impacts of natural and anthropogenic disturbances on vegetation (Fensholt et al. 2009; Mao et al. 2012; Pettorelli et al. 2005). However, there is an important botanical characteristic of this evergreen species that must be considered when using NDVI for water stress assessment: Tamarugo trees are heliotropic plants or 'solar trackers'. They sense the increasing solar irradiation during the day and adjust the orientation of leaves (leaf pulvinar movements) to avoid facing the sun rays at the hottest time of the day, causing a diurnal variation in the NDVI signal (Chávez et al. 2013a; Chávez et al. 2013b). Similarly, this mechanism gets more active in summer than in winter, causing a seasonal variation in the NDVI signal with low values in summer and high values in winter (Chávez et al. 2014).

In the study of Chávez et al. (2014), the authors showed that the NDVI signal in winter ($NDVI_W$) was negatively correlated to cumulative GW depletion, in other words $NDVI_W$ decreases as GWD increases. In the same study the authors proposed a new water stress indicator: the NDVI difference between winter and summer ($\Delta NDVI_{W-S}$), which was related to the capacity of Tamarugo to perform leaf pulvinar movements. Due to its nature, $\Delta NDVI_{W-S}$ was considered an early indicator of water stress, since the limitation of the leaf movements occurred under

stress before Tamarugo started shutting down green foliage (Chávez et al. 2013a; Chávez et al. 2013b). In this paper, we hypothesize that both indicators ($NDVI_W$ and $\Delta NDVI_{W-S}$) are spatially and temporally correlated to GWD, making a quantitative assessment of the impacts of GW extractions in the Pampa del Tamarugal aquifer possible. Furthermore, we aim to provide useful information for operational Tamarugo's conservation practices and GW management by combining the high temporal resolution of Landsat with high spatial resolution satellite images. Specifically we aim to:

1. Establish the spatial and temporal (1989-2013) relationship between the water status of the Tamarugo trees, as estimated by NDVI derived metrics, and changes in GWD caused by GW extraction.
2. Provide an up-to-date inventory and water status assessment of Tamarugo single trees using very high spatial resolution remote sensing.
3. Based on the spatio-temporal assessment of Tamarugo's water status, define a GWD threshold to ensure the conservation of the Tamarugo population.

5.2. Material and methods

5.2.1. Species description

Tamarugos are thorny desert trees highly specialized to survive the aridness of the hyper-arid Atacama Desert, a place considered among the more extreme environments for life (McKay et al. 2003; Navarro-González et al. 2003). This endemic species of the Atacama Desert belongs to the Leguminoseae family and exhibits a large range of phenotypes. In adverse conditions, Tamarugos express a shrub-like phenotype, about two m high and 2-3 m crown size, while Tamarugos express a tree-like phenotype under favourable conditions, reaching up to 25 m high and 20-30 m crown size (Altamirano 2006; Chávez et al. 2013a; Riedemann et al. 2006).

Several adaptations to survive the harsh conditions of the Atacama Desert have been described for Tamarugo. They are phreatophytic species (Aravena and Acevedo 1985; Mooney et al. 1980) with a dual root system: a deep taping root and a dense superficial root mat (Sudzuki 1985b). It has been suggested that

Tamarugos' root system moves water from the GW to the root mat layer during the night to ensure water supply during the growing season when the water demand at the capillary fringe increases (Mooney et al. 1980). Furthermore, like other Legiminoseae plants Tamarugo trees are solar trackers (Chávez et al. 2013a; Chávez et al. 2013b). They adjust the angle of the leaves as solar irradiation increases to avoid facing direct sun rays at the hottest time of the day (paraheliotropism) and this way enhance the photosynthetic process and avoid photoinhibition. Paraheliotropic leaf movements have been reported for many other desert plants and some major crops (Ehleringer and Forseth 1980; Pastenes et al. 2005; Pastenes et al. 2004). Another remarkable adaptation is its osmotic regulation capacity allowing rapid stomata closure as temperature and vapour pressure deficit increase during the day (Acevedo et al. 1985; Ortiz et al. 2010). In summary, Tamarugos optimize the water budget by enhancing the GW intake and by reducing evapotranspiration due to excessive solar irradiation.

5.2.2. Study area

The study area comprises all Tamarugo plantations of the 'Lote3' of Pampa del Tamarugal National Reserve and some plantation stands and natural vegetation located in private areas surrounding the Reserve (Figure 5.2). The study area covers the two sectors where most of the remaining Tamarugo population is concentrated: the Salar de Pintados and the Salar de Bellavista. Both sectors are located in the south-west part of the Pampa del Tamarugal aquifer where the GW table is relatively shallow (5-15 m). Since GW levels are close to the surface, these sectors show a high evaporation causing salt accumulation in the upper layers of the soil. This has led to the formation of salt-flats, locally known as 'salares', with Salar de Pintados and Salar de Bellavista as the largest ones in the Pampa del Tamarugal Aquifer.

The Pampa del Tamarugal aquifer is situated in the dry plains located between the Andes mountain range and the Pacific Ocean, covering an area of about 5,000 km^2 (Rojas and Dassargues 2007). It is 130-160 km long, 13-60 km wide and located 45 km away from the coast line at an altitude of 1,000 m (JICA-DGA-PCI 1995; Rojas and Dassargues 2007). Since precipitation is practically inexistent, the recharge comes laterally from the eastern sub-basins through infiltration and GW flow (Houston 2002; Rojas and Dassargues 2007). Several authors have estimated the recharge of the aquifer (DICTUC 2008; DICUC 1988; JICA-DGA-PCI 1995;

Rojas and Dassargues 2007), showing a general agreement on a value of about 1,000 l/s. However, artificial discharge (pumping) has dramatically increased since the 1980's causing a sustained negative water balance and an overall lowering of the GW table (CIDERH 2013; Rojas and Dassargues 2007).

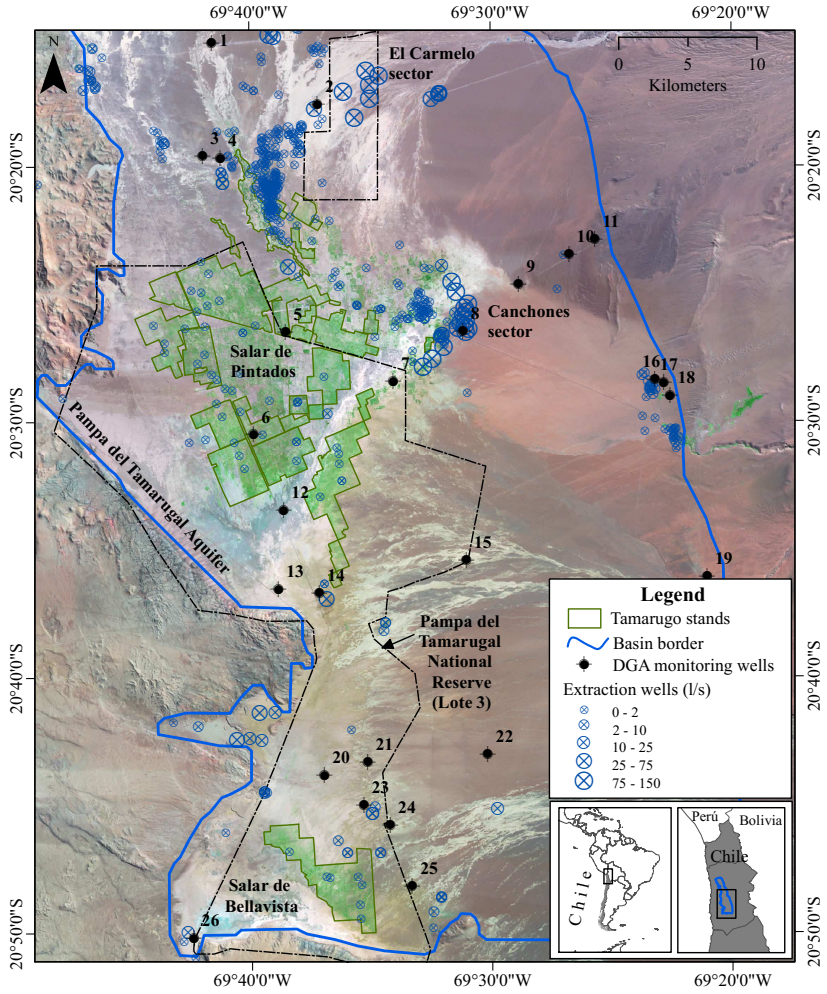

Figure 5.2. Landsat mosaic showing the study area in the Atacama Desert (Northern Chile). Monitoring wells are obtained from the DGA network (updated to 2013) and extraction wells from DGA (2011).

The natural Tamarugo trees were almost extinct in the 19th century due to overexploitation for wood supply and fuel for the saltpetre industry (Zelada 1986).

Although there were attempts to reforest Pampa del Tamarugal as early as 1936, it was not until the 1970's when an enormous reforestation effort was carried out by the Chilean government and about 13,000 hectares were planted. Trees were planted in 40 cm deep holes in a regular 10x10 m grid by removing the salt crust. Plants were put in the shadowed south base of the holes and watered during the first year of establishment till the root system was tapping the GW (Habit 1981; Mooney et al. 1980). During the reforestation of the Pampa del Tamarugal also some other *Prosopis* species were planted, sometimes mixed with Tamarugo. Nevertheless, only pure Tamarugo stands were considered in this study (see the highlighted green areas in Figure 5.2).

5.2.3. Hydrogeological data

We searched for all available data of extraction wells, monitoring wells and historical GWD maps of the Pampa del Tamarugal aquifer, complemented with precipitation records. Although precipitation hardly occurred in the study area, the few rainfall events can have an impact on the NDVI signal of the Tamarugo forest (Chávez et al. 2014). The sources of information used in this study are as follows:

Extraction well data (DGA 2011). We considered the 740 extraction wells used by DGA to calculate artificial discharge from the Pampa del Tamarugal aquifer (Figure 5.2). We obtained from each well the location, the authorized GW extraction (l/s) and the year in which the extraction request was issued. We assigned this year as the starting year of extraction, since the authorization year was absent for many wells.

Monitoring wells from the DGA network (1989-2013). We used 26 wells located in the center-south part of the aquifer with GWD records updated till December 31st, 2013 (Figure 5.2). These wells are part of the current operational DGA network. Only 13 wells had records for the period 1989-2013 and the other 13 for the period 1998-2013. The records obtained this way were used to calculate mean annual GWD values for each well considering only years with at least three measurements (see Table A1 in the Annex).

GWD grid maps (1988-2013). Sources for these maps were the study of JICA-DGA-PCI (1995) for the years 1988 and 1993 and GWD interpolations made in this study using the 27 DGA monitoring wells for the period 1998-2013. For the GWD interpolations 1998-2013 we used spatial interpolation by ordinary point

kriging, as implemented in the gstat package (Pebesma 2004) of the R software (R Core Team 2013). Assuming temporal stationarity of the spatial correlation structure, a single experimental variogram was computed by pooling point pairs from different years. Spatio-temporal interpolation was not attempted because of lack of data for fitting a spatio-temporal variogram. An exponential variogram model was fitted (nugget=15, psill=280, and range=7,000). GWD data for the period 1998-2013 were interpolated by ordinary point kriging to a square grid with 90 m spacing. We performed a leave-one-out cross-validation to check the kriging assumptions; Z-scores of the residuals were normally distributed with mean -0.01 and standard deviation of 1.28. The deviation from 1 of the standard deviation was caused by a few large residuals located outside the forested area (see Figure A2 in Annex 1), corresponding to wells close to the pumping areas.

Precipitation records (1992-2013). These were obtained from the DGA meteorological station Huara en Fuerte Baquedano, located about 30 km north from the study area (20°07'51"S, 69°44'59"W) at similar altitude (1,100 m).

5.2.4. Landsat NDVI derived metrics

We used all available Landsat 5 TM and Landsat 7 ETM data of the study area covering the period 1988-2013. A total of 667 cloud free L1T images of 30 m pixel resolution corresponding to path 1 and row 34 were downloaded and pre-processed using the Landsat Ecosystem Disturbance Adaptive Processing System (LEDAPS) to obtain surface reflectance values for all spectral bands (Masek et al. 2006). Subsequently, we used the red and near-infrared (NIR) surface reflectance values to compute the NDVI for each scene as follows: NDVI = (NIR-Red)/(NIR+Red). Using as a base the Tamarugo plantation map of CONAF (1997) and the 3-month average Landsat NDVI of the 1988 winter, we created a forest mask with all pixels inside the Tamarugo stands and NDVI values higher than 0.13. Then, a Landsat NDVI time series was calculated using the median value of the pixels for each scene inside the forest mask. Using this time series we calculated NDVI derived metrics for each year as follows:

(1) $NDVI_W$ = average of all NDVI scenes from the months May, June and July (winter);
(2) $NDVI_S$ = average of all NDVI scenes from the months November, December and January (summer);
(3) $\Delta NDVI_{W-S}$ = Landsat $NDVI_W$ – Landsat $NDVI_S$.

As stated before, we considered a minimum of three scenes for the summer and winter period to obtain a representative value of the respective season. Otherwise a gap in the time series occurred. For mapping NDVI derived metrics of specific years (1988, 1993, 1998, 2005, and 2013), no ETM SLC-off scenes (containing no-data stripes due to the failure of the Scan Line Corrector in 2003) were used. Only 2013 was mapped using ETM SLC-off data since the TM sensor was discontinued in November 2011.

5.2.5. Digital inventory using high spatial resolution imagery

A panchromatic Quickbird2 image with 0.6 m pixel resolution, acquired in November 2006, was used to automatically identify single Tamarugo trees in the study area. We used the procedure developed by Chávez and Clevers (2012), allowing discrimination of single trees even when the tree crowns were overlapping. This object-based algorithm provided object polygons with the crown area of each tree as output. Using this polygon layer, we extracted for each tree the digital values of the red and NIR bands of a WorldView2 multispectral image with 2 m pixel resolution, acquired in July 2011. The digital values of both bands were transformed into top-of-canopy reflectance (for details, see Updike and Comp (2010)) to finally calculate the $NDVI_W$ for each Tamarugo tree in 2011. The panchromatic WorldView2 image was not used for tree identification because of the large amount of pixels with shadows projected by the trees themselves at the time of the year the image was acquired. Following the recommendations of Chávez et al. (2013a), we performed the tree identification in summer (to avoid shadows) and the NDVI calculation in winter (the annual NDVI peak occurred in winter due to seasonal pulvinar movements). Although differences in canopy size may exist between 2006 and 2011, we believe that they can be neglected since the crown growing rate of adult trees is low, which was confirmed by visual comparison of the canopy size in the panchromatic images of 2006 and 2011. Thus, differences in crown size between 2006 and 2001 were most likely lower than the pixel resolution of the multispectral image.

During a field campaign carried out in January 2012, 50 Tamarugo trees were surveyed. We used the procedure proposed by Chávez et al. (2013a) to calculate the green canopy fraction (GCF) of each tree using digital pictures and an object-based image segmentation of the green and brown canopy elements. We regressed the GCF and NDVI values for single trees to obtain an empirical equation, which

was used to estimate GCF for all the trees identified in the digital inventory. This way, we obtained the total number of Tamarugo trees, the total and individual crown area and an estimation of the GCF at the tree level in 2011.

5.2.6. Data analysis

5.2.6.1. Temporal patterns

We analysed the relationship between the annual average time series of NDVI derived metrics ($NDVI_W$ and $\Delta NDVI_{W-S}$) and GWD of the Tamarugo areas by inspecting the trends and by calculating simple correlation coefficients (R). Annual average values were calculated by averaging all the cells (pixels) from the satellite images and GWD interpolation grids inside the forest mask (spatial mean).

5.2.6.2. Spatial patterns

We made maps for the years 1988, 1993, 1998, 2005 and 2013 showing the location of the pumping wells, the GWD iso-curves of 5, 10, 15 and 20 m and the NDVI derived metrics. In order to provide an up-to-date assessment of the condition of the Tamarugos after 50 years of GW extraction, we analysed the distribution of the Tamarugo population in the GWD range of the forested area in 2011 by using histograms of the number of trees as well as the proportion of trees sorted in four classes of GCF (0-0.25, 0.25-0.50, 0.50-0.75 and >0.75) at different GWD. In the same way we used histograms with the proportion of Landsat pixels sorted in four categories of $NDVI_W$ and $\Delta NDVI_{W-S}$ at different GWD.

Both the spatial and temporal dimensions were used in the discussion section to define GWD thresholds for the Tamarugos' survival.

5.3. Results

5.3.1. Groundwater depth and Landsat NDVI derived metrics in the period 1988-2013

The authorized GW extraction in the Pampa del Tamarugal aquifer increased from about 400 l/s in 1988 to about 2,200 l/s in 1998 (Figure 5.1), causing an average GW depletion of about 2 meters in the Tamarugo areas (Figure 5.3). By 2009, the year the aquifer was declared 'restricted area', the authorized GW extractions had

reached about 4,000 l/s. This amount constitutes the current (2013) legal water rights in the Pampa del Tamarugal aquifer, which is four times the natural recharge of the system (estimated at about 1,000 l/s). Since 1998 GWD has increased linearly (p-value <0.001, R^2=0.94), reaching an average of 14 m GWD in the Tamarugo area by 2013 and an average cumulative GW depletion of three meters.

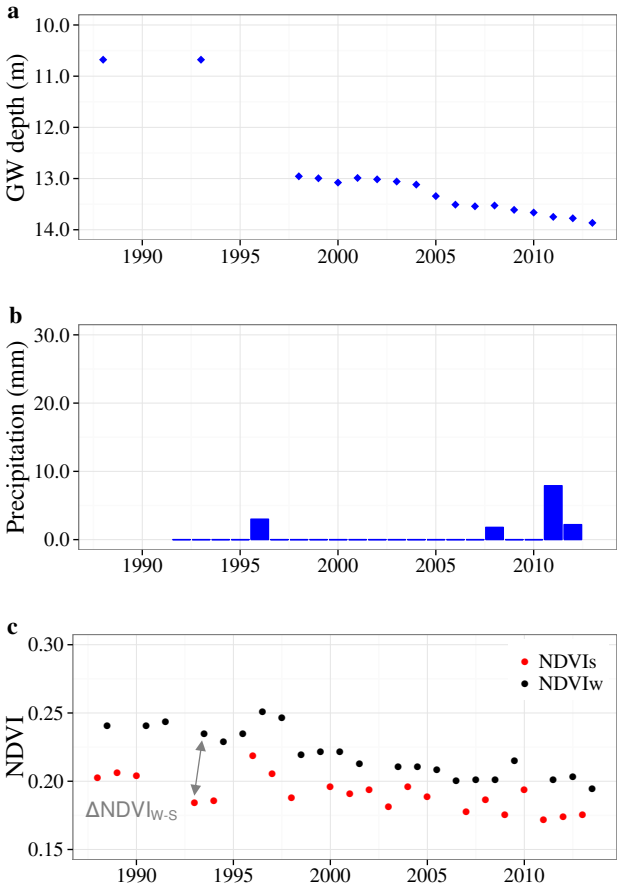

Figure 5.3. (a) Average groundwater depth (GWD), (b) precipitation, and (c) average NDVI in winter (black) and summer (red) for the area covered by Tamarugo in the Pampa del Tamarugal aquifer

As a consequence of the GW depletion, the mean annual $NDVI_W$ and $\Delta NDVI_{W-S}$ of the Tamarugo areas have decreased consistently in time, showing a negative linear trend (p-value <0.001, R^2=0.79 for $NDVI_W$ and p-value <0.01, R^2=0.38 for

$\Delta NDVI_{W-S}$) in the period 1988-2013, which was only interrupted by recovery jumps related to occasional precipitation events (Figure 5.3). These precipitation events had no effect on the GWD and only a temporary positive effect on the NDVI derived metrics. For the period 1988-2013, the $NDVI_W$ signal considering all Tamarugo areas decreased by 19%, while the $\Delta NDVI_{W-S}$ signal decreased by 51%. The annual time series of GWD was limited to the period 1998-2013. For this timeframe, $NDVI_W$ was negatively correlated to GWD with R=−0.82; however, $\Delta NDVI_{W-S}$ was not correlated to GWD (R=0.03). This low correlation may have occurred because of limited amount of data in this timeframe (no $\Delta NDVI_{W-S}$ values for 1999, 2002, 2005, and 2010), and/or because the main effects of GWD occurred before 1998 (see Figure 5.3c), and/or because $\Delta NDVI_{W-S}$ was more sensitive to the precipitation events of 2008, 2011 and 2012.

5.3.2. Spatial patterns of the impact of groundwater extraction in the period 1988-2013

5.3.2.1. Spatial patterns of groundwater depletion

Before 1988 the authorized GW extractions were lower than the natural recharge of about 1000 l/s and no significant changes in Tamarugo areas were reported for the period 1968-1984 (Canadell et al. 1996). Tamarugo was mainly distributed in areas with less than 15 m GWD and about 50% of the trees were in areas with less than 10 m GWD (Figure 5.4). JICA-DGA-PCI (1995) performed an extensive study of the hydrogeology of the Pampa del Tamarugal aquifer and provided GWD maps for the years 1960 and 1993. They concluded that no significant GW depletion occurred in the period 1960-1993, and for this reason we assumed the GWD map of 1960 also as representative for 1988. For the period 1993-1998, the pumping was concentrated in the north-western part of the study area (with a cluster of wells in the Canchones sector). Consequently, the GW depleted (especially in the north-west area), leaving few Tamarugo areas with less than 10 m GWD. No Tamarugo stands were in areas with over 20 m GWD by 1998.

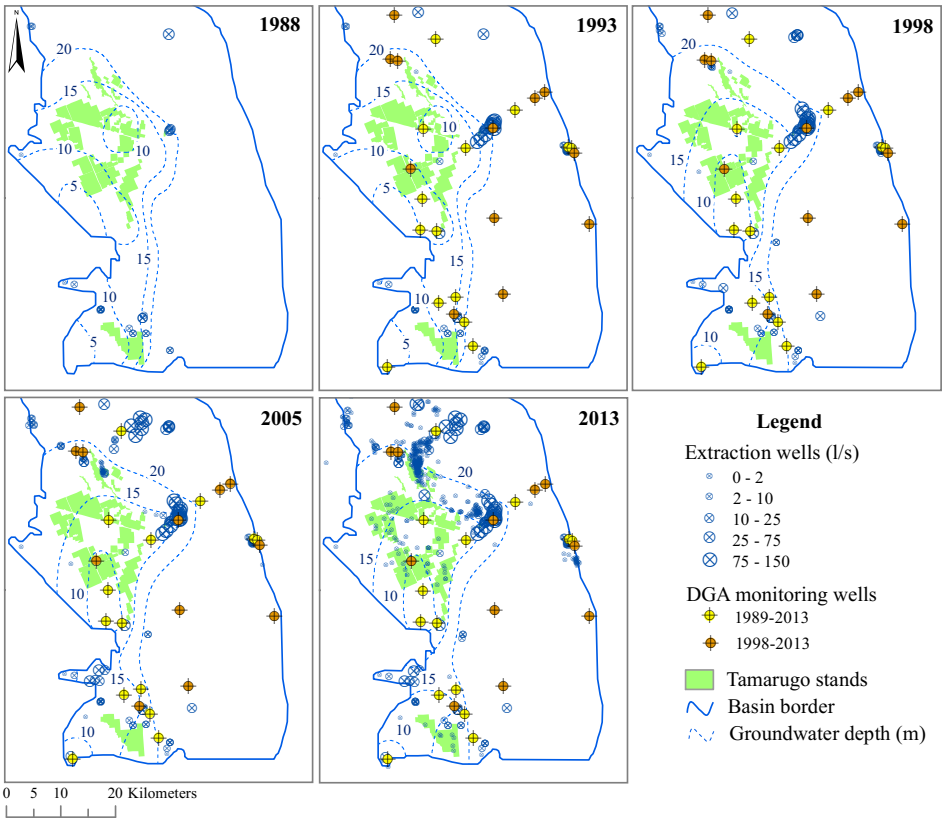

Figure 5.4. Extraction wells and groundwater depth in the Pampa del Tamarugal aquifer at different dates. Sources: 1988 and 1993 (JICA-DGA-PCI 1995), 1998, 2005 and 2013 (this study using the DGA monitoring network).

In 2005 a new cluster of pumping wells appeared in the northern part of the study area (El Carmelo sector) and for the period 2005-2013 the major GW depletion occurred around this new cluster. Some specific areas close to the Canchones cluster recovered in this period (see well JICA-6 in Tables A1 and A2 of the Annex), meaning that most of the pumping took place in El Carmelo rather than in Canchones after 2005. Besides the areas immediately close to Canchones, most of the Tamarugo areas faced GWD depletion in this period. By 2013 only few areas with Tamarugo had less than 10 m GWD and the line of 20 m GWD got close to the stands in the east and north of the study area, reaching the Tamarugo natural areas in the north (Figure 5.4).

5.3.2.2. Spatial patterns of Landsat $NDVI_W$

In Figure 5.5 we can visually observe a general trend of decreasing $NDVI_W$ values when comparing different years in the period 1988-2013, which is consistent with the time series shown in Figure 5.3. In the absence of GW depletion (1988-1993), the larger values of $NDVI_W$ (> 0.25) occurred mainly in areas with less than 10 m GWD in the center and south-west of the study area. Tamarugos located close to the Canchones pumping cluster with high $NDVI_W$ values in 1988 declined in the period 1988-1998. In 2013, after 50 years of GW extraction, only few sectors remained with $NDVI_W$ values higher than 0.25 and were concentrated in the few areas with less than 10 m GWD in the center-south of the study area (Figure 5.5).

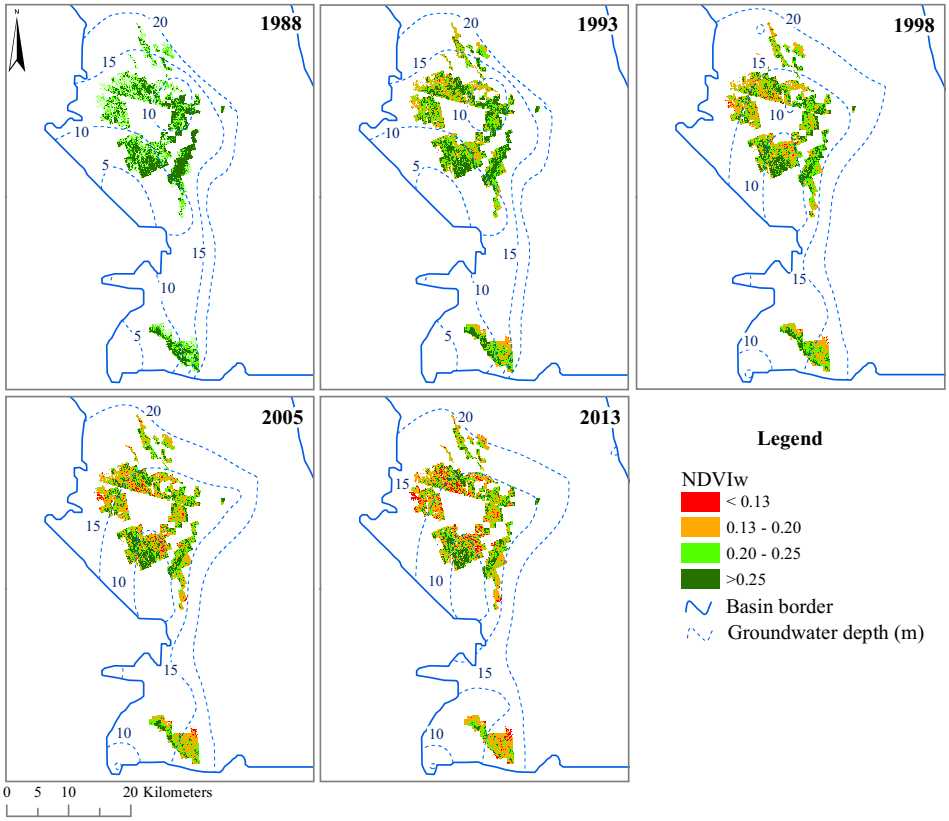

Figure 5.5. $NDVI_W$ and groundwater depth in the Pampa del Tamarugal aquifer at different dates.

5.3.2.3. *Spatial patterns of Landsat ΔNDVI$_{W\text{-}S}$*

The change in $\Delta NDVI_{W\text{-}S}$ for the period 1988-2013 was larger than the change in $NDVI_W$, as explained in section 5.3.1. This is also noticeable in Figure 5.6, which displays the spatial patterns of $\Delta NDVI_{W\text{-}S}$ at different points in time. Similarly to the case of $NDVI_W$, the areas close to the Canchones pumping cluster with larger values of $\Delta NDVI_{W\text{-}S}$ in 1988 declined in the period 1988-1998. $\Delta NDVI_{W\text{-}S}$ in 1993 showed the largest $\Delta NDVI_{W\text{-}S}$ values of the time series (Figure 5.3), which could not be related to any known precipitation event. By 2013 $\Delta NDVI_{W\text{-}S}$ reached the smallest values of the series and no clear clusters of large $\Delta NDVI_{W\text{-}S}$ values can be distinguished in the study area anymore.

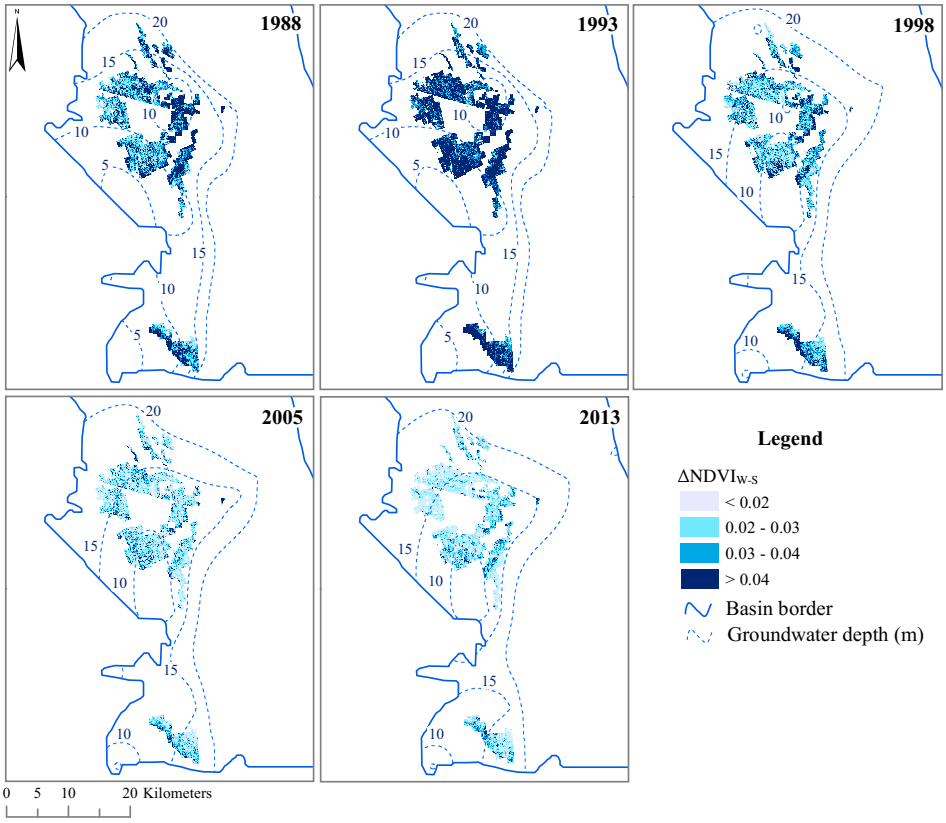

Figure 5.6. $\Delta NDVI_{W\text{-}S}$ and groundwater depth in the Pampa del Tamarugal aquifer at different dates.

5.3.3. Digital inventory using high spatial resolution remote sensing

From the previous sections it became clear that GW extraction had a negative effect on the water status of Tamarugos. The Landsat NDVI derived metrics were able to flag the areas where the effects took place, but they could not yet provide meaningful outputs for managers, like the number of trees affected by GW depletion. For this reason, we complemented our analysis with a digital inventory using high spatial resolution Quickbird2 and Worldview2 images to provide more operational outputs. According to the digital inventory of 2011 a total of 728,953 Tamarugo trees remained in the study area distributed over 13 plantation stands and some small patches of natural vegetation (see Table A3 in the Annex for details). From this total, only 5.4% of the trees corresponded to natural trees and the other 94.6% to plantations. The average crown size of the Tamarugo trees was 48.2 m^2 and the total tree crown coverage was 35.1 km^2.

As shown in Figure 5.7, there was a positive linear relationship (p-value <0.001, R^2=0.71) between GCF (obtained from digital pictures) and $NDVI_W$ (obtained from the WorldView2 satellite image) for the 50 Tamarugo trees surveyed during the field campaign. This empirical equation was used to estimate the GCF of all Tamarugo trees. From the 728,953 Tamarugo trees of the study area, 42% had less than 0.5 GCF and 5.2% less than 0.25 GCF. Most of the trees (75.6%) belonged to the range of 0.25-0.75 GCF and only 12.2% presented more than 0.75 GCF.

As shown in the histogram of Figure 5.8a, in 2011 99.5% of the trees were distributed in areas with less than 20 m GWD and most of them were in areas with less than 15 m GWD (84%). On the other hand, only 20% of the trees were in areas with less than 10 m GWD, which was a normal condition back in 1988 (Figure 5.4). Except for the extreme GWD values, the different GCF classes were homogeneously distributed over the GWD gradient (Figure 5.8b). From 17 m onwards the proportion of trees in lower GCF classes increased. The relatively even distribution over the GWD ranges between 10 and 18 m can be an indication of trees adapting to the new GWD condition. From the Landsat assessment, we know that the green foliage has declined about 19% since 1988 (Section 5.3.1). However, the depletion rate has been relatively low (3 m on average for the period 1989-2013, which equals 0.13 m/year) and trees may have adapted by shutting down part of the green foliage and/or elongating the roots while competing with each other for the available water. As a result this may give an even proportion of

the GCF classes for the GWD range of 10-15 m, but a lower total amount of green biomass. Most likely, the high classes of GCF were better represented in the past, when the Landsat $NDVI_W$ values were higher, than in 2011.

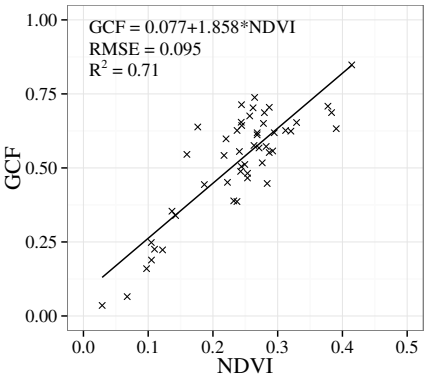

Figure 5.7. Relationship between NDVI and green canopy fraction (GCF) of 50 tamarugo trees in Pampa del Tamarugal

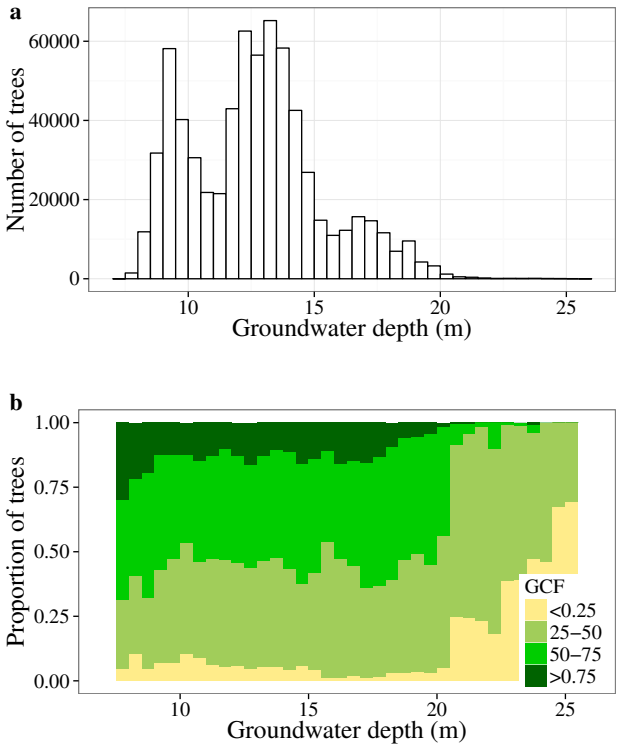

Figure 5.8. (a) Number of Tamarugo trees identified in the high spatial resolution satellite image and **(b)** proportion of trees sorted by green canopy fraction (GCF) for different groundwater depths in 2011.

5.3.4. Comparison between the high spatial resolution and Landsat assessments

Consistent with the results obtained in the high spatial resolution analysis, the observed trend for Landsat $NDVI_W$ values (Figure 5.9a) was similar to the trend for GCF at different GWD. This is expected since GCF is also an NDVI derived metric (Figure 5.7). Because of the lower spatial resolution of the Landsat images, scattered trees located in the 20-25 m GWD range were not included in the histogram of Figure 5.9 as it was the case of the high spatial resolution images (Figure 5.8). A different trend was observed for $\Delta NDVI_{W\text{-}S}$ where high classes of $\Delta NDVI_{W\text{-}S}$ decreased rapidly as GWD increased (Figure 5.9b). This metric is

related to leaf pulvinar movement that is controlled by changes in turgor pressure of the pulvinar cells (Chávez et al. 2014). Therefore, $\Delta NDVI_{W\text{-}S}$ is water driven. It is not surprising that the proportion of Tamarugos with high $\Delta NDVI_{W\text{-}S}$ decreased as GWD decreased, because water is less available for the root system. This decreasing trend of high $\Delta NDVI_{W\text{-}S}$ classes became very clear for trees at a GWD from 12 m onwards.

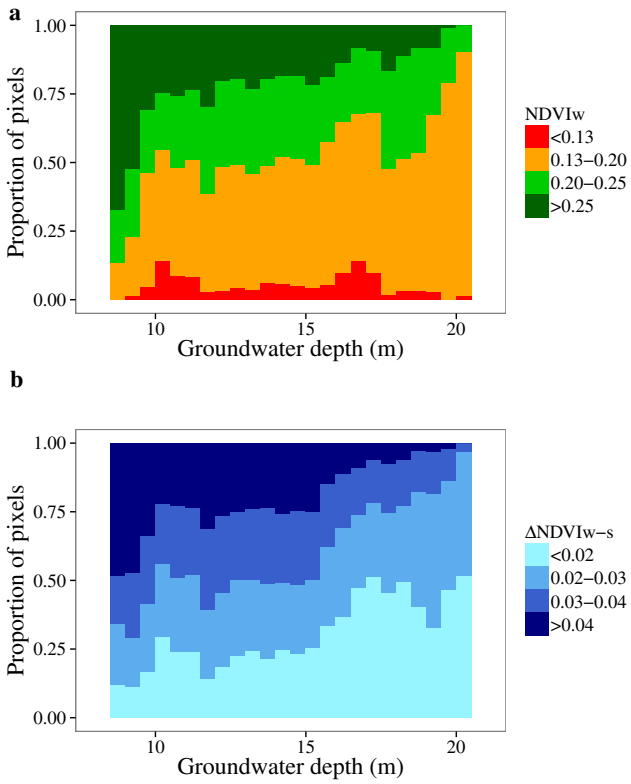

Figure 5.9. Proportion of all Landsat pixels of the Tamarugo stands sorted by **(a)** $NDVI_W$ and **(b)** $\Delta NDVI_{W\text{-}S}$ for different groundwater depths in 2011.

5.4. Discussion

Tamarugo trees were historically distributed mainly at GWD between 5 and 15 meter and rarely at GWD higher than 20 m. After 50 years of GW extractions some Tamarugo trees (about 1% of the population) started facing 20 m GWD

(Figure 5.8a). These trees showed an increasing proportion of green foliage loss (GCF<0.25). A previous study (Chávez et al. 2013a) showed that single Tamarugo trees with this level of green foliage loss were facing a predawn leaf water potential (the actual direct measurement of water supply at the root system) that was significantly below normal ranges. Consequently, this threshold of 20 m GWD is suggested as a threshold for Tamarugos' survival. This can be related to the maximum root elongation depth and the hydraulic lift capacity (Naumburg et al. 2005). In fact, only few plant species can reach such a GWD (Canadell et al. 1996; Phillips 1963). Although some trees and shrubs of exceptional species can reach a GW table deeper than 20 m (Stone and Kalisz 1991), including *Prosopis* species such as *P. juliflora* and probably some Tamarugo individuals, this is not the case for most of the Tamarugo population as shown in Figure 5.8a.

It is unlikely that Tamarugos can cope with the high solar irradiation of the hyper-arid Atacama Desert in the long-term without performing leaf angle adjustments (pulvinar movements). Our results showed that this regulatory mechanism, as estimated by $\Delta NDVI_{W\text{-}S}$, was strongly affected by GW overexploitation for the whole study area. In 2011 about 50% of the Tamarugos located at a GWD deeper than 16 m presented a severe limitation of the pulvinar movements ($\Delta NDVI_{W\text{-}S}$ < 0.02), which is an indication of high level of water stress (Figure 5.9b). Between 12 and 15 m GWD the proportion of trees with low $\Delta NDVI_{W\text{-}S}$ increased rapidly, evidencing the effects of GW depletion. A more even proportion of all $\Delta NDVI_{W\text{-}S}$ classes can be observed for trees located in areas with GWD lower than 12 m GWD, which can be interpreted as the optimal range for Tamarugo, consistent with the areas where Tamarugos were historically distributed and presenting good water status.

Most of the DGA monitoring wells showed a linear negative trend for the period 1998-2013 (see Table A2 in the Annex), and there is no reason to assume that the trend will change in the future. Besides the restraint on authorising new extractions in the aquifer, there is no policy towards limiting the already given water rights and the depletion rate is more likely to continue unaltered in the future. If that is the case, we can predict that the 15 m GWD line will reach the wells 5 and 6 in 2060 (see Table A2 in the Annex), causing a large area of Tamarugos in the north of the study area to have a GWD exceeding 15 m. Thus, these Tamarugos will be in great danger.

5.5. Conclusions

i. Since 1988 the water balance of the Pampa del Tamarugal has become increasingly negative, leading to a general depletion of the groundwater table. For the period 1988-2013, the groundwater table depleted about three meters on average in the areas where the Tamarugo population is distributed. The areas with higher depletion were located close to the main pumping clusters (Canchones and El Carmelo) in the north and north-east of the study area.

ii. As a consequence of the groundwater depletion in the Pampa del Tamarugal aquifer, the water status of the Tamarugos has declined by 19% as measured by the Landsat $NDVI_W$ (an indicator of green biomass) and 51% as measured by the Landsat $\Delta NDVI_{W-S}$ (an indicator of the available water in the trees needed to perform leaf pulvinar movements). The latter is an early indicator of water stress. Both temporal and spatial patterns were negatively correlated to groundwater depth.

iii. The digital inventory carried out in 2011 using very high spatial resolution imagery showed that about 730,000 Tamarugo trees remained in the study area (Salar de Pintados and Salar de Bellavista) with a total crown area of 35.1 km2. Regarding the water status of the trees, the analysis showed that 42% of the Tamarugo trees had less than 0.5 GCF and 5.2% less than 0.25 GCF, the latter is considered as a critical threshold for Tamarugos' water balance. Most of the trees (75.6%) were in the range of 0.25-0.75 GCF and only 12.2% had more than 0.75 GCF.

iv. We suggest a groundwater depth of 20 meters as a threshold for Tamarugos' survival since a) historically the distribution of Tamarugos (natural and planted) was at depths less than 20 m, b) recently trees facing this threshold showed a green canopy fraction lower than 0.25 (75% of green foliage loss), and c) trees facing this threshold cannot longer adjust their leaves to avoid high solar irradiation as shown by the Landsat $\Delta NDVI_{W-S}$ metric, accelerating the drying process.

v. We identified the range up to 12 m GWD as the optimal range for Tamarugo, considering its historical distribution and water status as shown by the $NDVI_W$ and $\Delta NDVI_{W-S}$ metrics. A GWD larger than 12 m increasingly limited the capability of this paraheliotropic species to perform pulvinar movements.

vi. We concluded that trees with a GWD range of 12-16 m were facing moderate water stress and trees at 16-20 m were facing high water stress, with 20 m as the limit for survival of Tamarugo trees.

Acknowledgements

This work has been supported by CONICYT-Chile and Wageningen University. The authors would like to thank Digital Globe for providing the WorldView2 and Quickbird2 imagery. Special thanks to N. Hosonuma for facilitating valuable bibliography.

Annex: additional material of chapter 5

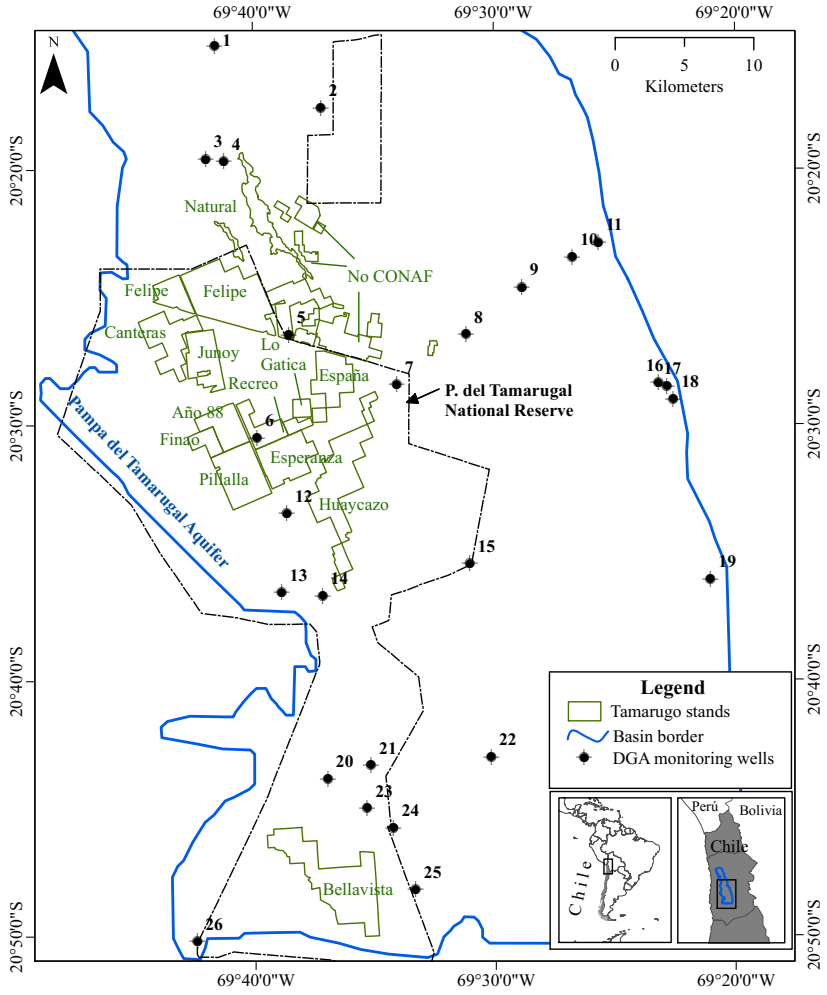

Figure A1. Location of DGA monitoring wells (Table A1) and forest stands (see Table A3).

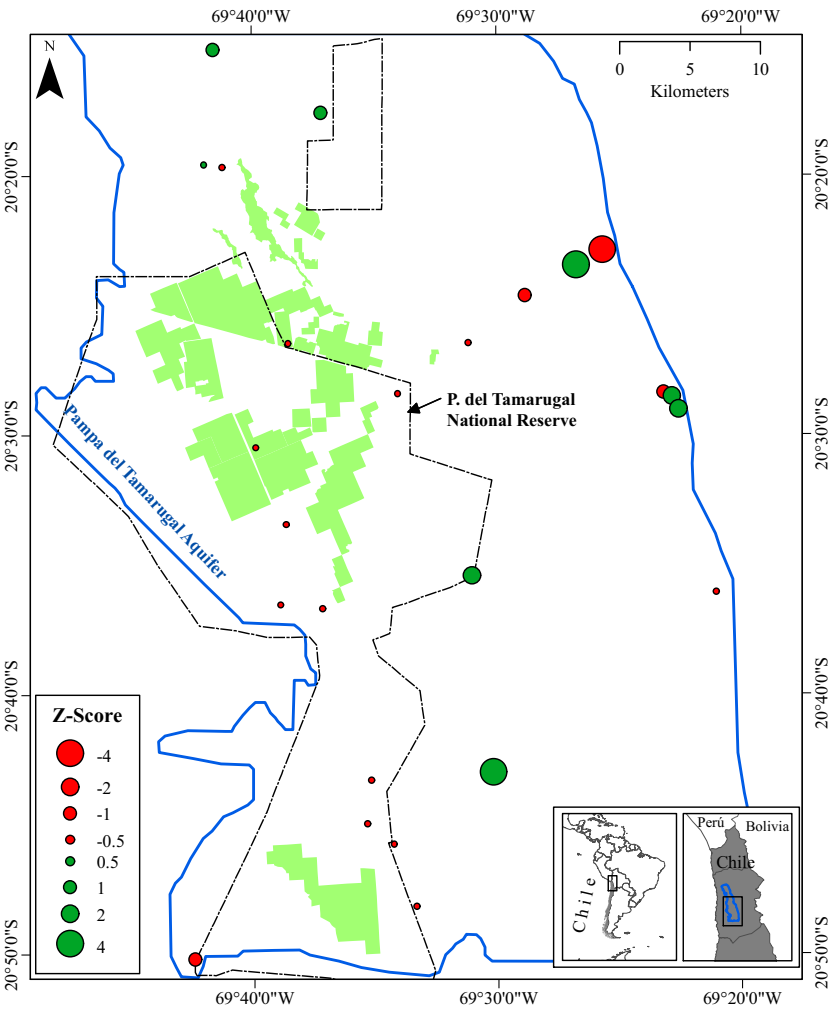

Figure A2. Z-scores of the residuals from the cross-validation of the GWD kriging interpolation.

Table A1. Annual mean groundwater depth for 26 DGA monitoring well in the period 1989 – 2013.

N	DGA code	Well	East	North	Annual mean groundwater depth																								
					1989	1990	1991	1992	1993	1994	1995	1996	1997	1998	1999	2000	2001	2002	2003	2004	2005	2006	2007	2008	2009	2010	2011	2012	2013
1	01700101-9	JICA-5	427654	7760416										29.56	29.69	29.79	29.88	30.03	30.17	30.31	30.65	30.79	30.91	31.00	31.15	31.42	31.59	31.77	31.91
2	01700030-6	El Carmelo	435314	7755955	24.53	24.56	24.58	24.76	24.88	24.98	25.09	25.21	25.30	25.40	25.65	26.09					28.76	29.36	29.47	29.75	30.05		30.62	30.86	31.36
3	01700032-2	Sara Tirana	427022	7752239					15.69	15.77	15.93	16.05	16.15	16.29	16.37	16.46	16.59	16.67	16.77	17.00	17.16	17.33	17.53	17.49	17.79	17.97	18.15	18.28	18.43
4	01700093-4	JICA- E	428308	7752047										13.70	13.80	13.94	14.05	14.17	14.32	14.49	15.19	15.29	15.41	15.59	15.76	15.63	15.92	16.05	16.31
5	01700063-2	Planta Ap Hispania	433019	7739545	7.97	8.11	8.25	8.33	8.47	8.68	8.82	8.87	9.03	9.08	9.04	9.27	9.10	9.37	9.53	9.60	9.71	9.84	9.93	9.87	10.04	10.13	10.21	10.26	10.31
6	01700103-5	JICA-7	430724	7732110										8.07	8.12	8.16	8.21	8.21	8.25	8.27		8.53	8.55	8.58	8.59	8.65	8.69	8.73	8.79
7	01700080-2	Luis Quispe	440798	7735969	9.90	9.91	10.41	10.36	10.67	11.32	11.28	11.47	11.91	11.88	12.08	12.35	12.35	11.87	11.70	11.87	12.10	13.21	12.97	12.53	12.67	12.86	13.30	13.11	12.56
8	01700102-7	JICA-6	445819	7739608										17.26	16.78	15.69	14.91	14.05	13.95	14.03	13.66	13.89	14.03	14.19	14.45	14.77	14.95	14.69	15.14
9	01700053-5	Esmeralda6	449838	7742996	16.50	16.56	16.89	17.08	17.56		18.37	18.66	19.00	19.27	19.52	19.68	19.65	19.64	19.63	19.63	19.73	19.82	19.86	19.92	19.97	20.13	20.26	20.37	20.46
10	01700052-7	La Calera2	453484	7745182				65.76	65.87	66.06	66.22	66.41	66.54	66.70	66.88	67.03	67.20	67.36	67.51	67.68	67.75	67.91	68.04	68.14	68.27	68.34	68.48	68.59	68.70
11	01700051-9	La Calera3	455355	7746253				19.26	19.39	19.47	19.57	19.55	19.49	19.58	19.75	19.94	19.93	20.16	20.31	20.29	19.48	17.80	16.98	17.54	16.12	16.36	16.34	15.40	14.16
12	01700069-1	Salar Pintados 237	432893	7726665	5.70	5.48	5.65	5.77	5.88	6.03	6.12	6.20	6.26	6.35	6.45	6.52	6.61	6.66	6.69	6.75	6.72	6.79	6.88	6.93	7.01	6.89	6.87	6.90	6.98
13	01700019-5	Salar Pintados	432508	7720947			4.78	4.77	4.86	4.96	5.04	5.12	5.19	5.25	5.34	5.42	5.48	5.53	5.64	5.65	5.73	5.77	5.82	5.87	5.91	5.97	6.01	6.06	6.10
14	01700034-9	Salar Pintados 256	435470	7720697	7.93	7.95	8.07	8.14	8.21	8.34	8.55	8.54	8.65	8.74	8.86	8.93	8.99	9.07	9.04	9.18	9.36	9.42	9.54	9.67	9.58	9.58	9.59	9.55	9.61
15	01700104-3	JICA-8	446078	7723065										39.27	39.27	39.00	38.73	38.51	38.40	38.36	38.53	38.69	38.74	38.93	38.94	39.08	39.13	39.12	39.05
16	01700054-3	Esmeralda11	459700	7736124	24.24	24.30	24.41	24.44	24.50	24.80	24.83	24.96	25.04	25.19	25.44	25.55	25.67	25.83	26.05	26.16	26.25	26.33	26.27	26.31	26.31	26.45	26.52	26.55	26.57
17	01700057-8	Esmeralda28	460316	7735866	39.23	39.32	40.14	40.07	40.38	40.45	40.54	40.87	40.77	41.30	41.83	41.82	42.10	42.38	42.66	42.66	42.81	42.89	42.90	43.05	43.02	42.87	43.00	43.01	43.25
18	01700059-4	Esmeralda34	460779	7734951			45.44	45.52	45.64	45.95	46.03	46.19	46.27	46.43	46.77	46.65	46.95	47.17	47.54	47.51	47.50	47.31	47.03	47.01	47.05	47.10	47.22	47.42	47.65
19	01700068-3	Puquio Nunez	463467	7721934				19.95	19.91	19.90	19.83	19.80	19.82	19.80	19.84	19.97	19.99	20.03	19.84	19.82	19.87	19.96	19.83	19.86	19.82	19.89	19.89	19.85	19.84

Table A1 (cont.). Annual mean groundwater depth for 26 DGA monitoring well in the period 1989 – 2013.

N	DGA code	Well	East	North	Annual mean groundwater depth																								
					1989	1990	1991	1992	1993	1994	1995	1996	1997	1998	1999	2000	2001	2002	2003	2004	2005	2006	2007	2008	2009	2010	2011	2012	2013
20	01700074-8	Bellavista275	435844	7707498	10.64	10.67	10.69	10.72	10.73	10.78	10.83	10.87	10.91	10.94	10.99	11.02	11.07	11.10	11.16	11.20	11.20	11.24	11.29	11.30	11.32	11.38	11.35	11.44	
21	01700043-8	Bellavista276	438959	7708487	15.75	15.68	15.78	15.74	15.76	15.79	15.83	15.84	15.86	15.89	15.93	15.97	16.02	16.03	16.05	16.12	16.06	16.15	16.12	16.13	16.13	16.17	16.20	16.33	16.23
22	01700094-2	JICA-F	447638	7709087										55.40	55.05	55.06	55.28	55.16	54.83	54.78	55.08	55.80	55.44	55.92	55.56	55.08	55.02	54.95	54.92
23	01700105-1	JICA-9	438684	7705394										13.14	13.19	13.23	13.28	13.31	13.35	13.40	13.63	13.70	13.71	13.76	13.76	13.87	13.93	13.98	14.04
24	01700076-4	Salar Bellavista	440585	7703953	18.26	18.25	18.20	18.20	18.21	18.23	18.23	18.23	18.40	18.34	18.36	18.37	18.42	18.48	18.51	18.51	18.53	18.59	18.61	18.60	18.61	18.67	18.72	18.75	18.79
25	01700026-8	Bellavista286	442180	7699530	19.57	19.47	19.54	19.52	19.53	19.57	19.58	19.63	19.59	19.66	19.73	19.76	19.83	19.89	19.96	20.06	20.14	20.32	20.31	20.28	20.49	20.61	20.71	20.80	20.89
26	01700024-1	Bellavista290	426420	7695746	2.39	2.47	2.58	2.50	2.52	2.55	2.58	2.61	2.65	2.67	2.70	2.73	2.77	2.79	2.84	2.86	2.90	2.93	2.97	2.99	3.01	3.06	3.10	3.22	3.15

Table A2. Linear model and projections for the annual mean groundwater depth (GWD) of 16 DGA monitoring well located <7 km from the Tamarugo stands.

N	DGA code	Well	Linear model	R^2	GW depletion		GWD in 2013	Year reaching GWD of	
					1989-1998	1998-2013		15 m	20 m
2	01700030-6	El Carmelo	y = 0.3156*x - 604.26	0.95	0.87	5.95	31.36	-	-
3	01700032-2	Sara Tirana	y = 0.1363*x-256.05	0.99	-	2.15	18.43	1993	2030
4	01700093-4	JICA-E	y = 0.1834*x-352.79	0.97	-	2.61	16.31	2005	2035
5	01700063-2	Planta Ap Hispania	y = 0.0964*x-183.58	0.98	1.11	1.23	10.31	2060	2115
6	01700103-5	JICA-7	y = 0.0496*x-91.057	0.97	-	0.71	8.79	2140	2240
7	01700080-2	Luis Quispe	y = 0.124*x-236.21	0.83	1.98	0.68	12.56	2030	2070
8	01700102-7	JICA-6	NL	NL	-	-2.12	15.14	-	-
12	01700069-1	Salar Pintados 237	y = 0.0612*x-116.12	0.92	0.65	0.63	6.98	2145	2225
13	01700019-5	Salar Pintados	y = 0.0626*x-119.93	0.99	0.62	0.85	6.10	2160	2240
14	01700034-9	Salar Pintados 256	y = 0.0779*x-146.92	0.96	0.81	0.87	9.61	2080	2145
20	01700074-8	Bellavista 275	y = 0.0355*x - 60.062	0.99	0.30	0.46	11.40	2115	2260
21	01700043-8	Bellavista 276	y = 0.0243*x - 32.566	0.96	0.14	0.35	16.23	1989	2165
23	01700105-1	JICA-9	y = 0.0631*x - 112.88	0.97	-	0.90	14.04	2030	2110
24	01700076-4	Salar Bellavista	y = 0.0251*x - 31.687	0.94	0.08	0.45	18.79	-	2060
25	01700026-8	Bellavista 286	y = 0.0588*x - 97.64	0.91	0.09	1.23	20.89	-	-
26	01700024-1	Bellavista 290	y = 0.0312*x - 59.731	0.98	0.28	0.48	3.15	>2300	>2300

Note: all linear models significative with P<0.01, except for well JICA-7, labelled as NL=non-linear trend

Table A3. Number of Tamarugo trees in the Pampa del Tamarugal aquifer sorted in four categories of green canopy fraction (GCF).

Origin	Sector	Plantation year	Number of trees per GCF category						Tree coverage per GCF category (Km^2)						Average crown size (m^2)
			<0.25	0.25-0.50	0.50-0.75	>0.75	ND	Total	<0.25	0.25-0.50	0.50-0.75	>0.75	ND	Total	
Plantation	Año 84	1983-86	165	1107	2090	1443	0	4805	0.002	0.030	0.104	0.101	0.000	0.237	49.3
	Bellavista	1968-69	596	29331	43947	15266	0	89140	0.011	1.258	2.587	1.093	0.000	4.949	55.5
	Canteras	1970-71	30	690	1739	714	28172	31345	0.000	0.023	0.105	0.056	1.275	1.459	46.5
	España	1971	3130	20139	15030	4360	34	42693	0.048	0.716	0.964	0.382	0.000	2.110	49.4
	Esperanza	1967-71	4750	22559	21688	6879	144	56020	0.070	0.662	1.088	0.483	0.001	2.303	41.1
	Felipe	1966-70	4623	46555	42491	13006	10563	117238	0.048	1.170	2.112	0.867	0.555	4.752	40.5
	Finao	1968-69	1512	10318	17109	4759	92	33790	0.021	0.308	0.934	0.346	0.000	1.610	47.6
	Huaycazo	1972	7740	39635	29347	7881	72	84675	0.133	1.464	1.812	0.658	0.000	4.067	48.0
	Junoy	1936	219	8183	11573	2150	1569	23694	0.005	0.388	0.973	0.219	0.126	1.711	72.2
	La Habana	1970	1258	4264	1734	218	24	7498	0.017	0.187	0.126	0.016	0.000	0.346	46.2
	Lo Gatica	1936	658	3430	1642	694	13	6437	0.010	0.105	0.098	0.062	0.000	0.275	42.8
	Pillalla	1967-69	3016	15344	22691	7869	169	49089	0.036	0.469	1.248	0.635	0.001	2.390	48.7
	Recreo	1971	2517	9854	7759	2600	55	22785	0.041	0.292	0.403	0.176	0.000	0.914	40.1
	No CONAF	-	6491	41992	51375	16365	409	120101	0.094	1.346	2.752	1.068	0.022	5.282	44.0
Natural	-	-	1447	12073	15264	5033	5826	39643	0.047	0.671	1.269	0.405	0.332	2.725	68.7
TOTAL			38152	265474	285479	89237	47142	728953	0.584	9.091	16.575	6.567	2.313	35.130	48.2

ND = no data. These trees were not covered by the WorldView2 image

Chapter

6

Synthesis

6.1. Main results

This thesis addresses the spectral reflectance signal coming from desert vegetation as measured by optical remote sensing, as well as the interpretation of these signals to assess water stress of desert vegetation. Desert ecosystems are environments characterized by high solar irradiation and scarce water resources. Yet, many plant species have evolved adaptations to successfully survive different levels of aridity. As shown by the case of the Tamarugo trees in the Atacama Desert, Northern Chile (this thesis), assessments of vegetation health condition using optical remote sensing need a proper understanding of how these adaptations influence canopy reflection properties. Many desert plants have developed adaptations to minimize leaf surface exposure to the high solar irradiation of deserts, having an impact on the reflection properties of the canopy. While some of these adaptations (e.g. leaf solar tracking) modify the reflection properties of the canopy on a diurnal basis, others such as leaf shedding modify the reflection properties at a seasonal or inter-annual level. Whichever the case, a time series of canopy spectral reflectance (or vegetation indices derived from it) cannot be correctly interpreted without considering the effects of this regulatory mechanism. Furthermore, anthropogenic or natural induced water stress altering the normal functioning of these plants can also have unexpected effects on canopy spectral reflectance.

The effects of water stress induced by groundwater pumping on relevant variables and physiological processes of desert woody vegetation were explained in Figure 1.3. Based on the main results obtained in chapters 2 to 5 of this thesis, the

unknown regulatory mechanism and relationships identified in Figure 1.3 as well as the expected response on remote sensing vegetation indices (black rectangles) are now given in Figure 6.1 for the case of Tamarugo vegetation.

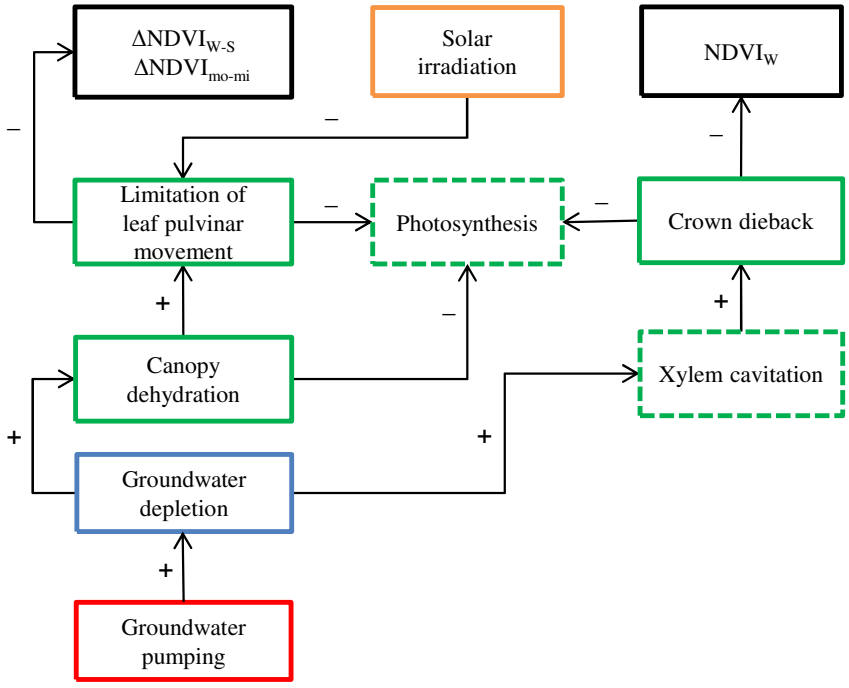

Figure 6.1. Causal diagram of the effects of groundwater pumping on water related variables and processes of Tamarugo vegetation and the response of NDVI derived metrics. Symbols indicate positive (+) or negative (−) effects. Dashed boxes correspond to processes/variables not studied in this thesis.

Section 6.1 provides a synthesis of the main results answering each of the research questions listed in Section 1.5. For each research question, I refer back to Figure 6.1 to explain how these results contribute to the understanding of the water related relationships of Tamarugo and how remote sensing can be used to assess water stress of this desert species. In Section 6.2 I provide the general conclusions of this thesis, and finally, in Section 6.3 I provide a reflection and outlook of this PhD research.

Research question A: what is the spectral response of the desert Tamarugo tree to water stress?

In **chapter 2** I described for the first time paraheliotropic leaf movements in Tamarugo plants and their effects on canopy spectral reflectance under laboratory conditions using the Soil-Leaf-Canopy (SLC) radiative transfer model. In the absence of water stress, empirical canopy reflectance changes occurring during the day were explained by pulvinar movements only, as shown by the SLC simulations. By varying the leaf inclination distribution function (LIDF) parameter of SLC from a random distribution (morning) to a more erectophyle distribution (after midday), the SLC model was able to accurately explain diurnal spectral changes, as measured by a spectroradiometer, caused by leaf pulvinar movements. Under water stress, changes in canopy reflectance were explained mainly by changes in the equivalent water thickness (EWT), a parameter of SLC accounting for the amount of water in the leaves, and in the LAI. The results suggested that remote sensing based assessment of Tamarugo should consider LAI and the canopy water content (CWC, being the product of LAI and EWT) as water stress indicators. Another important finding of this experiment was the fact that the difference in spectral reflectance between morning and afternoon, evident without water stress, declined as the Tamarugo plants were running out of water.

Once calibrated, the SLC model was used to test fifteen different vegetation indices and spectral absorption features proposed in literature for detecting changes in LAI and CWC, considering the effect of LIDF variations. A sensitivity analysis was carried out using SLC simulations with a broad range of LAI, LIDF and EWT values. The results showed that the Water Index (ratio of the reflectance at 900 and 970 nm) and the area under the curve for the spectral range 910-1070 nm were the most sensitive remote sensing features for estimating CWC. For estimating LAI, the red-edge chlorophyll index ($CI_{red\text{-}edge}$) was the most sensitive index. Although this study showed the potential of remote sensing for estimating important canopy variables related to water stress of Tamarugo plants, it also showed that diurnal leaf movements had an effect on all remote sensing features tested, particularly on those for detecting changes in CWC.

The contributions of this chapter to complete the causal diagram of Figure 6.1 are indicated as follows:

- The identification of the regulatory mechanism (leaf pulvinar movements) of Tamarugo to avoid high solar radiation around midday. Still at this stage, this mechanism needed to be studied under field conditions with actual changes in solar irradiation (a topic addressed in chapter 3).
- Leaf pulvinar movements have a positive effect on diurnal changes of canopy reflectance and of vegetation indices.
- Leaf pulvinar movements (triggered by changes in cell water turgor) can be limited by water stress, causing the diurnal changes in canopy reflectance to decrease.

Research question B: how can we assess the water condition of single Tamarugo trees using modern remote sensing techniques?

In **chapter 3**, I designed a field experiment to investigate three main issues: first, the water stress symptoms of Tamarugo trees under different levels of groundwater extraction; secondly, the usefulness of WorldView2 very high spatial resolution images to estimate LAI and green canopy fraction (GCF) of single trees; and thirdly, to study the effects of diurnal pulvinar movements on canopy reflectance under field conditions (sun position and intensity changing throughout the day).

In-situ measurements showed that Tamarugo trees under water stress showed significantly lower leaf water concentration, higher pigment concentration and lower GCF. Predawn water potential values (a measure of the actual water supply at the root system) were significantly lower for trees with GCF <0.25 than the rest of the GCF classes (0.25-0.50, 0.50-0.75, and 0.75-1.00). This means that Tamarugo is able to keep its water status at normal ranges till losing about 75% of green foliage. This value (GCF = 0.25) is therefore critical for Tamarugo's water balance and can be used as a threshold for conservation purposes.

Single tree identification, crown size delineation and estimations of LAI and GCF were successfully performed using WorldView2 images and an object based image analysis approach. The NDVI constituted the best estimator for LAI, while the red-edge chlorophyll index was the best one for estimating GCF for tree objects extracted from WorldView2 imagery.

Finally, I recorded pulvinar movements under field conditions (digital pictures) and measured the canopy spectral response using a field spectroradiometer. Hourly

values of NDVI obtained from the field spectral measurements were negatively correlated (R=-0.5) to solar irradiation records, showing a clear diurnal cycle with minimum values around midday.

The contributions of this chapter to complete the causal diagram of Figure 6.1 are indicated as follows:

- Confirmation of the fact that pulvinar movements of Tamarugo leaves are activated by increasing solar irradiation during the day, yielding minimum values of canopy reflectance and NDVI towards midday.
- Increasing groundwater depth has a negative effect on CWC and LAI of single Tamarugo trees.
- Empirical basis of the diurnal NDVI cycle to design the following NDVI derived metrics as early indicators of water stress (to be tested in chapter 4): NDVI difference between morning and midday ($\Delta NDVI_{mo\text{-}mi}$) and NDVI difference between winter and summer ($\Delta NDVI_{W\text{-}S}$).

Research question C: what is the impact of the regulatory mechanisms of Tamarugo (to avoid excessive transpiration and photoinhibition) on time series of canopy spectral reflectance and vegetation indices with and without water stress?

In **chapter 4**, I studied seasonal and diurnal variations of MODIS and Landsat NDVI time series of Tamarugo stands subject to different levels of groundwater depletion.

The diurnal NDVI cycles presented in chapter 3 showed that NDVI values in the morning were higher than NDVI values at midday. Consequently, I tested in this chapter whether the MODIS 16-days NDVI composites obtained with the Terra satellite (flying over the Atacama Desert at about 10 a.m. local time) were higher than the MODIS 16-days NDVI composites obtained with the Aqua satellite (flying over the Atacama Desert at about 1.30 p.m. local time). The results showed that Tamarugo stands located in areas with no groundwater depletion had a clear NDVI difference between midday and morning ($\Delta NDVI_{mo\text{-}mi}$) during the whole year, reaching its maximum towards winter time when the difference in solar irradiation between morning and midday was higher than in summer. In a similar

way, the NDVI signal of both MODIS and Landsat presented a strong seasonal variation, mainly explained by the seasonal variation of solar irradiation.

As expected, Tamarugo stands under groundwater depletion showed lower $\Delta NDVI_{mo\text{-}mi}$ and lower $\Delta NDVI_{W\text{-}S}$ as the amplitude of the natural NDVI diurnal and seasonal cycles was declining due to limitations on the functioning of the pulvinar mechanism. Consequently, long time series of Landsat $\Delta NDVI_{W\text{-}S}$ of Tamarugo stands showed a negative linear relationship with cumulative groundwater depletion, in other words $\Delta NDVI_{W\text{-}S}$ decreased as groundwater depth increased.

Annual time series of $NDVI_W$ (3-month averages of NDVI in winter) were also negatively correlated to cumulative groundwater depletion as a consequence of LAI losses. Both $\Delta NDVI_{mo\text{-}mi}$ and $\Delta NDVI_{W\text{-}S}$ can be used for early detection of water stress, since a limitation of the pulvinar mechanism is likely to occur before Tamarugos start losing green foliage.

The contributions of this chapter to complete Figure 6.1 are indicated as follows:

- Leaf pulvinar movements are the main factor explaining diurnal and seasonal variations of the NDVI signal.
- Ground water depth has a negative effect on $\Delta NDVI_{mo\text{-}mi}$ and $\Delta NDVI_{W\text{-}S}$ as a consequence of limitation in the pulvinar mechanism.
- Ground water depth has a negative effect on NDVIW due to LAI loss.

Research question D: how can we use remote sensing to assess the impact of groundwater extraction on the Tamarugo population at large scale?

Based on the findings of the previous chapters, in **chapter 5** I proposed and implemented a remote sensing based assessment of the effects of groundwater extraction on the water condition of Tamarugo vegetation. The assessment was carried out for Tamarugo areas located in the center-south part of the Pampa del Tamarugal aquifer, where most of the Tamarugo population is concentrated. To achieve this, I analysed a dense time series of Landsat $NDVI_W$ and $\Delta NDVI_{W-S}$ together with hydrogeological data for the period 1989-2013. In order to provide operational outputs for water managers, I complemented the analysis with an automated digital inventory and estimation of GCF for all single Tamarugo trees within the study area.

The results showed that the $NDVI_W$ and $\Delta NDVI_{W-S}$ of the Tamarugo vegetation declined 19% and 51% as groundwater depleted (3 meters on average considering all Tamarugo stands) between 1989 and 2013. $NDVI_W$ and $\Delta NDVI_{W-S}$ were negatively correlated to groundwater depth both temporally and spatially. A total of about 730.000 Tamarugo trees remained in the study area by 2011, from which 5.2% showed a GCF<0.25 that is associated to severe water stress. Based on this spatio-temporal analysis, I suggest that the survival of Tamarugo trees is limited to a maximum groundwater depth of 20 meters.

6.2. General conclusions

The objective of this PhD research was to analyse the usefulness of remote sensing for assessing water stress of desert woody vegetation, exemplified by the case of the *Prosopis tamarugo* Phil. trees in the Atacama Desert (Northern Chile). The aim was to propose a remote sensing based methodology to detect and monitor water stress effects induced by external perturbations. In this section, the main conclusions from the work presented in this thesis are given as follows.

i. Heliotropism or leaf 'solar tracking', a common adaptation among desert plants, has an important impact on canopy spectral reflectance. As shown in the case of the Tamarugo trees, the leaf lamina of this species adjusts to avoid facing high solar irradiation throughout the day (paraheliotropism), causing the canopy reflectance to decrease as solar irradiation increases. In this thesis, I showed that widely used vegetation indices such as the NDVI

were negatively correlated to solar irradiation, showing a distinct diurnal and seasonal cycle.

ii. The laboratory experiment and the time series analysis of satellite images performed in this thesis showed that normal diurnal and seasonal cycles of canopy reflectance and vegetation indices are affected by water stress. In the case of Tamarugo, paraheliotropic movements are controlled by changes in cell turgor of a pulvinar structure located in the base of the leaves. Under water stress pulvinar movements are limited. Thus, an early symptom of water stress is the decline of the amplitude of the diurnal and seasonal cycles of the NDVI.

iii. At the stand level, I showed that NDVI derived metrics from Landsat and MODIS Terra-Aqua satellites are good indicators of the effects of groundwater depletion on the water status of Tamarugo vegetation. The NDVI difference between morning and midday ($\Delta NDVI_{mo\text{-}mi}$) obtained from MODIS-Terra (morning) and MODIS-Aqua (midday), the NDVI difference between winter and summer ($\Delta NDVI_{W\text{-}S}$) obtained from MODIS-Terra or from Landsat, and the NDVI in winter ($NDVI_W$) obtained from Landsat were negatively correlated to in-situ measurements of cumulative groundwater depletion, in other words, these indices decreased as groundwater depth increased.

iv. At the tree level, very high spatial resolution images combined with object based image analysis and in-situ data provided accurate estimations of the leaf area index and green canopy fraction of single Tamarugo trees. For monitoring purposes, careful consideration of the time during the day and the season at which the images are taken needs to be taken to avoid misleading interpretations.

v. Time series analysis of historical satellite images combined with very high spatial resolution images and hydrogeological records provided a quantitative spatio-temporal assessment of the effects of long-term groundwater extraction on Tamarugo vegetation at the basin level.

6.3. Reflection and outlook

In this PhD, the scientific fields of biology and remote sensing meet together. Through the observation and study of physiological and ecological processes of a desert plant species at the leaf, tree, and stand level, we were able to interpret the canopy reflectance signal of this species measured by laboratory, field and satellite sensors. Specific contributions to biology were the functional and anatomical description of leaf pulvinar movements (paraheliotropism) of the desert tree *Prosopis tamarugo* Phil. (chapter 2, 3 and 4), the study of water relationships of Tamarugo plants under laboratory conditions (chapter 2) and of trees under field conditions (chapter 3) with and without water stress, and finally, the study of specific aspects of the Tamarugo population such as spatial distribution, number of trees, fractional canopy cover, and the spatio-temporal dynamic of its water status (chapter 5). Specific contributions to remote sensing science were the use of radiative transfer modelling to study the single and combined effects of leaf pulvinar movements and water stress on the canopy reflectance of a paraheliotropic desert plant (chapter 2) as well as the proposal of NDVI derived indices to assess and monitor the water status of desert paraheliotropic vegetation. Perhaps the most important societal benefit of this PhD thesis was the proposition of a remote sensing based framework to assess and monitor water stress of desert vegetation (Figure 6.1), which is one of the most important environmental impacts of human activities in desert ecosystems.

In this final section, I provide a reflection and outlook of three aspects related to my PhD research: i) implications for the use of remote sensing to study heliotropic vegetation, ii) implications for the use of remote sensing to assess water stress of paraheliotropic vegetation, and iii) implication for forest and water management of the Tamarugo ecosystem in the Atacama Desert in northern Chile.

6.3.1. Remote sensing of heliotropic vegetation

Optical remote sensing has been broadly used for assessing the health status of vegetation worldwide. Vegetation indices derived from canopy spectral reflectance measured by optical satellites such as the normalized difference vegetation index (NDVI) are good estimators of the green biomass of the vegetation, allowing scientists to study seasonal phenological cycles as well as natural and anthropogenic impacts on vegetation. For example, seasonal changes of NDVI are

used in global climate modelling as a proxy to describe the growing season dynamic of different vegetation land cover types (Bontemps et al. 2012; Menzel 2002). Furthermore, NDVI seasonal time series and more sophisticated spectral reflectance derived metrics (e.g. using radiative transfer modelling) are used in crop yield estimation models (Doraiswamy et al. 2004; Doraiswamy et al. 2005; Hochheim and Barber 1998; Huang et al. 2013). In most of these applications it is assumed that the canopy structure of vegetation is constant over a short period of time (daily, 16-days, monthly).

However, this is not the case for heliotropic species or "solar trackers", which adjust the leaf angle distribution according to the direction of the sun rays to either optimize (diaheliotropism) or minimize (paraheliotropism) the interception of solar radiation. In this thesis, we addressed the issue of using canopy reflectance derived indices, including NDVI, when the structure of the vegetation varies on a diurnal and seasonal basis. It showed the errors that can be made in time series analysis of satellite data if these structural variations are not taken into account. For example, Figure 6.2 shows a 5-years MODIS-Terra NDVI time series of a 1 km^2 Tamarugo stand in the Atacama Desert. The seasonal trend of the NDVI signal could have been interpreted as the effect of Tamarugos' growing season with a peak around July, for instance, in the framework of a climate modelling study. Because we know Tamarugo is a solar tracker, we can correctly interpret this signal as the effect of changes in the leaf slope of Tamarugos' canopy associated to seasonal fluctuations of solar irradiation (chapter 4).

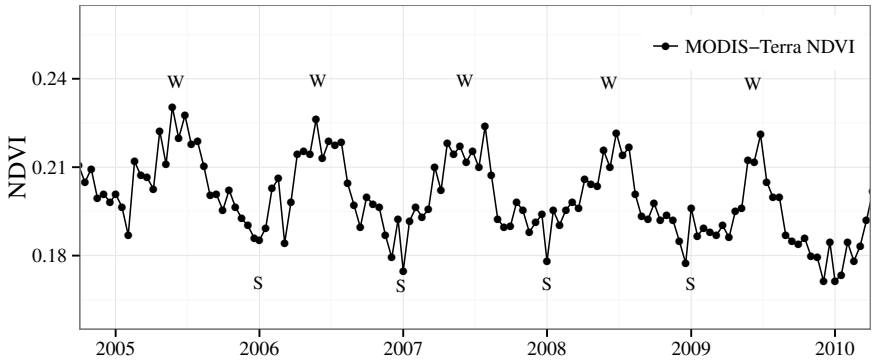

Figure 6.2. Time series of MODIS-Terra 16 days NDVI composites of a Tamarugo stand in the Atacama Desert, Northern Chile. W=winter, S=summer.

This PhD thesis gives evidence of the effects of solar tracking on canopy reflectance and spectral vegetation indices, and at the same time, it offers new research questions: is the case of Tamarugo an extreme example of heliotropism, considering the harsh conditions of the Atacama Desert? How common are solar trackers in nature? Is heliotropism a factor to take into account in local, regional or global remote sensing applications? Paraheliotropic species are common in arid ecosystems (Ehleringer and Forseth 1980), thus remote sensing of desert vegetation needs to take into account this mechanism as well as other adaptations to aridity with potential impacts on canopy reflectance such as leaf shedding. Besides desert vegetation, paraheliotropism has been identified as a particular trait of Leguminosae species, including major crops such as the common bean *Phaseolus vulgaris* L. (Pastenes et al. 2005; Pastenes et al. 2004), alfalfa *Medicago sativa* L. (Berg and Heuchelin 1990) and soybean *Glycine max* L. (Foster et al. 2013). Nevertheless, the effects of paraheliotropic leaf movements on remote sensing based yield estimations for 'solar tracking' crops, especially in areas with high solar radiation, remain poorly understood. For this reason, remote sensing of heliotropic vegetation needs to be further developed in order to provide accurate estimations of canopy properties of such species for environmental applications and crop yield modelling.

A recent publication entitled 'Remote sensing: A green illusion' (Soudani and Francois 2014) has brought the attention of the scientific community and policy makers towards the issue of the correct interpretation of remote sensing derived products for environmental applications. The authors reflected about this issue based on the results of Morton et al. (2014) showing how the apparent canopy greenness of the Amazon forest, interpreted as a positive response to more sunlight in the dry season, was caused by a bidirectional reflectance effect. In other words, this erroneous interpretation was caused by an optical artefact due to seasonal changes of the sun-sensor geometry. In this PhD thesis, we also discussed about the correct interpretation of remote sensing derived products, but this time for heliotropic vegetation. As shown in the case of Tamarugo, the seasonal changes in NDVI were related to leaf pulvinar movements, which also could have been interpreted as an apparent greening of the Tamarugo trees in winter (Figure 6.2). Considering the study of Morton et al. (2014), one may think that what in this thesis is interpreted as the effect of pulvinar movements (Figure 6.2) is actually caused by an optical artefact, similar to the case of the Amazon forest. However,

three pieces of evidence were provided in this PhD thesis to support that pulvinar movements are responsible for NDVI diurnal and seasonal changes of Tamarugo vegetation:

- Canopy spectral reflectance of Tamarugo plants simulated with the Soil-Leaf-Canopy (SLC) radiative transfer model showed that the SLC parameter LIDF (leaf inclination distribution function) could explain diurnal changes in canopy reflectance measured empirically with a spectroradiometer under laboratory conditions (lamp-sensor geometry was fixed). Thus, pulvinar movements, set in the SLC simulations as a 'random' LIDF in the morning and as an 'erectophile' LIDF after midday, governed diurnal changes in canopy reflectance in the absence of water stress.
- This study showed a negative empirical relationship between diurnal values of NDVI, measured for single Tamarugo trees, and solar irradiation under field conditions (Figure 3.12) as well as between seasonal NDVI values, measured by Landsat and MODIS satellites for Tamarugo stands, and solar irradiation (Figure 4.4). During the field campaign, I observed a predominantly erectophyle position of Tamarugo leaves around midday (Figure 3.11) as a response to the high solar irradiation at this time of the day. Furthermore, it is a known botanical fact that paraheliotropic movements are a response to increasing solar irradiation on the leaves (Ehleringer and Forseth 1980). Thus, pulvinar movements activated by changes in solar irradiation govern diurnal and seasonal changes on the NDVI signal of Tamarugo vegetation.
- In chapter 4, this study provided evidence that the amplitude of the seasonal NDVI trend ($\Delta NDVI_{W\text{-}S}$) of Tamarugo stands declined with water stress (Figure 4.6). If the NDVI seasonal trend measured by satellite remote sensing was governed by a sun-sensor artefact, then why would water stress cause the amplitude of the NDVI signal to decline?

In the southern hemisphere, more internal shadowing in satellite images (captured at nadir) is expected to occur in winter, and therefore, the bidirectional reflectance effect should cause an 'apparent greening' towards spring/summer (Morton et al. 2014). Due to the low canopy fractional cover of the Tamarugo vegetation, internal shadowing of the trees does occur in satellite images taken in winter. This is the

reason why it was recommended to use very high spatial resolution satellite images taken in summer to perform segmentation and classification of single Tamarugo trees (chapter 3). However, as shown in Figure 6.2, the peak of the NDVI signal of Tamarugo stands does not occur in summer, but in winter where the solar irradiation is lower. Although bidirectional reflectance effects may also occur in the case of Tamarugo vegetation, I believe that such effects are obscured by the stronger effect of seasonal pulvinar movements.

6.3.2. Early water stress detection of paraheliotropic desert vegetation using remote sensing

As explained in chapter 4, early water stress detection of paraheliotropic vegetation can be achieved by remotely sensing the decline of the pulvinar movement, using the NDVI difference between winter and summer ($\Delta NDVI_{W-S}$) as well as the NDVI difference between morning and midday ($\Delta NDVI_{mo-mi}$). However, in the case of Tamarugo vegetation, I faced some limitations to test the usefulness of these NDVI derived metrics, since the availability of in-situ groundwater depth records was limited and, for the case of $\Delta NDVI_{mo-mi}$, the temporal extent of the MODIS Terra and Aqua images (2003-2012) did not match the period of higher groundwater extraction levels (before 2005). Consequently, the relationship between groundwater depth or groundwater cumulative depletion and NDVI derived metrics related to pulvinar movements of Tamarugo vegetation was not always very strong.

For this reason, I believe that valuable research can be done to further explore the potential of remote sensing to detect the decline of paraheliotropic leaf movements related to water stress, specifically:

- Laboratory experiments to test differences in diurnal cycles of canopy reflectance for paraheliotropic plants under different controlled water stress levels.
- Field experiments using paraheliotropic crops to test the usefulness of spectral vegetation indices measured by proximal (field spectroradiometer), airborne or satellite remote sensing to detect pulvinar movements with and without water stress or under different irrigation regimes.

6.3.3. Forest and water management in Pampa del Tamarugal

Chapter 5 provided a detailed spatio-temporal assessment of the water status of the Tamarugo stands of the 'Lote 1' of the Pampa del Tamarugal National Reserve. These stands, located in the salt flats (or 'salares') of Bellavista and Pintados, contain most of the remaining population of this species. The results of this assessment showed a clear and consistent decline of the water status of Tamarugo vegetation since 1988 till now due to groundwater overexploitation, especially in the north and north-east stands of 'Lote 1'. The water unbalance of the Pampa del Tamarugal aquifer at the present time is enormous: groundwater extractions are currently 3 or 4 times the estimated natural recharge. Although these extractions are not expected to increase in the future (this aquifer was declared 'restricted area' by the Chilean Water Service in 2009), there is also no reduction in order to maintain the current groundwater depth. If the pumping continues unaltered in the future, the projected effects on the water status of the Tamarugo population, as shown in this study, indicate that most of the Tamarugo population will be in great danger in the next decades.

Important initial steps towards the conservation of the Tamarugo ecosystem have been made by the Chilean environmental agencies and policy makers. Most of the Tamarugo areas are currently under protection in the Pampa del Tamarugal National Reserve created in 1987 (CONAF 1997), and recently (2013) the species *Prosopis tamarugo* Phil. was officially classified as 'endangered' (Decreto Supremo Number 13/2013) in the framework of the Chilean law for species classification and conservation. In spite of these important and concrete steps, the key for ensuring the conservation of the Tamarugo ecosystem is still the protection of Tamarugos' water supply sources.

This PhD research offers the basis for the implementation of a monitoring system of Tamarugos' water condition using freely available remote sensing data (Landsat and MODIS). The future availability of remote sensing data is secured at least for 5-10 years in the case of the NASA Landsat-8 satellite (Kelly and Holm 2014) and for 20 years in the case of the ESA Sentinel-1, -2, and -3 satellites (Malenovský et al. 2012). Now it is the turn for the Chilean Environmental Agencies and policy makers to take further actions towards the monitoring of the Tamarugo trees' status and the conservation of the Tamarugo ecosystem. In view of the research carried out in my PhD, I consider that relevant future actions are:

- Continue and expand the in-situ and remote sensing based monitoring of the water status of the Tamarugo population to its complete distribution range (aquifers of Pampa del Tamarugal and Llamara). While free Landsat and MODIS satellite time series can be used to continuously monitor the Tamarugo stands, commercially available high spatial resolution satellite images (e.g. WorldView2 data or data from the upcoming WorldView3 satellite) can be used for detailed digital inventories and water status assessments (at the tree level) over larger timespans (each 5-10 years).
- Decrease the groundwater extraction in the Pampa del Tamarugal aquifer and limit the groundwater extraction in the Llamara aquifer, where a small native Tamarugo population still remains under good water condition.
- As it was already suggested by Carevic et al. (2012), the incorporation of the natural Tamarugo stands located in the sectors of Tirana and Llamara to the Pampa del Tamarugal National Reserve is an urgent matter. Most of the Tamarugo areas of this National Reserve are plantations and these relevant natural populations are currently unprotected. The protection of natural Tamarugo areas can be the key to future conservation actions, since they are likely to be a very rich source of genetic variation.

References

Acevedo, E., Ortiz, M., Franck, N., & Sanguineti, P. (2007). *Relaciones hídricas de Prosopis tamarugo Phil. Uso de isótopos estables*. Santiago (Chile): Universidad de Chile

Acevedo, E., Sotomayor, D., & Zenteno, V. (1985). Water uptake as affected by the environment in *Prosopis tamarugo* Phil. In M. Habit (Ed.), *The current state of knowledge on Prosopis tamarugo* (pp. 273–281): F.A.O.

Aguirre, J.J., & Wrann, J. (1985). The genus *Prosopis* and its management at the Tamarugal Pampa. In M. Habit (Ed.), *The current state of knowledge on Prosopis tamarugo* (pp. 3-32): F.A.O.

Aksoy, S., Yalniz, I.Z., & Taşdemir, K. (2012). Automatic detection and segmentation of orchards using very high resolution imagery. *IEEE Transactions on Geoscience and Remote Sensing, 50*, 3117-3131

Alpert, P., & Oliver, M.J. (2002). Drying without dying. In M. Black & H.W. Pritchard (Eds.), *Desiccation and survival in plants: drying without dying* (pp. 4-31). Wallingford (UK): CABI

Altamirano, H. (2006). *Prosopis tamarugo* Phil. Tamarugo. In C. Donoso (Ed.), *Las especies arbóreas de los bosques templados de Chile y Argentina. Autoecología* (pp. 534-540). Valdivia (Chile): Marisa Cuneo Ediciones

Aravena, R., & Acevedo, E. (1985). The use of environmental isotopes Oxigen-18 and deuterium in the study of water relations of *Prosopis tamarugo* Phil. In M. Habit (Ed.), *The current state of knowledge on Prosopis tamarugo* (pp. 251-262): F.A.O.

Asner, G.P. (1998). Biophysical and biochemical sources of variability in canopy reflectance. *Remote Sensing of Environment, 64*, 234-253

Asner, G.P., & Heidebrecht, K.B. (2002). Spectral unmixing of vegetation, soil and dry carbon cover in arid regions: comparing multispectral and hyperspectral observations. *International Journal of Remote Sensing, 23*, 3939-3958

Asner, G.P., Wessman, C.A., Bateson, C.A., & Privette, J.L. (2000). Impact of tissue, canopy, and landscape factors on the hyperspectral reflectance variability of arid ecosystems. *Remote Sensing of Environment, 74*, 69-84

Barchuk, A.H., & Valiente-Banuet, A. (2006). Comparative analysis of leaf angle and sclerophylly of Aspidosperma quebracho-blanco on a water deficit gradient. *Austral Ecology, 31*, 882-891

Baret, F., de Solan, B., Lopez-Lozano, R., Ma, K., & Weiss, M. (2010). GAI estimates of row crops from downward looking digital photos taken perpendicular to rows at 57.5° zenith angle: Theoretical considerations based on 3D architecture models and application to wheat crops. *Agricultural and Forest Meteorology, 150*, 1393-1401

Baret, F., Houlès, V., & Guérif, M. (2007). Quantification of plant stress using remote sensing observations and crop models: The case of nitrogen management. *Journal of Experimental Botany, 58*, 869-880

Berg, V.S., & Heuchelin, S. (1990). Leaf orientation of soybean seedlings. I. Effect of water potential and photosynthetic photon flux density on paraheliotropism. *Crop Science, 30*, 631-638

Berni, J.A.J., Zarco-Tejada, P.J., Suárez, L., & Fereres, E. (2009). Thermal and narrowband multispectral remote sensing for vegetation monitoring from an unmanned aerial vehicle. *IEEE Transactions on Geoscience and Remote Sensing, 47*, 722-738

Birdsey, R., Angeles-Perez, G., Kurz, W.A., Lister, A., Olguin, M., Pan, Y., Wayson, C., Wilson, B., & Johnson, K. (2013). Approaches to monitoring changes in carbon stocks for REDD+. *Carbon Management, 4*, 519-537

Blaschke, T. (2010). Object based image analysis for remote sensing. *ISPRS Journal of Photogrammetry and Remote Sensing, 65*, 2-16

Bontemps, S., Herold, M., Kooistra, L., Van Groenestijn, A., Hartley, A., Arino, O., Moreau, I., & Defourny, P. (2012). Revisiting land cover

observation to address the needs of the climate modeling community. *Biogeosciences, 9*, 2145-2157

Boochs, F., Kupfer, G., Dockter, K., & Kuhbauch, W. (1990). Shape of the red edge as vitality indicator for plants. *International Journal of Remote Sensing, 11*, 1741-1753

Borzuchowski, J., & Schulz, K. (2010). Retrieval of leaf area index (LAI) and soil water content (WC) using hyperspectral remote sensing under controlled glass house conditions for spring barley and sugar beet. *Remote Sensing, 2*, 1702-1721

Bowman, W.D. (1989). The relationship between leaf water status, gas exchange, and spectral reflectance in cotton leaves. *Remote Sensing of Environment, 30*, 249-255

Briones, L. (1985). Retrospective anthropological vision of *Prosopis*. In M. Habit (Ed.), *The current state of knowledge on Prosopis tamarugo* (pp. 49-51): F.A.O.

Burkart, A. (1976). A monograph of the genus *Prosopis* (Leguminosae subfam. Mimosoideae). [Part 1.]. *Journal of the Arnold Arboretum, 57*, 219-249

Burke, A. (2003). Practical measures in arid land restoration after mining - A review for the southern Namib. *South African Journal of Science, 99*, 413-417

Burke, A. (2005). Endemic plants of the arid succulent karoo in Namibia: Towards hypotheses for their evolution. *Ecography, 28*, 171-180

Canadell, J., Jackson, R.B., Ehleringer, J.R., Mooney, H.A., Sala, O.E., & Schulze, E.D. (1996). Maximum rooting depth of vegetation types at the global scale. *Oecologia, 108*, 583-595

Carevic, F., Carevic, A., & Delatorre, J. (2012). Natural history of genus prosopis at Tarapaca region. *Historia natural del género prosopis en la región de Tarapacá, 30*, 113-117

Carter, G. (1991). Primary and Secondary Effects of Water Content on the Spectral Reflectance of Leaves *American Journal of Botany, 78*, 916-924

Carter, G. (1993). Responses of leaf spectral reflectance to plant stress. *American Journal of Botany, 80*, 239-243

Carter, G.A., & Knapp, A.K. (2001). Leaf optical properties in higher plants: linking spectral characteristics to stress and chlorophyll concentration. *American Journal of Botany, 88*, 677-684

Chaerle, L., & Van Der Straeten, D. (2000). Imaging techniques and the early detection of plant stress*, 5*, 495-501

Chávez, R., & Clevers, J.G.P.W. (2012). Object-based analysis of 8-bands WorldView2 imagery for assessing health condition of desert trees. In: *CGI Report 2012-001* (p. 15). Wageningen: Wageningen University

Chávez, R.O., Clevers, J.G.P.W., Herold, M., Acevedo, E., & Ortiz, M. (2013a). Assessing water stress of desert tamarugo trees using in situ data and very high spatial resolution remote sensing. *Remote Sensing, 5*, 5064-5088

Chávez, R.O., Clevers, J.G.P.W., Herold, M., Ortiz, M., & Acevedo, E. (2013b). Modelling the spectral response of the desert tree *Prosopis tamarugo* to water stress. *International Journal of Applied Earth Observation and Geoinformation, 21*, 53-65

Chávez, R.O., Clevers, J.G.P.W., Verbesselt, J., Naulin, P.I., & Herold, M. 2014). Detecting leaf pulvinar movements on NDVI time series of desert trees: a new approach for water stress detection. *PLOS One (in press)*

CIDERH (2013). *Recursos hídricos de la región de Tarapacá. Diagnóstico y sistematización de la información*. Iquique (Chile): Universidad Arturo Prat

Clark, R.N., & Roush, T.L. (1984). Reflectance spectroscopy: quantitative analysis techniques for remote sensing applications. *Journal of Geophysical Research, 89*, 6329-6340

Clevers, J.G.P.W., De Jong, S.M., Epema, G.F., Van Der Meer, F., Bakker, W.H., Skidmore, A.K., & Addink, E.A. (2001). MERIS and the red-edge position*, 3*, 313-320

Clevers, J.G.P.W., Kooistra, L., & Schaepman, M.E. (2008). Using spectral information from the NIR water absorption features for the retrieval of canopy water content. *International Journal of Applied Earth Observation and Geoinformation, 10*, 388-397

Clevers, J.G.P.W., Kooistra, L., & Schaepman, M.E. (2010). Estimating canopy water content using hyperspectral remote sensing data. *International Journal of Applied Earth Observation and Geoinformation, 12*, 119-125

Cohen, W.B., & Goward, S.N. (2004). Landsat's role in ecological applications of remote sensing. *BioScience, 54*, 535-545

Colombo, R., Meroni, M., Marchesi, A., Busetto, L., Rossini, M., Giardino, C., & Panigada, C. (2008). Estimation of leaf and canopy water content in poplar plantations by means of hyperspectral indices and inverse modeling. *Remote Sensing of Environment, 112*, 1820-1834

Combal, B., Baret, F., Weiss, M., Trubuil, A., Macé, D., Pragnère, A., Myneni, R., Knyazikhin, Y., & Wang, L. (2003). Retrieval of canopy biophysical variables from bidirectional reflectance using prior information to solve the ill-posed inverse problem. *Remote Sensing of Environment, 84*, 1-15

CONAF (1997). *Plan de manejo reserva nacional Pampa del Tamarugal*: Corporación Nacional Forestal (CONAF). Ministerio de Agricultura. Gobierno de Chile

CONAMA (2008). *Biodiversidad de Chile, patrimonio y desafíos*. Santiago de Chile: Ocho Libros Editores

Curran, P.J. (1989). Remote sensing of foliar chemistry. *Remote Sensing of Environment, 30*, 271-278

Curran, P.J., Dungan, J.L., & Peterson, D.L. (2001). Estimating the foliar biochemical concentration of leaves with reflectance spectrometry: Testing the Kokaly and Clark methodologies. *Remote Sensing of Environment, 76*, 349-359

Dai, A. (2011). Drought under global warming: a review. *Wiley Interdisciplinary Reviews: Climate Change, 2*, 45-65

Danielopol, D.L., Griebler, C., Gunatilaka, A., & Notenboom, J. (2003). Present state and future prospects for groundwater ecosystems. *Environmental Conservation, 30*, 104-130

Danson, F.M., & Plummer, S.E. (1995). Red-edge response to forest leaf area index. *International Journal of Remote Sensing, 16*, 183-188

Danson, F.M., Steven, M.D., Malthus, T.J., & Clark, J.A. (1992). High-spectral resolution data for determining leaf water content. *International Journal of Remote Sensing, 13*, 461-470

Darvishzadeh, R., Atzberger, C., Skidmore, A., & Schlerf, M. (2011). Mapping grassland leaf area index with airborne hyperspectral imagery: A comparison study of statistical approaches and inversion of radiative transfer models. *ISPRS Journal of Photogrammetry and Remote Sensing, 66*, 894-906

Dean, W.R.J., Milton, S.J., & Seymour, C.L. (2004). Landuse and biodiversity: Examples from arid Southern Africa. *Annals of Arid Zone, 43*, 255-276

DGA (2011). *Actualización de la oferta y la demanda de recursos hídricos subterráneos del sector hidrogeológico de aprovechamiento común Pampa del Tamarugal*. Santiago, Chile: Dirección General de Aguas, Ministerio de Obras Públicas, Gobierno de Chile

DICTUC (2008). Anexo VIII.2 Modelación de la evolución del nivel de la napa en la Pampa del Tamarugal. In: *EIA proyecto Pampa Hermosa* (p. 169)

DICUC (1988). *Modelo de simulación hidrogeológico de la Pampa del Tamarugal*. Santiago, Chile: Dirección General de Aguas, Ministerio de Obras Públicas, Gobierno de Chile

Dobrowski, S.Z., Pushnik, J.C., Zarco-Tejada, P.J., & Ustin, S.L. (2005). Simple reflectance indices track heat and water stress-induced changes in steady-state chlorophyll fluorescence at the canopy scale. *Remote Sensing of Environment, 97*, 403-414

Doraiswamy, P., Hatfield, J., Jackson, T., Akhmedov, B., Prueger, J., & Stern, A. (2004). Crop condition

and yield simulations using Landsat and MODIS. *Remote Sensing of Environment, 92*, 548-559

Doraiswamy, P.C., Sinclair, T.R., Hollinger, S., Akhmedov, B., Stern, A., & Prueger, J. (2005). Application of MODIS derived parameters for regional crop yield assessment. *Remote Sensing of Environment, 97*, 192-202

Ehleringer, J., & Forseth, I. (1980). Solar tracking by plants. *Science, 210*, 1094-1098

Elmore, A.J., Manning, S.J., Mustard, J.F., & Craine, J.M. (2006). Decline in alkali meadow vegetation cover in California: the effects of groundwater extraction and drought. *Journal of Applied Ecology, 43*, 770-779

Elmore, A.J., Mustard, J.F., & Manning, S.J. (2003). Regional patterns of plant community response to changes in water: Owens Valley, California. *Ecological Applications, 13*, 443-460

Estades, C.F. (1996). Natural history and conservation status of the Tamarugo Conebill in northern Chile. *Wilson Bulletin, 108*, 268-279

Estades, C.F., & López-Calleja, M.V. (1995). First Nesting Record of the Tamarugo Conebill (*Conirostrum tamarugense*). *The Auk, 112*, 797-800

Ezcurra, E. (2006). *Global deserts outlook*. Nairobi: United Nations Environment Programme

Ezcurra, E., Arizaga, S., Valverde, P.L., Mourelle, C., & Flores-Martínez, A. (1992). Foliole movement and canopy architecture of *Larrea tridentata* (DC.) Cov. in Mexican deserts. *Oecologia, 92*, 83-89

Fensholt, R., Rasmussen, K., Nielsen, T.T., & Mbow, C. (2009). Evaluation of earth observation based long term vegetation trends — Intercomparing NDVI time series trend analysis consistency of Sahel from AVHRR GIMMS, Terra MODIS and SPOT VGT data. *Remote Sensing of Environment, 113*, 1886-1898

Feret, J.-B., François, C., Asner, G.P., Gitelson, A.A., Martin, R.E., Bidel, L.P.R., Ustin, S.L., le Maire, G., & Jacquemoud, S. (2008). PROSPECT-4 and 5: Advances in the leaf optical properties model separating photosynthetic pigments. *Remote Sensing of Environment, 112*, 3030-3043

Filella, I., & Penuelas, J. (1994). The red edge position and shape as indicators of plant chlorophyll content, biomass and hydric status. *International Journal of Remote Sensing, 15*, 1459-1470

Flexas, J., Briantais, J.M., Cerovic, Z., Medrano, H., & Moya, I. (2000). Steady-state and maximum chlorophyll fluorescence responses to water stress in grapevine leaves: A new remote sensing system. *Remote Sensing of Environment, 73*, 283-297

Flexas, J., Escalona, J.M., Evain, S., Gulías, J., Moya, I., Osmond, C.B., & Medrano, H. (2002). Steady-state chlorophyll fluorescence (Fs) measurements as a tool to follow variations of net CO2 assimilation and stomatal conductance during water-stress in C3 plants. *Physiologia Plantarum, 114*, 231-240

Foster, K., Ryan, M.H., Real, D., Ramankutty, P., & Lambers, H. (2013). Seasonal and diurnal variation in the stomatal conductance and paraheliotropism of tedera (Bituminaria bituminosa var. albomarginata) in the field. *Functional Plant Biology, 40*, 719-729

Gajardo, R. (1994). *La vegetación natural de Chile. Clasificación y distribución geográfica.* Santiago de Chile: Editorial Universitaria

Gamon, J.A., Field, C.B., Goulden, M.L., Griffin, K.L., Hartley, A.E., Joel, G., Penuelas, J., & Valentini, R. (1995). Relationships between NDVI, canopy structure, and photosynthesis in three Californian vegetation types. *Ecological Applications, 5*, 28-41

Gao, B.C. (1996). NDWI - A normalized difference water index for remote sensing of vegetation liquid water from space. *Remote Sensing of Environment, 58*, 257-266

Geohidrología-SQM (2012). Informe semestral 2. In: *Plan de segumiento ambiental hidrogeológico proyecto Pampa Hermosa* (p. 118)

Gibbes, C., Adhikari, S., Rostant, L., Southworth, J., & Qiu, Y. (2010). Application of object based classification and high resolution satellite imagery for savanna ecosystem analysis. *Remote Sensing, 2*, 2748-2772

Gillon, D., Dauriac, F., Deshayes, M., Valette, J.C., & Moro, C. (2004). Estimation of foliage moisture

content using near infrared reflectance spectroscopy, *124*, 51-62

Giordano, M., & Villholth, K.G. (2007). *The agricultural groundwater revolution: opportunities and threats to development*: The agricultural groundwater revolution: opportunities and threats to development. 2007. xii + 419 pp. many ref.

Gitelson, A., & Merzlyak, M.N. (1994). Spectral relfectance changes associated with autumn senescence of *Aesculus hippocastanum* L. and *Acer platanoides* L. leaves. Spectral features and relation to chlorophyll estimation. *Journal of Plant Physiology, 143*, 286-292

Gitelson, A.A. (2004). Wide Dynamic Range Vegetation Index for Remote Quantification of Biophysical Characteristics of Vegetation. *Journal of Plant Physiology, 161*, 165-173

Gitelson, A.A., Keydan, G.P., & Merzlyak, M.N. (2006). Three-band model for noninvasive estimation of chlorophyll, carotenoids, and anthocyanin contents in higher plant leaves. *Geophys. Res. Lett., 33*, L11402

Govender, M., Dye, P.J., Weiersbye, I.M., Witkowski, E.T.F., & Ahmed, F. (2009). Review of commonly used remote sensing and ground-based technologies to measure plant water stress. *Water SA, 35*, 741-752

Guo, Q. (2004). Slow recovery in desert perennial vegetation following prolonged human disturbance. *Journal of Vegetation Science, 15*, 757-762

Habit, M.A. (1981). *Prosopis tamarugo: fodder tree for arid zones*. Rome: F.A.O.

Hapke, B. (1981). Bidirectional Reflectance Spectroscopy 1. Theory. *J. Geophys. Res., 86*, 3039-3054

Herrmann, I., Pimstein, A., Karnieli, A., Cohen, Y., Alchanatis, V., & Bonfil, D.J. (2011). LAI assessment of wheat and potato crops by VENμS and Sentinel-2 bands. *Remote Sensing of Environment, 115*, 2141-2151

Hochheim, K.P., & Barber, D.G. (1998). Spring wheat yield estimation for western Canada using NOAA NDVI data. *Canadian Journal of Remote Sensing, 24*, 17-27

Horler, D.N.H., Dockray, M., & Barber, J. (1983). The red edge of plant leaf reflectance. *International Journal of Remote Sensing, 4*, 273-288

Houston, J. (2002). Groundwater recharge through an alluvial fan in the Atacama Desert, northern Chile: mechanisms, magnitudes and causes. *Hydrological processes, 16*, 3019-3035

Houston, J. (2006). Evaporation in the Atacama Desert: An empirical study of spatio-temporal variations and their causes. *Journal of Hydrology, 3*, 402-412

Houston, J., & Hartley, A.J. (2003). The central andean west-slope rainshadow and its potential contribution to the origin of hyper-aridity in the Atacama desert. *International Journal of Climatology, 23*, 1453-1464

Huang, J., Wang, X., Li, X., Tian, H., & Pan, Z. (2013). Remotely Sensed Rice Yield Prediction Using Multi-Temporal NDVI Data Derived from NOAA's-AVHRR. *PLOS One, 8*, e70816

Huang, Z., Turner, B.J., Dury, S.J., Wallis, I.R., & Foley, W.J. (2004). Estimating foliage nitrogen concentration from HYMAP data using continuum removal analysis. *Remote Sensing of Environment, 93*, 18-29

Huber, S., Kneubühler, M., Psomas, A., Itten, K., & Zimmermann, N.E. (2008). Estimating foliar biochemistry from hyperspectral data in mixed forest canopy. *Forest Ecology and Management, 256*, 491-501

Hunt Jr, E.R., & Rock, B.N. (1989). Detection of changes in leaf water content using Near- and Middle-Infrared reflectances. *Remote Sensing of Environment, 30*, 43-54

Jacquemoud, S., & Baret, F. (1990). PROSPECT: A model of leaf optical properties spectra. *Remote Sensing of Environment, 34*, 75-91

Jacquemoud, S., Ustin, S.L., Verdebout, J., Schmuck, G., Andreoli, G., & Hosgood, B. (1996). Estimating leaf biochemistry using the PROSPECT leaf optical properties model. *Remote Sensing of Environment, 56*, 194-202

Jacquemoud, S., Verhoef, W., Baret, F., Bacour, C., Zarco-Tejada, P.J., Asner, G.P., François, C., & Ustin, S.L. (2009). PROSPECT + SAIL models: A review of use for vegetation characterization. *Remote Sensing of Environment, 113*, S56-S66

JICA-DGA-PCI (1995). *The study on the development of water resources in northern Chile*. Santiago, Chile: Gobierno de Chile

Jonckheere, I., Fleck, S., Nackaerts, K., Muys, B., Coppin, P., Weiss, M., & Baret, F. (2004). Review of methods for in situ leaf area index determination: Part I. Theories, sensors and hemispherical photography. *Agricultural and Forest Meteorology, 121*, 19-35

Jong, S.M., & Meer, F.D. (2005). *Remote Sensing Image Analysis: Including the Spatial Domain*. Dordrecht: Springer Science + Business Media, Inc.

Jordan, C.F. (1969). Derivation of Leaf-Area Index from Quality of Light on the Forest Floor. *Ecology, 50*, 663-666

Julio Hirschmann, R. (1973). Records on solar radiation in Chile. *Solar Energy, 14*, 129-138

Karnieli, A., & Dall'Olmo, G. (2003). Remote-sensing monitoring of desertification, phenology, and droughts. *Management of Environmental Quality, 14*, 22-38

Karydas, C.G., & Gitas, I.Z. (2011). Development of an IKONOS image classification rule-set for multi-scale mapping of Mediterranean rural landscapes. *International Journal of Remote Sensing, 32*, 9261-9277

Kelly, F.P., & Holm, T.M. (2014). Landsat: Sustaining earth observations beyond landsat 8. *Photogrammetric Engineering and Remote Sensing, 80*, 15

Kesler, S.E., Gruber, P.W., Medina, P.A., Keoleian, G.A., Everson, M.P., & Wallington, T.J. (2012). Global lithium resources: Relative importance of pegmatite, brine and other deposits. *Ore Geology Reviews, 48*, 55-69

Kimes, D.S., & Kirchner, J.A. (1983). Diurnal variations of vegetation canopy structure. *International Journal of Remote Sensing, 4*, 257-271

Knipling, E.B. (1970). Physical and physiological basis for the reflectance of visible and near-infrared radiation from vegetation. *Remote Sensing of Environment, 1*, 155-159

Kokaly, R.F., & Clark, R.N. (1999). Spectroscopic Determination of Leaf Biochemistry Using Band-Depth Analysis of Absorption Features and Stepwise Multiple Linear Regression. *Remote Sensing of Environment, 67*, 267-287

Kokaly, R.F., Despain, D.G., Clark, R.N., & Livo, K.E. (2003). Mapping vegetation in Yellowstone National Park using spectral feature analysis of AVIRIS data. *Remote Sensing of Environment, 84*, 437-456

Koller, D. (1990). Light-driven leaf movements*. *Plant, Cell & Environment, 13*, 615-632

Koller, D. (2001). Solar navigation by plants. In: *Comprehensive Series in Photosciences* (pp. 833-895)

Laliberte, A.S., Fredrickson, E.L., & Rango, A. (2007). Combining decision trees with hierarchical object-oriented image analysis for mapping arid rangelands. *Photogrammetric Engineering and Remote Sensing, 73*, 197-207

Laliberte, A.S., Rango, A., Havstad, K.M., Paris, J.F., Beck, R.F., McNeely, R., & Gonzalez, A.L. (2004). Object-oriented image analysis for mapping shrub encroachment from 1937 to 2003 in southern New Mexico. *Remote Sensing of Environment, 93*, 198-210

Laurent, V.C.E., Verhoef, W., Clevers, J.G.P.W., & Schaepman, M.E. (2011a). Estimating forest variables from top-of-atmosphere radiance satellite measurements using coupled radiative transfer models. *Remote Sensing of Environment, 115*, 1043-1052

Laurent, V.C.E., Verhoef, W., Clevers, J.G.P.W., & Schaepman, M.E. (2011b). Inversion of a coupled canopy–atmosphere model using multi-angular top-of-atmosphere radiance data: A forest case study. *Remote Sensing of Environment, 115*, 2603-2612

Le Maitre, D.C., Scott, D.F., & Colvin, C. (1999). A review of information on interactions between vegetation and groundwater. *Water SA, 25*, 137-152

Leinonen, I., & Jones, H.G. (2004). Combining thermal and visible imagery for estimating canopy temperature and identifying plant stress. *Journal of Experimental Botany, 55*, 1423-1431

LI-COR (1992). *LAI-2000 plant canopy analyser. Instruction manual*. Lincoln, NE, USA: LICOR

Lichtenthaler, H.K. (1983). Determination of total carotenoids and chlorophyll a and b of leaf extract in different solvents. *Biochemical Society Transactions*, 591-592

Lichtenthaler, H.K., & Wellburn, A.R. (1983). Determination of total carotenoids and chlorophyll a and b of leaf extract in different solvents. . *Biochemical Society Transactions*, 591-592

Liu, C.C., Welham, C.V.J., Zhang, X.Q., & Wang, R.Q. (2007). Leaflet movement of *Robinia pseudoacacia* in response to a changing light environment. *Journal of Integrative Plant Biology, 49*, 419-424

Liu, J., Pattey, E., & Admiral, S. (2013). Assessment of in situ crop LAI measurement using unidirectional view digital photography. *Agricultural and Forest Meteorology, 169*, 25-34

Lovich, J.E., & Bainbridge, D. (1999). Anthropogenic degradation of the southern California desert ecosystem and prospects for natural recovery and restoration. *Environmental Management, 24*, 309-326

Malenovský, Z., Bartholomeus, H.M., Acerbi-Junior, F.W., Schopfer, J.T., Painter, T.H., Epema, G.F., & Bregt, A.K. (2007). Scaling dimensions in spectroscopy of soil and vegetation. *International Journal of Applied Earth Observation and Geoinformation, 9*, 137-164

Malenovský, Z., Rott, H., Cihlar, J., Schaepman, M.E., García-Santos, G., Fernandes, R., & Berger, M. (2012). Sentinels for science: Potential of Sentinel-1,-2, and-3 missions for scientific observations of ocean, cryosphere, and land. *Remote Sensing of Environment, 120*, 91-101

Mao, D., Wang, Z., Luo, L., & Ren, C. (2012). Integrating AVHRR and MODIS data to monitor NDVI changes and their relationships with climatic parameters in Northeast China. *International Journal of Applied Earth Observation and Geoinformation, 18*, 528-536

Masek, J.G., Vermote, E.F., Saleous, N.E., Wolfe, R., Hall, F.G., Huemmrich, K.F., Gao, F., Kutler, J., & Lim, T.K. (2006). A landsat surface reflectance dataset for North America, 1990-2000. *IEEE Geoscience and Remote Sensing Letters, 3*, 68-72

McGlynn, I.O., & Okin, G.S. (2006). Characterization of shrub distribution using high spatial resolution remote sensing: Ecosystem implications for a former Chihuahuan Desert grassland. *Remote Sensing of Environment, 101*, 554-566

McKay, C.P., Friedmann, E.I., Gómez-Silva, B., Cáceres-Villanueva, L., Andersen, D.T., & Landheim, R. (2003). Temperature and moisture conditions for life in the extreme arid region of the atacama desert: Four years of observations including the El Niño of 1997-1998. *Astrobiology, 3*, 393-406

Menzel, A. (2002). Phenology: its importance to the global change community. *Climatic Change, 54*, 379-385

Meyer, W.S., & Ritchie, J.T. (1980). Resistance to water flow in the Sorghum plant. *Plant Physiology, 65*, 33-39

Mooney, H.A., Gulmon, S.L., Rundel, P.W., & Ehleringer, J. (1980). Further observations on the water relations of *Prosopis tamarugo* of the northern Atacama Desert. *Oecologia, 44*, 177-180

Moorthy, I., Miller, J.R., & Noland, T.L. (2008). Estimating chlorophyll concentration in conifer needles with hyperspectral data: an assessment at the needle and canopy level. *Remote Sensing of Environment, 112*, 2824-2838

Moran, M.S., Clarke, T.R., Inoue, Y., & Vidal, A. (1994). Estimating crop water deficit using the relation between surface-air temperature and spectral vegetation index. *Remote Sensing of Environment, 49*, 246-263

Moran, M.S., Pinter Jr, P.J., Clothier, B.E., & Allen, S.G. (1989). Effect of water stress on the canopy architecture and spectral indices of irrigated alfalfa. *Remote Sensing of Environment, 29*, 251-261

Morton, D.C., Nagol, J., Carabajal, C.C., Rosette, J., Palace, M., Cook, B.D., Vermote, E.F., Harding, D.J., & North, P.R.J. (2014). Amazon forests maintain consistent canopy structure and greenness during the dry season. *Nature, 506*, 221-224

Naumburg, E., Mata-Gonzalez, R., Hunter, R.G., McLendon, T., & Martin, D.W. (2005). Phreatophytic vegetation and groundwater fluctuations: A review of current research and application of ecosystem response modeling with an emphasis on great basin vegetation. *Environmental Management, 35*, 726-740

Navarro-González, R., Rainey, F.A., Molina, P., Bagaley, D.R., Hollen, B.J., De La Rosa, J., Small, A.M., Quinn, R.C., Grunthaner, F.J., Cáceres, L., Gomez-Silva, B., & McKay, C.P. (2003). Mars-Like Soils in the Atacama Desert, Chile, and the Dry Limit of Microbial Life. *Science, 302*, 1018-1021

Noy-Meir, I. (1985). Desert ecosystem structure and function. *Ecosystems of the world, 12A. Hot deserts and arid shrublands, A*, 93-103

Ogle, K., & Reynolds, J.F. (2004). Plant responses to precipitation in desert ecosystems: Integrating functional types, pulses, thresholds, and delays. *Oecologia, 141*, 282-294

Olson, D.M., Dinerstein, E., Wikramanayake, E.D., Burgess, N.D., Powell, G.V.N., Underwood, E.C., D'Amico, J.A., Itoua, I., Strand, H.E., Morrison, J.C., Loucks, C.J., Allnutt, T.F., Ricketts, T.H., Kura, Y., Lamoreux, J.F., Wettengel, W.W., Hedao, P., & Kassem, K.R. (2001). Terrestrial ecoregions of the world: A new map of life on Earth. *BioScience, 51*, 933-938

Ortega, A., Escobar, R., Colle, S., & de Abreu, S.L. (2010). The state of solar energy resource assessment in Chile. *Renewable Energy, 35*, 2514-2524

Ortiz, M., Silva, P., & Acevedo, E. (2010). Leaf water parameters in *Prosopis tamarugo* Phil. subject to a lowering of the water table. *Nivel freático en la Pampa del Tamarugal y crecimiento de Prosopis tamarugo Phil. Tesis para optar al Grado Académico de Doctor en Ciencias Silvoagrpecuarias y Veterinarias* (pp. 15-42). Santiago, Chile: Universidad de Chile

Oyarzún, J., & Oyarzún, R. (2011). Sustainable development threats, inter-sector conflicts and environmental policy requirements in the arid, mining rich, Northern Chile territory. *Sustainable Development, 19*, 263-274

Pastenes, C., Pimentel, P., & Lillo, J. (2005). Leaf movements and photoinhibition in relation to water stress in field-grown beans. *Journal of Experimental Botany, 56*, 425-433

Pastenes, C., Porter, V., Baginsky, C., Norton, P., & González, J. (2004). Paraheliotropism can protect water-stressed bean (*Phaseolus vulgaris* L.) plants against photoinhibition. *Journal of Plant Physiology, 161*, 1315-1323

Patten, D.T., Rouse, L., & Stromberg, J.C. (2008). Isolated spring wetlands in the Great Basin and Mojave deserts, USA: Potential response of vegetation to groundwater withdrawal. *Environmental Management, 41*, 398-413

Pebesma, E.J. (2004). Multivariable geostatistics in S: The gstat package. *Computers and Geosciences, 30*, 683-691

Penuelas, J., Gamon, J.A., Fredeen, A.L., Merino, J., & Field, C.B. (1994). Reflectance indices associated with physiological changes in nitrogen- and water-limited sunflower leaves. *Remote Sensing of Environment, 48*, 135-146

Peñuelas, J., Pinol, J., Ogaya, R., & Filella, I. (1997). Estimation of plant water concentration by the reflectance Water Index WI (R900/R970). *International Journal of Remote Sensing, 18*, 2869-2875

Peper, P.J., & McPherson, E.G. (2003). Evaluation of four methods for estimating leaf area of isolated trees. *Urban Forestry and Urban Greening, 2*, 19-29

Pérez-Priego, O., Zarco-Tejada, P.J., Miller, J.R., Sepulcre-Cantó, G., & Fereres, E. (2005). Detection

of water stress in orchard trees with a high-resolution spectrometer through chlorophyll fluorescence In-Filling of the O 2-A band. *IEEE Transactions on Geoscience and Remote Sensing, 43*, 2860-2868

Pettorelli, N., Vik, J.O., Mysterud, A., Gaillard, J.-M., Tucker, C.J., & Stenseth, N.C. (2005). Using the satellite-derived NDVI to assess ecological responses to environmental change. *Trends in Ecology & Evolution, 20*, 503-510

Phillips, W.S. (1963). Depth of roots in soil. *Ecology, 44*, 424-424

Portnov, B.A., & Safriel, U.N. (2004). Combating desertification in the Negev: Dryland agriculture vs. dryland urbanization. *Journal of Arid Environments, 56*, 659-680

Pringle, C.M. (2001). Hydrologic connectivity and the management of biological reserves: a global perspective. *Ecological Applications, 11*, 981-998

Proctor, M.C., & Pence, V.C. (2002). Vegetative tissues: bryophytes, vascular resurrection plants and vegetative propagules. In: *Desiccation and survival in plants: Drying without dying. Black M, Pritchard HW* (pp. 207-237)

R Core Team (2013). R: A Language and Environment for Statistical Computing. R Foundation for Statistical Computing, Vienna, Austria. http://www.R-project.org/

Ramírez-Leyton, G., & Pincheira-Donoso, D. (2005). *Fauna del Altiplano y Desierto de Atacama. Vertebrados de la Provncia de El Loa.* Calama, Chile: Phrynosaura Ediciones

Raven, P.H., Evert, R.F., & Eichhorn, S.E. (2005). *Biology of plants*. New York, NY: Freeman

Richardson, A.D., & Berlyn, G.P. (2002). Changes in foliar spectral reflectance and chlorophyll fluorescence of four temperate species following branch cutting. *Tree Physiology, 22*, 499-506

Richter, H. (1997). Water relations of plants in the field: some comments on the measurement of selected parameters. *Journal of Experimental Botany, 48*, 1-7

Riedemann, P., Aldunate, G., & Teillier, S. (2006). *Flora nativa de valor ornamental. Chile, Zona Norte. Identificación y propagación*. Santiago, Chile: Productora Gráfica Andros Ltda

Rojas, R., Batelaan, O., Feyen, L., & Dassargues, A. (2010). Assessment of conceptual model uncertainty for the regional aquifer Pampa del Tamarugal - North Chile. *Hydrology and Earth System Sciences, 14*, 171-192

Rojas, R., & Dassargues, A. (2007). Groundwater flow modelling of the regional aquifer of the Pampa del Tamarugal, Northern Chile. *Hydrogeology Journal, 15*, 537-551

Romero, H., Méndez, M., & Smith, P. (2012). Mining development and environmental injustice in the Atacama Desert of Northern Chile. *Environmental Justice, 5*, 70-76

Romm, J. (2011). Desertification: The next dust bowl. *Nature, 478*, 450-451

Schaepman-Strub, G., Schaepman, M.E., Painter, T.H., Dangel, S., & Martonchik, J.V. (2006). Reflectance quantities in optical remote sensing-definitions and case studies. *Remote Sensing of Environment, 103*, 27-42

Schmidhalter, U. (1997). The gradient between pre-dawn rhizoplane and bulk soil matric potentials, and its relation to the pre-dawn root and leaf water potentials of four species. *Plant, Cell and Environment, 20*, 953-960

Scholander, P.F., Hammel, H.T., Bradstreet, E.D., & Hemmingsen, E.A. (1965). Sap pressure in vascular plants. *Science, 148*, 339-346

Schwinning, S., & Sala, O.E. (2004). Hierarchy of responses to resource pulses in arid and semi-arid ecosystems. *Oecologia, 141*, 211-220

Seelig, H.D., Hoehn, A., Stodieck, L.S., Klaus, D.M., Adams Iii, W.W., & Emery, W.J. (2009). Plant water parameters and the remote sensing R 1300/R 1450 leaf water index: Controlled condition dynamics during the development of water deficit stress. *Irrigation Science, 27*, 357-365

Shibayama, M., Takahashi, W., Morinaga, S., & Akiyama, T. (1993). Canopy water deficit detection

in paddy rice using a high resolution field spectroradiometer. *Remote Sensing of Environment, 45*, 117-126

Soudani, K., & Francois, C. (2014). Remote sensing: A green illusion. *Nature, 506*, 165-166

Stone, E.L., & Kalisz, P.J. (1991). On the maximum extent of tree roots. *Forest Ecology and Management, 46*, 59-102

Suárez, L., Zarco-Tejada, P.J., Sepulcre-Cantó, G., Pérez-Priego, O., Miller, J.R., Jiménez-Muñoz, J.C., & Sobrino, J. (2008). Assessing canopy PRI for water stress detection with diurnal airborne imagery. *Remote Sensing of Environment, 112*, 560-575

Sudzuki, F. (1985a). Environmental influence on foliar anatomy of *Prosopis tamarugo* Phil. In M. Habit (Ed.), *The current state of knowledge on Prosopis tamarugo*. Rome: F.A.O.

Sudzuki, F. (1985b). Environmental moisture utilization by *Prosopis tamarugo* Phil. In M. Habit (Ed.), *The current state of knowledge on Prosopis tamarugo*. Rome: F.A.O.

Taiz, L., & Zeiger, E. (2010). *Plant physiology*. Sunderland, MA: Sinauer Associates

Trobok, S. (1985). Fruit and seed morphology of Chilean Prosopis (Fabaceae-Mimosoidae). In M. Habit (Ed.), *The current state of knowledge on Prosopis tamarugo*. Rome: F.A.O.

Tucker, C.J. (1979). Red and photographic infrared linear combinations for monitoring vegetation. *Remote Sensing of Environment, 8*, 127-150

Updike, T., & Comp, C. (2010). Radiometric use of WorldView2 imagery. *Digital Globe technical note*, 17

Vargas, H.A., & Bobadilla, D. (2000). Insectos asociados al bosque de tamarugo. In A.B.L. Pancel (Ed.), *Agentes de daño en el bosque nativo* (pp. 283-318). Santiago: Editorial Universitaria S.A

Verbesselt, J., Robinson, A., Stone, C., & Culvenor, D. (2009). Forecasting tree mortality using change metrics derived from MODIS satellite data. *Forest Ecology and Management, 258*, 1166-1173

Verbesselt, J., Zeileis, A., & Herold, M. (2012). Near real-time disturbance detection using satellite image time series. *Remote Sensing of Environment, 123*, 98-108

Verhoef, W. (1984). Light scattering by leaf layers with application to canopy reflectance modeling: The SAIL model. *Remote Sensing of Environment, 16*, 125-141

Verhoef, W., & Bach, H. (2003). Simulation of hyperspectral and directional radiance images using coupled biophysical and atmospheric radiative transfer models. *Remote Sensing of Environment, 87*, 23-41

Verhoef, W., & Bach, H. (2007). Coupled soil-leaf-canopy and atmosphere radiative transfer modeling to simulate hyperspectral multi-angular surface reflectance and TOA radiance data. *Remote Sensing of Environment, 109*, 166-182

Veste, M., Staudinger, M., & Küppers, M. (2008). Spatial and temporal variability of soil water in drylands: plant water potential as a diagnostic tool. *Forestry Studies in China, 10*, 74-80

Viña, A., & Gitelson, A.A. (2005). New developments in the remote estimation of the fraction of absorbed photosynthetically active radiation in crops. *Geophysical Research Letters, 32*, 1-4

Viña, A., Gitelson, A.A., Nguy-Robertson, A.L., & Peng, Y. (2011). Comparison of different vegetation indices for the remote assessment of green leaf area index of crops. *Remote Sensing of Environment, 115*, 3468-3478

Vohland, M., Mader, S., & Dorigo, W. (2010). Applying different inversion techniques to retrieve stand variables of summer barley with PROSPECT + SAIL. *International Journal of Applied Earth Observation and Geoinformation, 12*, 71-80

Walter, H., & Mueller-Dombois, D. (1971). *Ecology of tropical and subtropical vegetation*: Edinburgh, UK, Oliver & Boyd

Wang, J., Guo, N., Wang, X., & Yang, J. (2007). Comparisons of normalized difference vegetation index from MODIS Terra and Aqua data in northwestern China. In: *International Geoscience and Remote Sensing Symposium (IGARSS)* (pp. 3390-3393)

Wang, P., Yu, J., Pozdniakov, S.P., Grinevsky, S.O., & Liu, C. (2014). Shallow groundwater dynamics and its driving forces in extremely arid areas: A case study of the lower Heihe River in northwestern China. *Hydrological processes, 28*, 1539-1553

Williams, D.L., Goward, S., & Arvidson, T. (2006). Landsat: Yesterday, today, and tomorrow. *Photogrammetric Engineering and Remote Sensing, 72*, 1171-1178

Wolfe, R.E., Nishihama, M., Fleig, A.J., Kuyper, J.A., Roy, D.P., Storey, J.C., & Patt, F.S. (2002). Achieving sub-pixel geolocation accuracy in support of MODIS land science. *Remote Sensing of Environment, 83*, 31-49

Wu, A., Xiong, X., & Cao, C. (2008). Terra and Aqua MODIS inter-comparison of three reflective solar bands using AVHRR onboard the NOAA-KLM satellites. *International Journal of Remote Sensing, 29*, 1997-2010

Yu, G., Miwa, T., Nakayama, K., Matsuoka, N., & Kon, H. (2000). A proposal for universal formulas for estimating leaf water status of herbaceous and woody plants based on spectral reflectance properties. *Plant and Soil, 227*, 47-58

Zarco-Tejada, P.J., Rueda, C.A., & Ustin, S.L. (2003). Water content estimation in vegetation with MODIS reflectance data and model inversion methods. *Remote Sensing of Environment, 85*, 109-124

Zelada, L. (1986). The influence of the productivity of *Prosopis tamarugo* on livestock production in the Pampa del Tamarugal - a review. *Forest Ecology and Management, 16*, 15-31

Summary

Water stress assessment of natural vegetation plays a key role in water management of desert ecosystems. It allows scientists and managers to relate water extraction rates to changes in vegetation water condition, and consequently to define safe water extraction rates for maintaining a healthy ecosystem. Previous research has shown that optical remote sensing constitutes a powerful tool for assessing vegetation water stress due to its capability of quantitatively estimating important parameters of vegetation such as leaf area index (LAI), green canopy fraction (GCF), and canopy water content (CWC). However, the estimation of these parameters using remote sensing can be challenging in the case of desert vegetation. Desert plants have to cope with high solar irradiation and limited water. In order to maintain an adequate water balance and to avoid photoinhibition, desert plants have evolved different adaptations. A common one is heliotropism or 'solar tracking', an ability of many desert species to move their leaves to avoid facing direct high solar irradiation levels during the day and season. This adaptation (paraheliotropism) can have an important effect on the canopy spectral reflectance measured by satellites as well as on vegetation indices such as the normalized difference vegetation index (NDVI). In this thesis, I propose a remote sensing based approach to assess water stress of desert vegetation, exemplified in the case of the Tamarugo (*Prosopis tamarugo* Phil) tree in the Atacama Desert (Northern Chile), a 'solar tracker' species, which is threatened by groundwater overexploitation.

In the first chapter of this thesis (general introduction), I explained the motivation of the PhD project and elaborated four research questions, which are later discussed in chapters 2, 3, 4, and 5. The thesis concluded with chapter 6, where I provide a synthesis of the main results, general conclusions and a final reflection and outlook.

In the second chapter, I studied the effects of water stress on Tamarugo plants under laboratory conditions and modelled the light-canopy interaction using the Soil-Leaf-Canopy radiative transfer model. I described for the first time pulvinar movement of Tamarugo and quantified its effects on canopy spectral reflectance with and without stress. I showed that different spectral indices have potential to assess water stress of Tamarugo by means of LAI and CWC. In the third chapter, I measured the effects of pulvinar movements on canopy reflectance for Tamarugos

under field conditions and used high spatial resolution images to assess water stress at the tree level. I developed an automated process to first identify single trees and delineate their crowns, and secondly, to estimate LAI and GCF using spectral vegetation indices. These indices (NDVI and chlorophyll red-edge index) were negatively correlated to diurnal values of solar irradiation as a consequence of leaf pulvinar movements. For this reason, higher values of both vegetation indices are expected to occur in the morning and in winter (low solar radiation) than at midday or summer.

In the fourth chapter I studied the effects of diurnal pulvinar movements on NDVI time series from the MODIS-Terra satellite (acquired in the morning) and the MODIS-Aqua satellite (acquired at midday) for the period 2003-2012 and the seasonal effects of pulvinar movements on NDVI time series of Landsat images for the period 1998-2012 for Tamarugo areas with and without water stress. NDVI values measured by MODIS-Terra (morning) were higher than the NDVI values measured by MODIS-Aqua (afternoon) and the difference between the two, the $\Delta NDVI_{mo\text{-}mi}$, showed good potential as water stress indicator. In a similar way, I observed a strong seasonal effect on the Landsat NDVI signal, attributed to pulvinar movements, and the difference between winter and summer, the $\Delta NDVI_{W\text{-}S}$, also showed good potential for detecting and quantifying water stress. The $\Delta NDVI_{mo\text{-}mi}$, the $\Delta NDVI_{W\text{-}S}$ and the NDVI itself measured systematically in winter time ($NDVI_W$) were negatively correlated with in situ groundwater depth measurements.

In chapter five I used a dense NDVI time series of Landsat images for the period 1989-2013, combined with high spatial resolution satellite imagery and hydrogeological records, to provide a quantitative assessment of the water status of Tamarugo vegetation after 50 years of increasing groundwater extraction. The results showed that the $NDVI_W$ and $\Delta NDVI_{W\text{-}S}$ of the Tamarugo vegetation declined 19% and 51%, respectively, as groundwater depleted (3 meters on average) for the period 1989-2013. Both variables were negatively correlated to groundwater depth both temporally and spatially. About 730.000 Tamarugo trees remained in the study area by 2011, from which 5.2% showed a GCF<0.25 which is associated to severe water stress. Based on this spatio-temporal analysis, I suggest that the survival of Tamarugo trees is limited to a maximum groundwater depth of 20 meters.

The main conclusions of this PhD thesis are summarized as follows:

i. Heliotropism or leaf 'solar tracking', a common adaptation among desert plants, has an important impact on canopy spectral reflectance. As shown in the case of the Tamarugo trees, widely used vegetation indices such as the NDVI were negatively correlated to solar irradiation (the stimulus for leaf solar tracking), showing a distinct diurnal and seasonal cycle.

ii. An early symptom of water stress in paraheliotropic plants (leaves facing away the sun) is the decline of the amplitude of the diurnal and seasonal NDVI cycles. Thus, remote sensing estimations of this amplitude (e.g. the NDVI difference between winter and summer or the difference between midday and morning) can be used to detect and map early water stress of paraheliotropic vegetation.

iii. At the tree level, very high spatial resolution images combined with object based image analysis and in-situ data provided accurate estimations of the water status of small desert vegetation features, such as isolated trees. For monitoring purposes, careful consideration of the time during the day and the season at which the images are taken needs to be taken to avoid misleading interpretations.

iv. Time series analysis of historical satellite images combined with very high spatial resolution images and hydrogeological records can provide a quantitative spatio-temporal assessment of the effects of long-term groundwater extraction on desert vegetation.

Samenvatting

De bepaling van waterstress bij natuurlijke vegetatie speelt een belangrijke rol in het waterbeheer van woestijn-ecosystemen. Het stelt wetenschappers en managers in staat om de waterextractie-snelheid te relateren aan veranderingen in de waterconditie van vegetatie, en bijgevolg om veilige waterextractie-snelheden vast te stellen voor het behoud van een gezond ecosysteem. Eerder onderzoek heeft aangetoond dat optische remote sensing een krachtig hulpmiddel vormt voor het bepalen van waterstress bij vegetatie omdat het belangrijke parameters van de vegetatie, zoals de bladoppervlakte-index (LAI), de fractie groene vegetatie (GCF) en het watergehalte (CWC), kwantitatief kan schatten. Toch kan de schatting van deze parameters met behulp van remote sensing een uitdaging zijn in het geval van woestijnvegetatie. Woestijnplanten hebben te kampen met een hoge instraling en een beperkte hoeveelheid water. Om een geschikte waterbalans in stand te houden en om foto-inhibitie te vermijden, hebben woestijnplanten verschillende aanpassingen ontwikkeld. Een veelvoorkomende aanpassing is heliotropisme of 'solar tracking', een vermogen van veel woestijnplanten om hun bladeren af te wenden van de zon om te voorkomen dat hoge niveaus direct zonlicht op de bladeren vallen. Deze aanpassing (paraheliotropisme) kan een belangrijk effect hebben op de spectrale reflectie van vegetatie gemeten door satellieten en op vegetatie-indices zoals de ‘normalized difference vegetation index’ (NDVI). In dit proefschrift stel ik een op remote sensing gebaseerde benadering voor om waterstress van woestijnvegetatie te bepalen, met als voorbeeld het geval van de Tamarugo boom (*Prosopis tamarugo* Phil.) in de Atacama woestijn (Noord-Chili), een 'solar tracker' die bedreigd wordt door overexploitatie van grondwater.

In het eerste hoofdstuk van dit proefschrift (algemene inleiding) heb ik de motivatie van het promotieproject uitgelegd en vier onderzoeksvragen uitgewerkt, die later worden besproken in de hoofdstukken 2, 3, 4, en 5. Het proefschrift wordt afgesloten met hoofdstuk 6, waar ik een synthese van de belangrijkste resultaten, algemene conclusies en een uiteindelijke reflectie en vooruitzichten geef.

In het tweede hoofdstuk heb ik de effecten van waterstress op Tamarugo planten onder laboratoriumomstandigheden bestudeerd en de interactie van licht met vegetatie gemodelleerd met het Soil-Leaf-Canopy stralingsinteractiemodel. Ik heb voor het eerst de beweging van de pulvinus van Tamarugo beschreven en de effecten hiervan op de spectrale reflectie van vegetatie met en zonder stress

gekwantificeerd. Ik heb aangetoond dat verschillende spectrale indices potentie hebben om waterstress van Tamarugo te bepalen door middel van LAI en CWC. In het derde hoofdstuk, heb ik de effecten van bewegingen van de pulvinus op de vegetatiereflectie voor Tamarugo onder veldomstandigheden gemeten en beelden met een hoge ruimtelijke resolutie gebruikt om waterstress te bepalen op boomniveau. Ik heb een geautomatiseerd proces ontwikkeld om eerst afzonderlijke bomen te identificeren en hun kronen af te bakenen, en vervolgens om LAI en GCF te schatten met behulp van spectrale vegetatie-indices. Deze indices (NDVI en de chlorofyl red-edge index) waren negatief gecorreleerd met dagelijkse waarden van inkomende zonnestraling ten gevolge van bladbewegingen veroorzaakt door de pulvinus. Om deze reden worden hogere waarden van beide vegetatie-indices verwacht in de ochtend en in de winter (minder zonnestraling) dan midden op de dag of in de zomer.

In het vierde hoofdstuk bestudeerde ik de effecten van dagelijkse bewegingen van de pulvinus op NDVI-tijdreeksen van de MODIS-Terra satelliet (opgenomen in de ochtend) en de MODIS-Aqua satelliet (opgenomen rond de middag) voor de periode 2003-2012 en de seizoenseffecten van bewegingen van de pulvinus op NDVI-tijdreeksen van Landsat-beelden over de periode 1998-2012 voor Tamarugo met en zonder waterstress. NDVI-waarden gemeten door MODIS-Terra (ochtend) waren hoger dan de NDVI-waarden gemeten door MODIS-Aqua (middag) en het verschil tussen de twee, de $\Delta NDVI_{mo\text{-}mi}$, toonde potentie als indicator voor waterstress. Op soortgelijke wijze heb ik een sterk seizoenseffect op het NDVI-signaal van Landsat waargenomen, te verklaren door bewegingen van de pulvinus, en het verschil tussen winter en zomer, de $\Delta NDVI_{W\text{-}S}$, bleek ook goede mogelijkheden te hebben voor het opsporen en kwantificeren van waterstress. De $\Delta NDVI_{mo\text{-}mi}$, de $\Delta NDVI_{W\text{-}S}$ en de NDVI zelf systematisch gemeten in de winter ($NDVI_W$) waren negatief gecorreleerd met in-situ metingen van de grondwaterdiepte.

In hoofdstuk vijf heb ik een dichte NDVI-tijdreeks van Landsat-beelden voor de periode 1989-2013 gebruikt, in combinatie met hoge ruimtelijke resolutie satellietbeelden en hydrogeologische gegevens, om een kwantitatieve bepaling van de waterstatus van Tamarugo vegetatie na 50 jaar van toenemende grondwaterextractie uit te voeren. De resultaten toonden aan dat de $NDVI_W$ en $\Delta NDVI_{W\text{-}S}$ van de Tamarugo vegetatie met respectievelijk 19% en 51% daalden bij dalende grondwaterstand gedurende de periode 1989-2013 (daling gemiddeld 3

meter). Beide variabelen waren negatief gecorreleerd met grondwaterdiepte zowel temporeel als spatiaal. Ongeveer 730.000 Tamarugo bomen waren in 2011 nog over in het studiegebied, waarvan 5,2% een GCF<0,25 vertoonde, die wordt geassocieerd met ernstige waterstress. Op basis van deze spatio-temporele analyse veronderstel ik dat het voortbestaan van Tamarugo bomen is beperkt tot een maximale grondwaterdiepte van 20 meter.

De belangrijkste conclusies van dit proefschrift worden als volgt samengevat:

i. Heliotropisme of 'solar tracking' van bladeren, een veelvoorkomende aanpassing onder woestijnplanten, heeft een belangrijke impact op de spectrale reflectie van vegetatie. Zoals aangetoond in het geval van de Tamarugo bomen waren op grote schaal gebruikte vegetatie-indices zoals de NDVI negatief gecorreleerd met de hoeveelheid inkomende zonnestraling (de prikkel voor de 'solar tracking' van de bladeren), met een duidelijke dagelijkse en seizoensgebonden cyclus.

ii. Een vroegtijdig symptoom van waterstress bij paraheliotropische planten (bladeren die zich afwenden van de zon) is de daling van de amplitude van de dagelijkse en seizoensgebonden NDVI cycli. Zo kunnen remote sensing schattingen van deze amplitude (bijvoorbeeld het NDVI-verschil tussen winter en zomer of het verschil tussen middag en ochtend) worden gebruikt om vroegtijdige waterstress bij paraheliotropische vegetatie te detecteren en in kaart te brengen.

iii. Op boomniveau gaven beelden met hoge ruimtelijke resolutie gecombineerd met een object-gebaseerde beeldanalyse en in-situ gegevens nauwkeurige schattingen van eigenschappen van kleine woestijnvegetatie, zoals geïsoleerde bomen. Voor monitoring moet een zorgvuldige afweging gemaakt worden van het moment op de dag en het seizoen waarin de beelden worden genomen om misleidende interpretaties te vermijden.

iv. Tijdreeksanalyse van historische satellietbeelden in combinatie met beelden met een hoge ruimtelijke resolutie en hydrogeologische gegevens kunnen een kwantitatieve spatio-temporele bepaling van de gevolgen van langdurige grondwaterwinning op vegetatie bieden.

Resumen

La evaluación del estrés hídrico de la vegetación nativa es clave para el manejo hídrico de ecosistemas desérticos. Estas evaluaciones permiten tanto a científicos como a profesionales del área ambiental relacionar diferentes tasas de extracción de agua con el estado hídrico de la vegetación, y de esta forma, definir umbrales de extracción que permitan conservar el ecosistema. Investigaciones previas han demostrado el gran potencial que la percepción remota (o teledetección) óptica tiene para la evaluación del estrés hídrico de la vegetación, puesto que permite estimar cuantitativamente importantes parámetros tales como índice de área foliar (LAI), fracción de copa verde (GCF) y contenido de agua de la copa (CWC). Sin embargo, la estimación de estos parámetros mediante sensores remotos puede ser compleja en el caso de la vegetación desértica. Las especies vegetales desérticas experimentan extrema radiación solar y escasez de agua. A fin de mantener su balance hídrico y evitar fotoinhibición, estas especies han desarrollado diferentes adaptaciones, entre las que se incluyen los movimientos heliotrópicos. Heliotropismo es la habilidad de muchas plantas desérticas de mover o ajustar la posición de sus hojas durante el día, o a lo largo de las estaciones del año, a fin de evitar altos niveles de radiación solar directamente sobre las láminas de las hojas. Esta adaptación (paraheliotropismo) puede tener un importante efecto en la reflectancia espectral de la copa medida a través de satélites así como en índices espectrales de vegetación, como el índice de vegetación de diferencia normalizada (NDVI). En esta tesis, se propone una metodología basada en sensores remotos para evaluar estrés hídrico de la vegetación desértica, ejemplificada en el caso de la especie arbórea Tamarugo (*Prosopis tamarugo* Phil) del desierto de Atacama (Norte de Chile). Tamarugo es una especie paraheliotrópica que se encuentra actualmente bajo amenaza debido a sobrexplotación de los acuíferos subterráneos.

En el primer capítulo de esta tesis (introducción general), se explica la motivación del proyecto de PhD y se elaboran cuatro preguntas de investigación, las que son posteriormente abordadas en los capítulos 2, 3, 4 y 5. Esta tesis concluye con el capítulo 6, el cual proporciona una síntesis de los principales resultados, seguido de conclusiones generales, y finalmente, una reflexión y sugerencias para futuras investigaciones.

En el segundo capítulo, se estudió los efectos del estrés hídrico en plantas de Tamarugo bajo condiciones de laboratorio y se modeló la interacción de la luz y el

follaje de las plantas usando el modelo de transferencia de radiación Soil-Leaf-Canopy. Se describió por primera vez movimientos pulvinares de esta especie y se cuantificó su efecto en la reflectancia espectral del follaje con y sin estrés hídrico. En este experimento se mostró que diferentes índices espectrales tienen potencial para evaluar estrés hídrico en Tamarugo, en términos de cambios en LAI y CWC. En el tercer capítulo, se midió en terreno los efectos de los movimientos pulvinares en la reflectancia espectral de la copa en Tamarugos y se utilizó imágenes satelitales de alta resolución para evaluar estrés hídrico a nivel de árboles individuales. Para tales efectos, se desarrolló un proceso automatizado para identificar árboles individuales y delinear sus copas, y además, estimar LAI y GCF para cada árbol usando índices espectrales de vegetación. Estos índices (NDVI y chlorophyll red-edge index) mostraron una correlación negativa con valores diarios de radiación solar debido al efecto de los movimientos pulvinares de las hojas de Tamarugo. De esta forma, es esperable que valores más altos de ambos índices ocurran en la mañana y en invierno (baja radiación solar) en comparación con valores medidos a medio día o en el verano (alta radiación solar).

En el cuarto capítulo, se estudió el efecto de movimientos pulvinares durante el día en series de tiempo de NDVI obtenidas del satélite MODIS-Terra (mañana) y del satélite MODIS-Aqua (medio día) para el periodo 2003-2012, así como el efecto de movimientos pulvinares estacionales sobre series de tiempo de NDVI obtenidas del satélite Landsat para el periodo 1998-2012 en áreas de Tamarugo con y sin stress hídrico. Los valores de NDVI medidos por MODIS-Terra (mañana) fueron mayores que los valores medidos por MODIS-Aqua (medio día), y la diferencia entre ambos ($\Delta NDVI_{mo\text{-}mi}$), resultó ser un buen indicador de estrés hídrico. Análogamente, se observó un efecto estacional marcado en la señal de NDVI registrada por Landsat, y la diferencia de NDVI entre invierno y verano ($\Delta NDVI_{W\text{-}S}$), también mostró potencial para detectar y cuantificar stress hídrico en Tamarugo. Tanto $\Delta NDVI_{mo\text{-}mi}$, $\Delta NDVI_{W\text{-}S}$ y NDVI medido sistemáticamente en invierno ($NDVI_W$) presentaron una correlación negativa con valores de profundidad de la napa subterránea.

En el quinto capítulo, se utilizó una densa serie temporal de NDVI obtenida del satélite Landsat para el periodo 1989-2013, junto con imágenes de alta resolución espacial y registros hidrogeológicos, para realizar una evaluación cuantitativa del estado hídrico de las formaciones de Tamarugo luego de 50 años de creciente extracción de agua subterránea. Los resultados de este estudio mostraron que tanto

$NDVI_W$ como $\Delta NDVI_{W-S}$ decrecieron un 19% y 51%, respectivamente, conforme la napa subterránea descendió durante el periodo 1989-2013 (3 metros en promedio). Ambas variables presentaron una correlación negativa con la profundidad de la napa tanto en su dimensión espacial como temporal. Alrededor de 730.000 tamarugos prevalecían aún en el área de estudio en 2011, de los cuales el 5.2% presentó valores de GCF<0.25, los que están asociados con un severo nivel de estrés hídrico. Este análisis espacio temporal, sugiere que la supervivencia de tamarugos está limitada por un valor máximo de profundidad de napa de 20 metros.

Las principales conclusiones de esta tesis de PhD se indican a continuación:

i. Heliotropismo es una adaptación común de plantas de desierto, la cual tiene un impacto importante en la reflectancia espectral de copa de estas especies. Tal como se muestra en el caso de Tamarugo, índices espectrales de vegetación ampliamente usados en literatura como el NDVI, presentan una correlación negativa con la radiación solar (que es el estímulo que activa el movimiento de las hojas), mostrando un ciclo muy particular a lo largo del día y también durante las estaciones del año.

ii. Un síntoma temprano de estrés hídrico en plantas paraheliotrópicas (hojas que evitan la radiación solar en forma directa) es la disminución en amplitud de los ciclos diarios y estacionales de NDVI. De esta forma, estimaciones de esta amplitud utilizando sensores remotos (por ej. la diferencia en NDVI entre el invierno y el verano o entre la mañana y el medio día), pueden ser utilizados para detectar y mapear estrés hídrico en forma temprana en vegetación paraheliotrópica.

iii. A nivel de árboles individuales, el uso de imágenes satelitales de alta resolución espacial combinado con técnicas de análisis de imágenes basadas en objetos e información de campo, permitió estimar en forma precisa el estado hídrico de pequeños elementos de vegetación desértica, como árboles aislados. Para fines de seguimiento o monitoreo, se debe considerar en forma cuidadosa el momento del día y la estación del año en que las imágenes son capturadas a fin de evitar interpretaciones incorrectas de los resultados.

iv. Análisis de series de tiempo de imágenes satelitales combinado con imágenes de alta resolución espacial y registros hidrogeológicos permiten efectuar un análisis cuantitativo y espacio-temporal de los efectos de largo plazo de la extracción de agua subterránea sobre vegetación desértica.

Acknowledgements

This PhD was funded by the scholarship 'CONICYT-Wageningen' number 540900001, granted by the government of Chile and Wageningen University.

It is hard to express my gratitude to so many people who played an important role in the long process of getting my PhD. All help, support, and kindness, no matter little or big, build up the success of a PhD student. I will make here my best attempt.

First of all, I have to acknowledge my parents who put me on the way of the education in times where economic and social conditions were difficult in Chile. To be fair, I will make it in Spanish: '*a mis queridos padres (tío Pollo y tía Tencha) quienes con todo su esfuerzo y cariño me permitieron volar tan alto en el camino del saber que, sin saber cómo, logré obtener el grado de doctor en una de las universidades más prestigiosas de Europa. Esto es para ustedes*!' I had the fortune to start and finish the adventure of studying abroad with my own family: all my love to my wife Marcela, without whom I don't think I'd have gotten this far. Thank you for your listening, your patience, and your unconditional support and love.

I also want to thank to my supervision team, starting with Prof. Edmundo Acevedo, who played a key role at the beginning of this journey, advising me to follow a PhD in Wageningen University. Many thanks to all academics of Wageningen University who contributed to reach this point: my promotor Prof. Martin Herold, Prof. Arnold Bregt, Harm Bartholomeus, Jan Verbesselt, Sytze de Bruin, Lammert Kooistra, Arend Ligtenberg, Ron van Lammeren, and especially to my daily supervisor Jan Clevers, who spent a significant amount of time guiding me through this wild science jungle. Thank you for all the chats, meetings, advices, and critical revisions of all my scientific work. Thanks also to Truus, Antoinette, Frans, Willy, Roland, John, and Phillip, who helped me a lot in the zone of the science jungle where academics can't help.

And last but not least, I'd like to thank my colleagues and friends who made my life in The Netherlands, and particularly in Wageningen, an unforgettable experience beyond the PhD. To my officemates: Lukasz, Noriko, Arun, and Hannes who not only had to stand me all these years, but also shared with me those thousands of hours that a PhD requires. Thank you guys! To my PhD colleagues of

these ‘more than four’ years: Gerd and Jochem; the ‘Danis’ Cangrejo and Daniela; ‘the girls’ Valérie, Lucie, Lucía, Titia and Petra, thank you for your good humor and all the moments we shared in Wageningen and Zurich; Richard and Kim, my contemporary colleagues: we went through all the PhD stages together, always with laughs and optimism despite the different trouble we faced, c’mon guys almost there! Also many thanks to my lovely neighbors in Bennekom, Nandika and Sukhad, and now Misheel, for the good time we shared within and outside the office. And for all the moments, help, coffee breaks, beers and so on and so on this long road: thanks to Ben, Niki, Loïc, María, Michi, Sarah, Yang, Peter, Erika, Brice, Valerio, Juha, Jalal, José, Manos, Angela, Qijun, Eliakim, Eskender, Giulia, and Marcio. Few PhD’s in the world can have the chance to share with such as cool international group and make friends from all around the globe!

Special thanks to my paranymphs: you guys will be at my side that day in the Aula, but not only that day. You have offered me a great friendship all these years, which I hope we can keep alive when we become old (and bold) researchers. Richard all the best for you and your lovely family, together with Marce, we have the best memories of our dinners and wine tastings with Steffi and Louis. Mathieu, together we survived the Atacama fieldwork, a milestone in this PhD. Thank you for all the travelling, the dinners, the countless beers, the board games nights, and those fish you promised and hopefully one day you will be able to catch (especially the Chilean ones).

Important friends that contributed with joy to my PhD were not only within the Gaia building. Thanks to Lukasz and his family: Magda, Anthony and Jan, who were always with us offering their friendship and support. Dziekuje bardzo! To Matthijs and Andrea, all the best guys! And finally, many thanks to the Chilean gang, who was very important when I felt homesick or when I thought that the PhD was a mountain too high to climb. Special thanks to Francisco and Lena; Tomás, Pía and Matías; Carlitos, Ali, Mateo and Renato; Daniela and Marcelo; Ninoska and Lawrence; Gabo and Deni; Álvaro, Anita and Maida; and also Gabi, Mane, Lucero, Tati, and Nico. Son lo máximo y espero verlos siempre!

Now, wherever you are, be with me and celebrate!

Roberto O. Chávez. Valdivia, August 2014

List of publications

Peer reviewed journals

Chávez, R.O., Clevers, J.G.P.W., Decuyper, M., De Bruin, S., & Herold, M. (In review). 50 years of groundwater extraction in the Pampa del Tamarugal basin: can Tamarugo trees survive in the hyper-arid Atacama Desert? *Ecological Applications*

Chávez, R.O., Clevers, J.G.P.W., Verbesselt, J., Naulin, P.I., & Herold, M. (2014). Detecting leaf pulvinar movements on NDVI time series of desert trees: a new approach for water stress detection. *PLOS One* (in Press)

Laurent, V.C.E., Schaepman, M.E., Verhoef, W., Weyermann, J., & **Chávez, R.O.** 2014. Bayesian object-based estimation of LAI and chlorophyll from a simulated Sentinel-2 top-of-atmosphere radiance image. Remote Sensing of Environment, 140, 318-329

Chávez, R.O., Clevers, J.G.P.W., Herold, M., Ortiz, M., & Acevedo, E. (2013b). Modelling the spectral response of the desert tree *Prosopis tamarugo* to water stress. *International Journal of Applied Earth Observation and Geoinformation, 21*, 53-65

Chávez, R.O., Clevers, J.G.P.W., Herold, M., Acevedo, E., & Ortiz, M. (2013a). Assessing water stress of desert tamarugo trees using in situ data and very high spatial resolution remote sensing. *Remote Sensing, 5*, 5064-5088

Other scientific publications

Chávez, R.O., Naulin, P., Clevers, J.G.P.W., Verbesselt, J. , & Herold, M. (2014). Early water stress detection by accounting for pulvinar movements in desert trees (Chile) using Landsat and MODIS NDVI time series. In: International Conference "Global Vegetation Monitoring and Modeling" (GV2M), 3-7 February 2013, Avignon, France. - Avignon, France, 2014. Abstract book – p. 183 - 184.

Chávez, R.O., & Clevers, J.G.P.W. (2012). Object-based analysis of 8-bands WorldView2 imagery for assessing health condition of desert trees. In: CGI Report 2012-001 (p. 15). Wageningen: Wageningen University

Chávez, R.O., Clevers, J.G.P.W., & Herold, M. (2012). Earth observation for assessing water condition of arid vegetation. The case of the Atacama desert. In: *Proceedings Encuentros 2012 Conference*, Paris, France, 4-6 July 2012. - Paris, France, 2012 - ISBN 9788468638607 - p. 36 - 37.

Chávez, R.O., Clevers, J.G.P.W., & Herold, M. (2012). Spectral response of desert trees (*Prosopsis tamarugo* Phil.) to water stress: basis for a remote sensing assessment. In: Proceedings 2nd Terrabites Symposium 2012, 06-08 February 2012, Frascati, Italy. - p. 58.

Short biography

Roberto O. Chávez Oyanadel was born in Santiago (Chile) in 1977. He followed primary and secondary school in Colegio Licarayén, and studied forestry at University of Chile in Santiago (Chile). He obtained his bachelor degree in forestry in 1999 and the professional title of Forest Engineer in 2001.

He started working in forestry as early as 1999 in Tierra del Fuego Island (Chilean Patagonia) and moved back in Santiago in 2001 where he started a consultancy career for environmental projects and environmental impact assessment. First as a project engineer (2003-2006) and later as a project leader (2006-2009), Roberto participated in several projects of national importance in the sectors of mining, energy, and forestry as well as in conservation projects, being the project "Contrafuertes Cordilleranos (GEFF/World Bank/Protege): development of a master plan for conservation of the mountain ecosystem in Santiago foothills" one of the most relevant of this period.

In 2009, Roberto was granted with the CONICYT-Wageningen PhD scholarship and joined the Laboratory of Geo-information Sciences and Remote Sensing of Wageningen University (The Netherlands). Under the supervision of Prof. Dr. Martin Herold and Dr. Jan Clevers, he realized deep studies of the use of remote sensing to detect and quantify water stress of desert vegetation. During his PhD, Roberto published four peer-reviewed articles and four other scientific publications and conference proceedings. In 2011 he won the 8-band challenge research organized by Digital Globe, leader in the sub-metric satellite industry, with the article entitled "Object-based analysis of 8-bands WorldView2 imagery for assessing health condition of desert trees". Finally, he accomplished his PhD in 2014.

Roberto's primary research interests are related to the use of quantitative remote sensing for vegetation monitoring, field and laboratory spectroscopy, and radiative transfer modelling. The nature of his research is also strongly connected to the fields of forest ecology, plant physiology and environmental impact assessment.

PE&RC Training and Education Statement

With the training and education activities listed below the PhD candidate has complied with the requirements set by the C.T. de Wit Graduate School for Production Ecology and Resource Conservation (PE&RC) which comprises of a minimum total of 32 ECTS (= 22 weeks of activities)

Review of literature (6 ECTS)

- Spectroscopic analysis of water stressed vegetation in Atacama Desert, and its applicability on water management

Writing of project proposal (4.5 ECTS)

- Assessment and monitoring water stress condition of arid vegetation using remote sensing techniques: the Atacama Desert (Chile) case

Post-graduate courses (7.1 ECTS)

- Introduction to R for statistical analysis; PE&RC (2010)
- Multivariate analysis; PE&RC (2010)
- The art of modelling; SENSE-PE&RC (2011)
- Eco-physiology of plants; University of Groningen (2011)

Invited review of (unpublished) journal manuscript (1 ECTS)

- PLOS One: the effect of differential growth rates across plants on spectral predictions of physiological parameters (2014)

Competence strengthening / skills courses (2.6 ECTS)

- Information literacy, including introduction Endnote; WUR library (2010)
- PhD Competence assessment; Wageningen Graduate Schools (2010)
- Scientific writing; Wageningen Graduate Schools (2013)

PE&RC Annual meetings, seminars and the PE&RC weekend (1.5 ECTS)

- PE&RC introduction weekend (2010)
- PE&RC Day (2011)
- PE&RC Day (2012)

Discussion groups / local seminars / other scientific meetings (5.0 ECTS)

- Mathematics and Statistics Network (2010)
- Remote Sensing symposium (2011)
- Encuentros Paris – a conference to discuss the state of Chilean research (2012)
- Ecological Theory and Application discussion group (2012-2013)
- Discussion seminars at Universidad de Chile and Universidad Austral de Chile (2009, 2012-2013)
- Dies Natalis Wageningen University (2014)

International symposia, workshops and conferences (6 ECTS)

- 2nd Terrabites Symposium, poster presentation, Frascati, Italy (2012)
- GV2M: Global Vegetation Monitoring and Modelling; poster presentation; Avignon, France (2014)

Lecturing / supervision of practical's / tutorials (3 ECTS)

- Advanced Earth Observation Course (2011-2013)

Supervision of MSc students (1.8 ECTS)

- Quantify the spatial and temporal aspects of vegetation succession on green beaches; Schiermonnikoog, The Netherlands

Cover illustration adapted from Sudzuki, F. 1969. Absorción foliar de humedad atmosférica en Tamarugo, *Prosopis tamarugo*, Phil. Boletin técnico de la Facultad de Agronomía, Universidad de Chile, 30, 1-23